Electrochemically Switchable Calixarene Ionophores

by

Gary Dougherty

Thesis submitted in accordance with the requirements of

The University of Liverpool

for the degree of

Doctor of Philosophy

September 1994

To Denise and Sean.

Acknowledgements

I would like to thank Dr. D. Bethell for his advice and support throughout the period of this research, and for his patience during the last year. Thanks are also due to ICI for financial support and access to their research facilities, in particular Dr.D. Cupertino and Dr. M. Charlton, and to Prof. I.O. Sutherland for the time spent on secondment in his research group. Thanks are also due to the technical staff for their assistance.

I would like to thank all those people whom I have had the pleasure of working with during my time at Liverpool (especially D.F.L., J.H. & D.H.K.).

Finally, I would like to express my deepest gratitude to my wife Denise, for her understanding, patience and support both during the research period and the writing of this thesis. I would also like to thank Sean for giving me a reason to finish this work.

Abstract

The synthesis of a series of *p-tert*-butylcalix[4]arene based, electrochemically switchable, ionophores (**1**), (**2**), (**3**), (**4**) and (**5**) is described. Their electrochemical properties were investigated in the presence of added Group I metal perchlorates. Both compounds (**1**) and (**2**) displayed no enhancement of binding for metal ions, due to electrostatic interactions, upon electrochemical reduction. This behaviour is explained on steric grounds, as deduced by molecular modelling. Compounds (**3**), (**4**) and (**5**) all display significant enhancements of metal ion binding upon electrochemical reduction. Compounds (**4**) and (**5**) appear to display a high selectivity for sodium ions over other Group I metal ions. Compound (**3**) displayed the highest binding enhancements yet recorded for both sodium (3.138×10^5) and potassium (1.398×10^3) ions.

Compound (**6**) (from which (**3**), (**4**) and (**5**) were made) could be converted to many other compounds in which the side arms bear different functional groups in an effort to control selectivity. For example thio esters or thio amides for silver, ethyl groups for potassium.

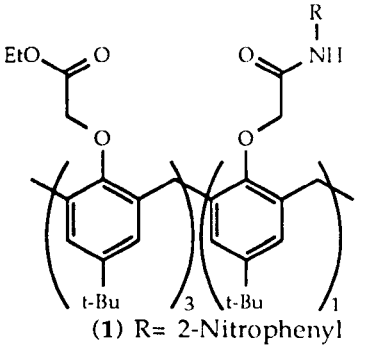

(**1**) R= 2-Nitrophenyl
(**2**) R= 1-Anthraquinone

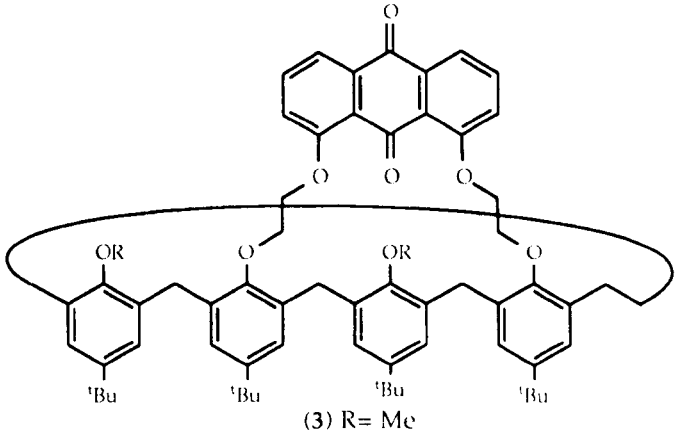

(**3**) R= Me
(**4**) R= CH_2CO_2Et
(**5**) R= CH_2CONEt_2
(**6**) R= H

Chapter 1

Introduction

Since Pedersen's discovery that crown ethers were capable of forming stable complexes with alkali and alkali earth metal cations,[1] chemists have striven to create increasingly elaborate ionophores capable of complexing a wide variety of metal ions. Part of the driving force behind this is for analytical (sensing) applications, but part is the need for effective ionophores in hydrometallurgic processes. Hydrometallurgy is concerned with the extraction of metals from an aqueous phase into an organic phase for the purpose of purification and recovery. An effective ionophore therefore, is one that is capable of selective, high strength, reversible binding.

Thus far the development of ionophores has revolved around the design of ionophores that display very high selectivities and very high binding abilities. The disadvantage with this approach is that as binding strength is increased, the host-guest interaction becomes so strong that the host becomes reluctant to give up its guest, i.e. binding becomes stoichiometric and irreversible.

In order to overcome this problem of irreversibility it would be convenient to be able to alter the strength of binding in a controllable way such that there are two binding states, i.e. to switch the ligand between binding and non-binding states. It is this approach to ionophore design that has led to the concept of the electrochemically switchable ionophore. Chapter 1 contains a brief outline of the development of "classical" ionophores (crown ethers, etc.) and a survey of the approaches that have been made towards switched ionophores.

Crown Ethers, Cryptands and Spherands.

Crown Ethers, cryptands and spherands represent a convenient progression in the design of ionophores that display increasing binding strength and higher selectivities.

[18]-Crown-6 (**2**) was one of the first crown ethers to be synthesised,[2] (Scheme 1.1), this original synthesis has now been greatly improved and it can be obtained in up to 93% yield (Table 1.1, Scheme 1.2).[3, 4, 5, 6]

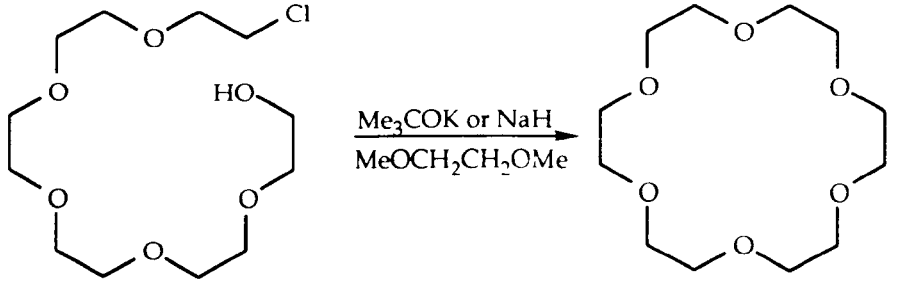

(**1**) (**2**)

Scheme 1.1

Table 1.1: Methods for the Synthesis of [18]-crown-6

Method	X	Base	Solvent	yield(%)	Ref.
i	OTs	Me_3COK	Me_3COH/ benzene	33	3
ii	OTs	Me_3COK	THF	30-60	4
iii	OTs	Me_3COK	DMSO	84	4
iv	OTs	Me_3COK	DME	93	4
v	Cl	KOH	THF/H_2O	40-60	5
vi	Cl	KOH	THF	30	6

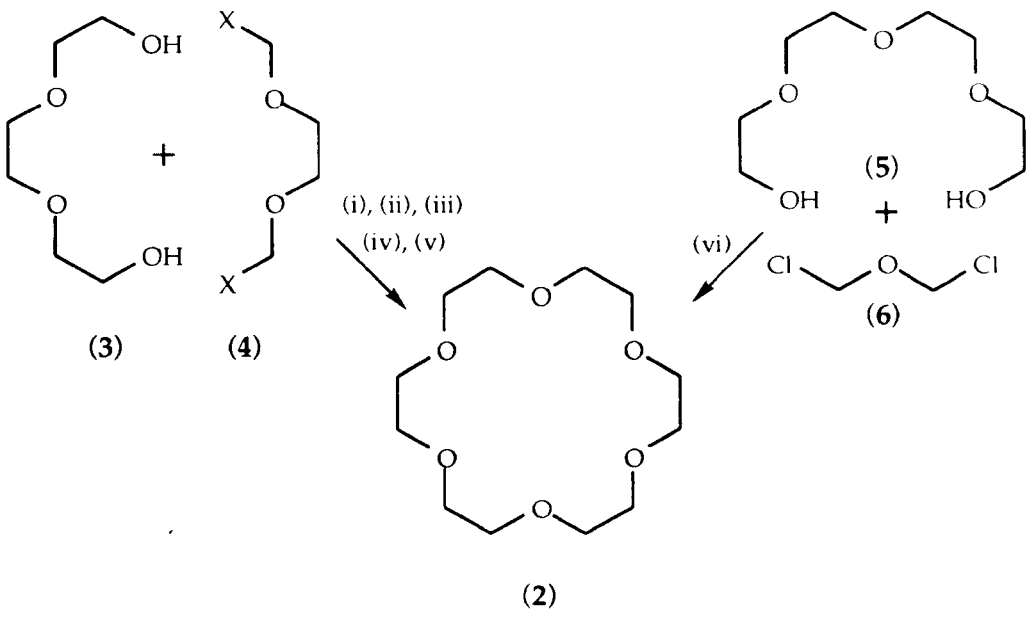

Scheme 1.2

The ability of [18]-crown-6 to complex metal ions, particularly potassium ions, is now well documented.[7] The molecule has this ability by virtue of its regular hexagonal arrangement of the six oxygens. When a metal ion is present, the lone pairs of the oxygens can donate electron density or charge towards the centre of the ring in a co-ordinated way. This acts to solvate the metal ion. This ability to complex metal ions can be expressed numerically by comparing the concentrations of free and complexed metal ion. An equilibrium constant, K_a, can then be calculated for the reaction (equ. 1.1).

$$M^+_{(solv)} + L_{(solv)} \underset{k_{-1}}{\overset{k_1}{\rightleftharpoons}} ML^+_{(solv)}$$

$$K_a = \frac{k_1}{k_{-1}} = \frac{[ML^+]}{[M^+]\,[L]} \qquad \text{(equ. 1.1)}$$

K_a is usually expressed as a log value, (log K_a), and is known as either the binding or stability constant (sometimes given the symbol K_s). The binding constant for the [18]-crown-6/potassium ion interaction (in methanol) is 6.1.[8] This means that complexation is

over a million times faster than decomplexation. The value for the acyclic analogue, pentaglyme, is 2.2. Closing the ring has led to an improvement by a factor of *ca.* 10,000. Part of the reason behind this improvement is that the crown ether is pre-organised for complexation. For the linear ionophore to complex a metal ion it must undergo a large change in conformation, this has an associated free energy cost and thus reduces the complexing ability of the ionophore. The [18]-crown-6 molecule is constrained in a cyclic form and does not need to undergo such a large change in conformation. There is, however, some loss of conformational freedom for the [18]crown-6 molecule, as it does not normally exist in the correct conformation for optimum binding. The oxygen lone pairs would not normally all face inwards due to electrostatic repulsion; the molecule must therefore reorganise itself to bind the metal ion. This low degree of pre-organisation led to the development of more complex host molecules in which the conformation is even more restricted and therefore shows a higher degree of pre-organisation. This development was the invention of the cryptands.[9,10,11]

Cryptands were created by simply substituting two trivalent nitrogen centres for divalent oxygens, on opposite sides of a crown ring. This opens up the possibility of attaching a bridge between the nitrogens, thus forming a bicyclic system (Scheme 1.3). This fixes the cryptand in the binding form, reducing the loss of conformational freedom. There is another consequence of the addition of the second ring; the "cavity" in the centre of the macrocycle is now better defined, improving the selectivity of the cryptand. The sum of these effects is to raise log K_a for the K^+/cryptand interaction in MeOH to 10.4,[12] an improvement by a factor of more than 10^4.

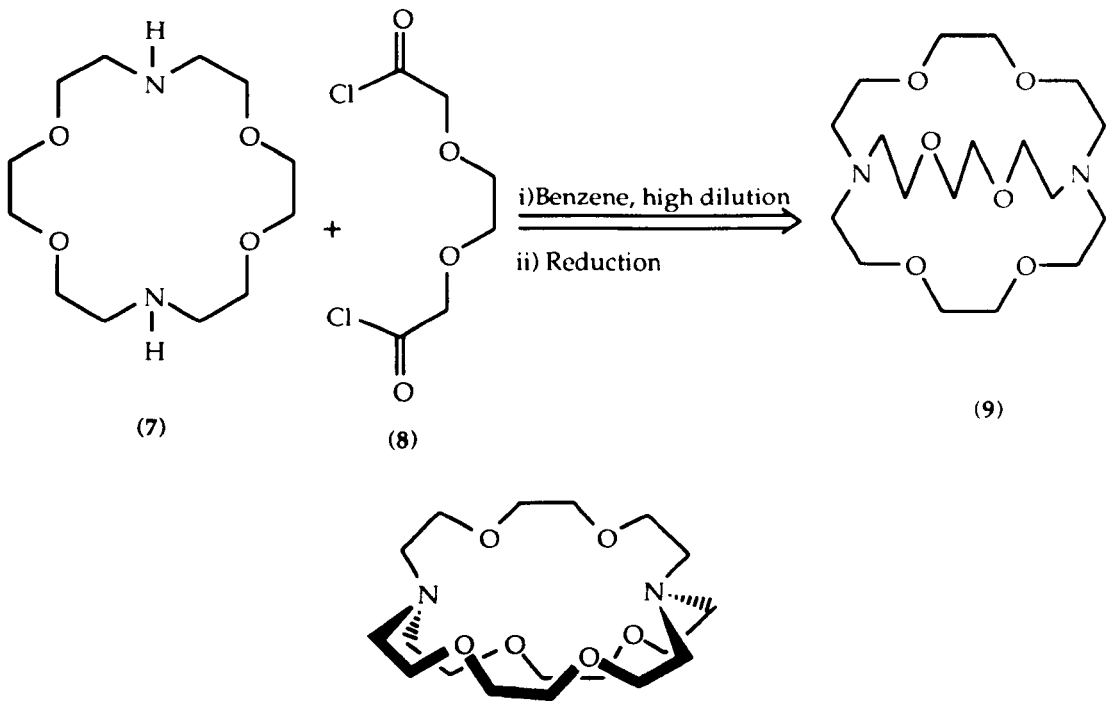

(7) (8) (9)

Scheme 1.3: Synthesis and 3D representation of Cryptand [2.2.2]

Despite this massive improvement, the cryptand still has a disadvantage, this is that the conformation is not completely rigid; there is still some loss of conformational freedom upon binding to a metal ion. Cram overcame this final hurdle with the invention of spherands.[13] Spherands are extremely rigid molecules composed of anisole moieties in a circular array; these molecules undergo no change in conformation upon binding a metal ion and can be described as fully pre-organised. In the example given, (10), optimum binding is for lithium ions (log K_a 16.85, in $CDCl_3$),[14] due to the small cavity size. This extremely high value for the binding constant equates to complexation taking place 7×10^{16} times faster than decomplexation.

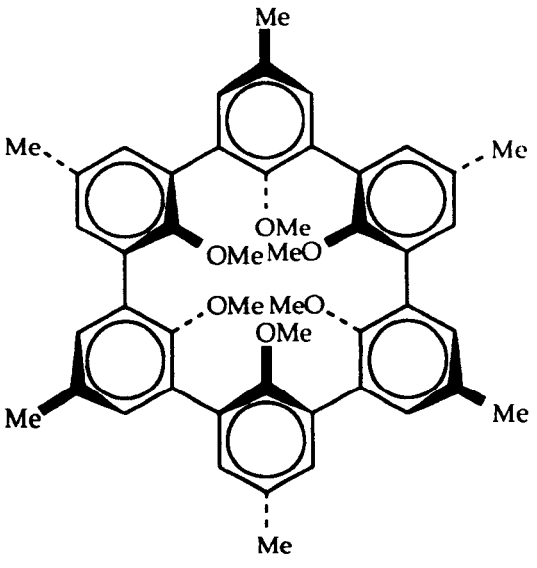

(10)

Switchable Ionophores

In the last section we have seen how the traditional approach to ionophore design, which involved increasing the degree of pre-organisation and improving the fit between host and guest, led to an increase in binding constants. The disadvantage with this approach to metal extraction is that the binding becomes irreversible and stoichiometric. Thus to extract one mole of metal ion would require one mole of, usually expensive, ligand and the host molecule will not give up its guest. One response to this problem is to introduce a switching mechanism into the ionophore. This allows the control of binding, by switching it between binding and non-binding states. Switching could then be used as a method for the control of transport of metal ions through membranes.

Switching between binding states can be achieved photochemically, electrochemically, by changes in pH and by chemical oxidation/reduction procedures.

Photochemically Switched Ionophores

Photochemical switching of binding has been particularly well studied by Shinkai *et al.*, the photoresponsive unit being azobenzene. Shinkai *et al.*, have produced a crown ether into which has been incorporated an azobenzene moiety (**11**),[15] a bis-benzocrown ether with an azo link (**12**),[16,17] and a cryptand-like molecule with an azobenzene bridging unit, (**13**).[18] All these molecules exhibit a degree of reversible binding when the azobenzene is switched between the *cis* (binding or "on state") and *trans* (non-binding or "off state") forms, with (**11**) displaying an "all or nothing" type binding. Compound (**12**) can be used in a light driven transport process.[19]

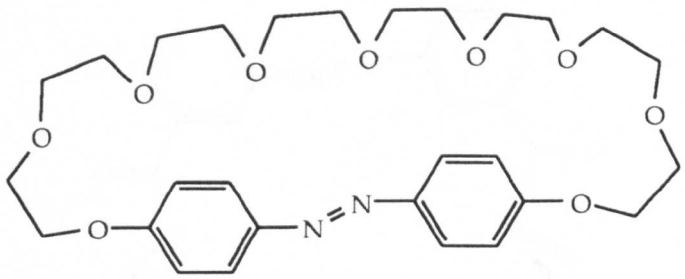

trans -(**11**) (non-complexing form)

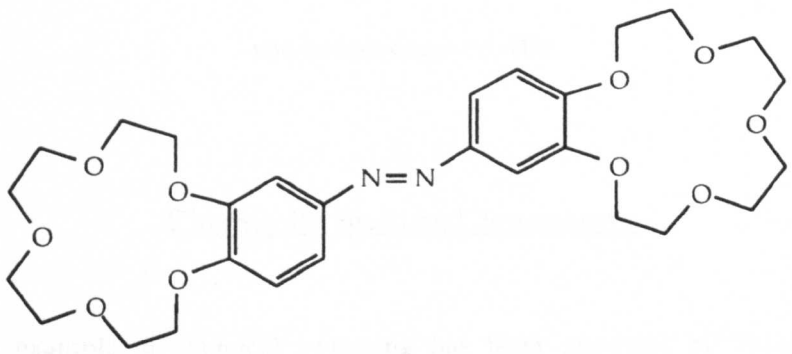

trans -(**12**)

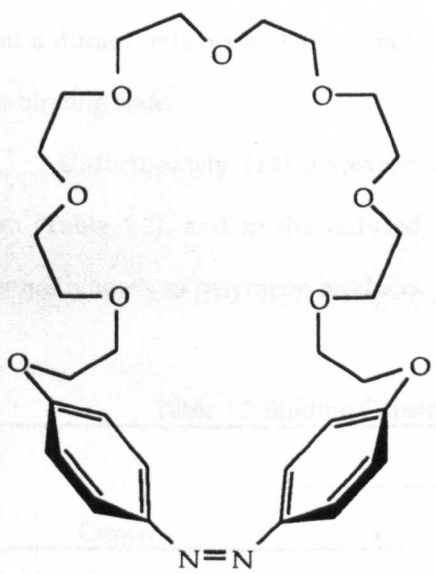

cis -(**11**) (complexing form)

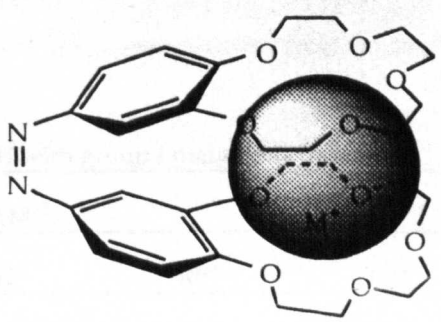

cis - (**12**) M^+ complex

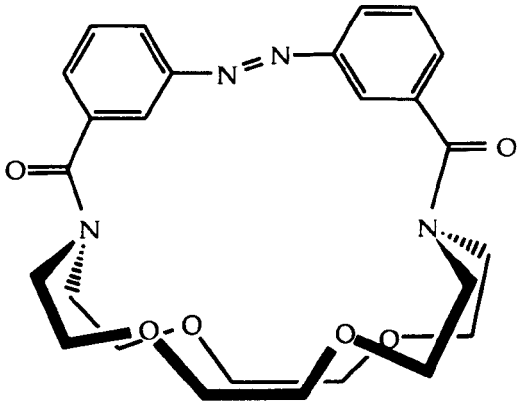

non complexing *trans* -(13)

Chemically Switched Ionophores

An example of chemical switching has been provided by Shinkai *et al.* [20] Compound (14) can exist in either an oxidised or reduced form. In the oxidised form it contains a disulphide linkage, the binding state. Reduction cleaves the disulphide link to form a dithiol, this open chain form having a lower affinity for metal ions and being the non-binding state.

Unfortunately (14) displayed very low affinities for metal ions in the oxidised form (Table 1.2), and in the reduced form it is very prone to aerial oxidation, which eventually leads to polymeric products.

Table 1.2 Binding Constants for (14) with group I metal ions

	K_a (M^{-1})			
Crown	Na^+	K^+	Rb^+	Cs^+
(14) $_{ox}$	≈ 30	180	290	320
monobenzo-21-crown-7	410	1270	1850	2070

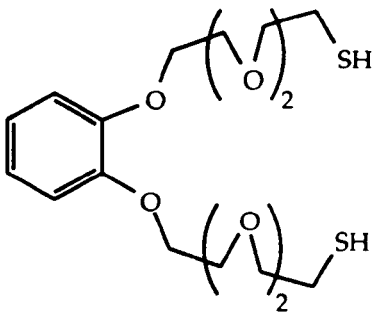

(14) (open, reduced)

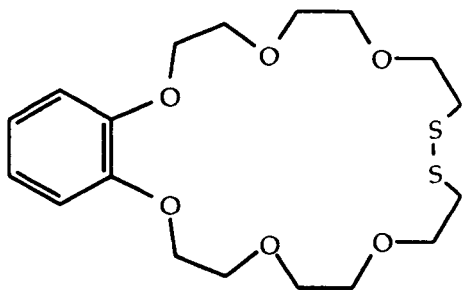

(14) (cyclised, oxidised)

pH-Switched Ionophores

Although not as elegant as photochemical switching, pH switching offers an excellent method of controlling binding. The control of pH is relatively simple and a wide variety of buffer systems are available. There are also a large number of molecular or conformational changes known to be affected by changes in pH. Changes in pH are also associated with the formation of a charged centre, this can lead to large increases in binding due to electrostatic forces. This has led to a multitude of pH controlled ionophores, a few representative examples are given here.

Phenolic Switches

Two examples of ionophores which include phenolic switches are (15; n=1,2) and (16; n=1,2).[21] Compounds (15) and (16) are lariat ether type ionophores which upon de-protonation of the phenol can be used to detect the presence metal ions. As the pH is increased the phenol is deprotonated causing colouration of the ligand. At an appropriate pH the ligand can extract metal ions into an organic phase, this metal extraction is signalled by a further colour change. The initial colour of the deprotonated form is yellow/orange but the inclusion of a metal ion in the crown ring shifts the absorption band to longer wavelengths, changing the colour to blue/violet. The crown ether portion of the

molecule affects the metal ion selectivity in the normal way (i.e. [15]-crown-5: Na^+ selective, [18]-crown-6: K^+ selective).

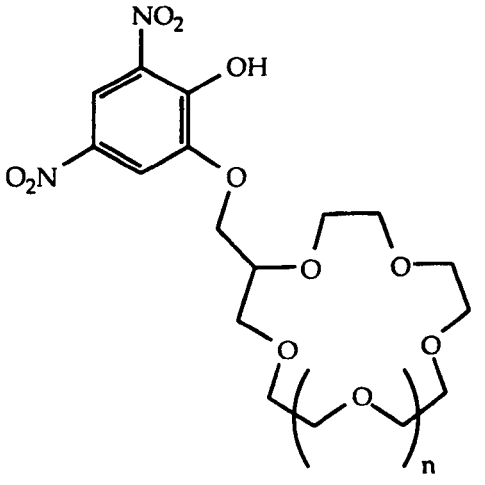

(15)

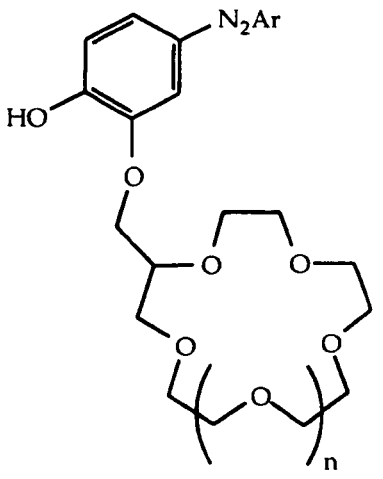

(16)

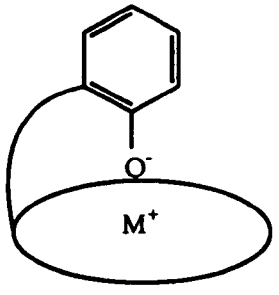

Schematic representation of the binding state for lariat crowns (15) and (16)

A second type of phenol based pH switchable ionophore is the calixarene compound (17).[22] Calixarenes are the macrocyclic condensation products of *p-tert*-butylphenol and formaldehyde, (for a more detailed description of the chemistry of calixarenes see Chapter 2). The cyclic arrangement of phenolic oxygens creates a hydrogen bonding array. This tends to hold the compound in the "cone conformation" with all the oxygens at the apex, in effect creating a pre-organised binding site. In the neutral state however there is a low barrier to rotation of the phenol through the annulus of the ring defined by the methylene groups. The compound is therefore a rather poor ionophore. In the deprotonated form though, the

ion pair that is formed is ideally solvated by the cone form. The onset of transport is therefore controlled by a change in pH; below *ca.* 12 no transport is observed and above this value it steadily increases. Transport rates for (17) with group I metal hydroxides across a $CH_2Cl_2/CHCl_3$ membrane are given in Table 1.3. The large ring in compound (17) gives it a selectivity towards the large caesium ion.

Table 1.3. Rates for the transport of group I metal ions from basic solution by (17), and three model compounds.

	Transport rate x 10^8/ mol s^{-1} m^{-2}			
Source Phase	(17)	18-Crown-6	Phenol	*p-tert*-butylphenol
LiOH	2.0 ± 0.2	a	a	a
NaOH	9 ± 2	a	a	a
KOH	10 ± 4	a	a	a
RbOH	340 ± 20	a	a	a
CsOH	996 ± 280	a	a	a

a/ less than 0.9 x 10^{-8} mol s^{-1} m^{-2}

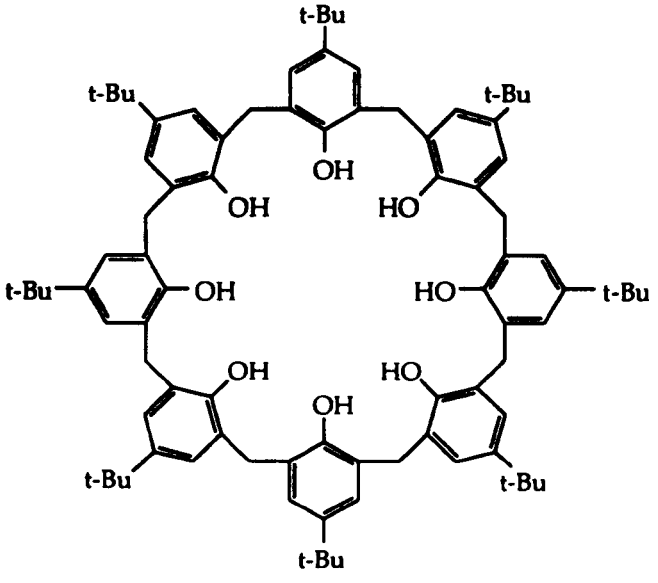

(17)

Switched Lariat Ionophores

Examples of pH-switched ionophores are compounds (**18**), (**19**), (**20**) and (**21**). All these compounds are crown ethers with both (**18**) and (**19**) bearing phosphonic acid side arms and compounds (**20**) and (**21**) bearing carboxylic acid side arms.[23] Binding constants were only given for the deprotonated forms of these compounds, and thus any enhancement of binding cannot be calculated.

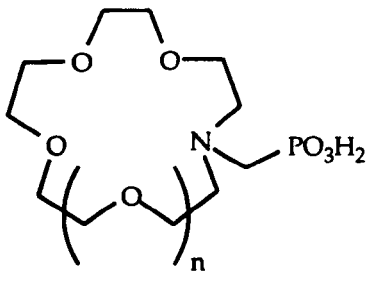

(**18**; n=1,2)

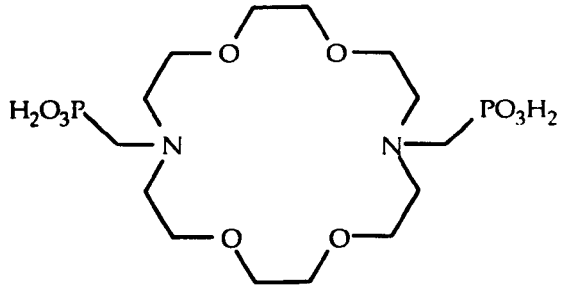

(**19**)

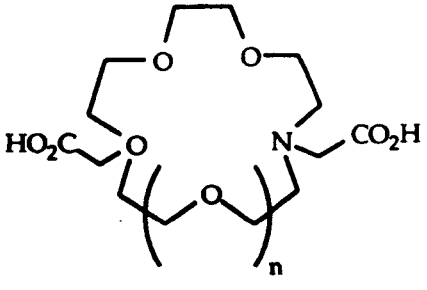

(**20**; n=1,2)

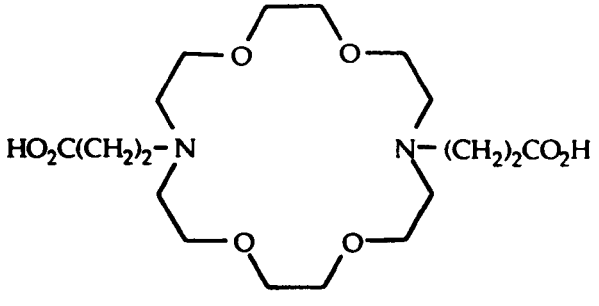

(**21**)

The structurally similar compound (**22**) has been made by Shinkai *et al.*[24] Transport of potassium ions across a chloroform membrane was shown to be very dependent on the pH of the receiving phase; the maximum rate being observed at around pH 5. This was attributed to transport by the zwitterionic species ($22^{\pm}$). Transport by metal ions is accompanied by the reverse transport of protons. At higher or lower pH, (**22**) exists in either the fully protonated (22^{+}) or fully deprotonated form (22^{-}). Neither of these species is as effective at transport; above *ca.* pH 9 reverse transport of protons is hindered, below

ca. pH 3 uptake of metal ion is no longer favoured as the acid side arm is now in its protonated form.

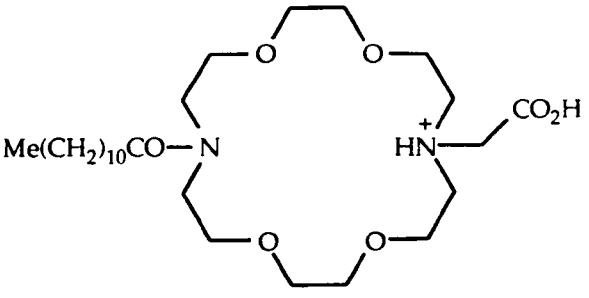

(22^{+})

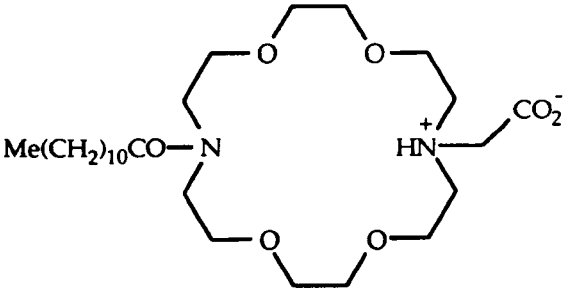

(22$^{\pm}$)

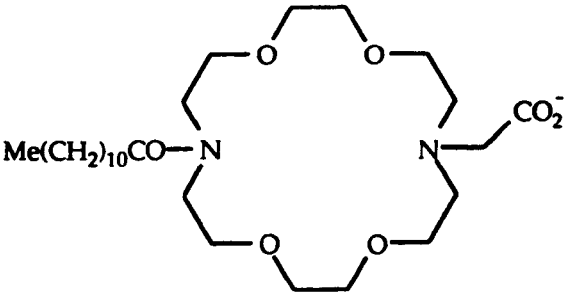

(22^{-})

Macrocyclic polyamines have been used extensively as pH switched ionophores, utilising both the basicity of the nitrogen and carboxylic acid bearing side arms.

Compounds such as (23)[25] and (24)[26] bear carboxylic acid side arms. They were studied exclusively in the deprotonated state for their binding with transition and group II metal ion- Although not strictly pH switchable ionophores the potential for switching exists.

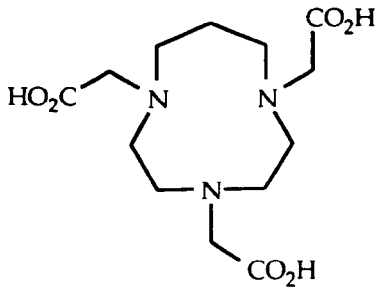

(23)

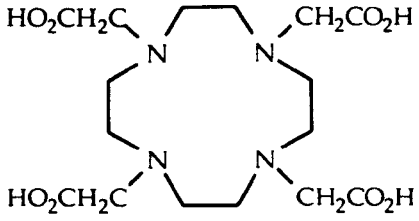

(24)

Tsukube has used compound (25), structurally similar to compound (24), to transport amino-acid and oligopeptide anions across a chloroform membrane.[27] Optimum transport was observed at a pH of *ca.* 5 (Table 1.4). Counter-transport of another anion was necessary; chloride proved to be the most effective.

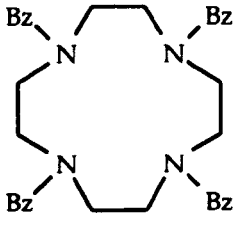

(25)

Table 1.4 : Transport rates for amino acid and related anions (mol h^{-1}).

Guest anion	pH	Counter-transported anion	Transport rate x 10^6 for (25)
Z-Asn	11.3	Cl^-	0.3
	5.6	Cl^-	0.8
	4.7	Cl^-	4.9
Z-Gln	4.3	Cl^-	7.8
Z-Gly	4.8	Cl^-	2.4
Z-Asp	9.2	Cl^-	0
	5.9	Cl^-	2.2
	4.7	Cl^-	5.4
	4.7	ClO_4^-	5.0
	4.7	none	0
Z-Glu	4.0	Cl^-	7.6
terephthalate	5.5	Cl^-	0
isophthalate	5.4	Cl^-	0.1
phthalate	5.4	Cl^-	5.2

Electrochemically Switched Ionophores

For the present investigation we have chosen electrochemical switching as it offers several advantages.

- Binding enhancements should be large since charge/charge interactions are responsible for strong bonding, e.g. ionic bonds.
- There exists a range of molecules whose electrochemical behaviour is well studied and understood (e.g. anthraquinone, ferrocene and nitro-aromatics).
- The changes induced in the binding of metal ions due to electrochemical change are easily measured using cyclic voltammetry.
- Highly accurate apparatus for the control of potentials and the measurement of current is available.

This study has centred on reductive switching, which involves electrochemical reduction of the ligand to form the radical anion, (the addition of one electron), or dianion, (the addition of two electrons). The radical anion can interact with a cation in the same way as a conventional anion, but if the ligand has been constructed in a suitable manner it can also provide efficient solvation of the cation.

Nitrobenzene Based Switches

The most notable contributors to the whole area of research into electrochemically switched ionophores have been Gokel and co-workers. They have produced a series of nitrobenzene based lariat and podand-type ionophores, as well as anthraquinone based compounds.

The first report of an electrochemically switchable ionophore was in 1983, when Gokel *et al.* made (**26**; n=1).[28] This [15]crown-5 based lariat-type ionophore could be reduced electrochemically to give the radical anion, (the charge being localised on the nitro group). When (**26**; n=1) is reduced in the presence of metal ions however a new redox

couple is observed at a more anodic potential than for the ligand in the presence of $(NR_4)^+$ (non-complexing). This is attributed to the interaction of the ligand with the metal ion. The presence of a positively charged ion in the [15]crown-5 cavity assists transfer of an electron to the ligand and serves to stabilise the reduced ligand/metal ion complex via a charge/charge interaction. Therefore the metal/ligand complex is easier to reduce, shifting the potential to a more anodic value. This effect has been termed the binding enhancement, and is expressed numerically by the binding enhancement factor (BEF) (equ. 1.2 c.f. Scheme 1.4).[29] The binding enhancement shows an exponential dependence on the shift in the reduction potential. A shift of *ca.* 10mV represents a simple ion pairing interaction, a shift of 200mV represents an enhancement of 2400, a shift of 300mV, 118,000, 400mV... 5,778,000. For the (**26**; n =1)/Na^+ interaction the BEF is 750, i.e. the reduced ligand binds 750 times more strongly than the neutral ligand. Control experiments, performed using molecules (**27**; n =1) and (**28**), did not show the same effects, [although (**28**) did show some ion pairing effects]. In (**27**) the nitro group is remote from the crown ring and cannot interact with the metal ion, (**28**) does not possess a crown ring to bind the metal ion. The 2-nitroanisyl and [15]crown-5 moieties are therefore acting in synergy. This last point is reinforced by comparison of (**26**; n =1) to (**29**) and (**30**), which can potentially interact with the metal ion using the polyethylene glycol side arms.[30] Both (**29**) and (**30**) behave in a similar way to (**28**), and the potentially ligating side arm has no synergistic effect. This demonstrates the need for ligating and reducible parts of the molecule to be in proximity for the effect to be appreciable.

$$K^2/K^1 = \exp\left\{-\frac{F}{RT}\left(E^{o1} - E^{o2}\right)\right\} \qquad \text{(equ. 1.2)}$$

K^1: binding constant for neutral ligand

K^2: binding constant for reduced ligand

E^{o1}: redox potential for free ligand

E^{o2}: redox potential for the complex

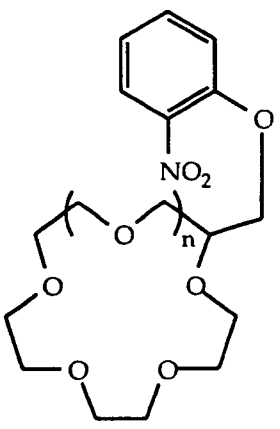

(26)

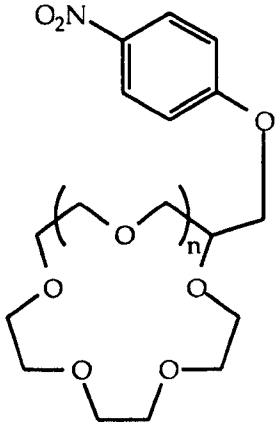

(27)

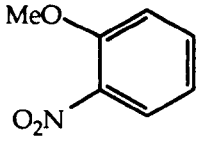

(28)

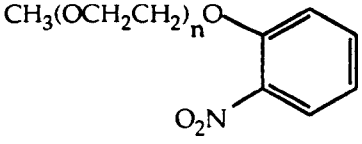

(29) n=8

(30) n=12

Gokel *et al.* went on to produce (**31**; n=1) and the model compound (**32**). Here the pivot point has been changed from carbon, in (**26**) and (**27**), to nitrogen and the linkage is one atom shorter.[31] This brings the reducible group closer to the macro-ring, enabling a stronger charge/charge interaction. The sum of these changes was to increase the BEF for the Na^+/(**31**; n=1) interaction to 25,000. In the model compounds the nitro group is remote from the macro-ring and they show only ion pairing effects. This dramatic improvement in the BEF, as compared to (**26**; n =1), led Gokel *et al.* to develop this chemistry further.[32] The range of lariat ionophores was expanded to include (**26**; n =2), (**27**; n =2), and a bibrachial lariat (**33**; n=1, 2). Binding enhancements are given in Table 1.5. The enhancements for (**31**; n=1) and (**33**; n=1,2) are particularly large, of the order of 10^6. This large difference between binding in the neutral and reduced ionophore is essentially a switch between on and off states.

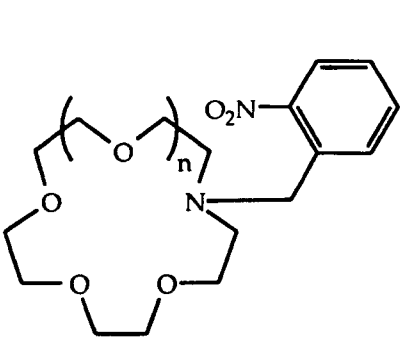

(31)

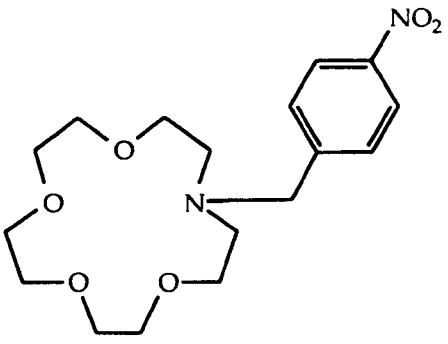

(32)

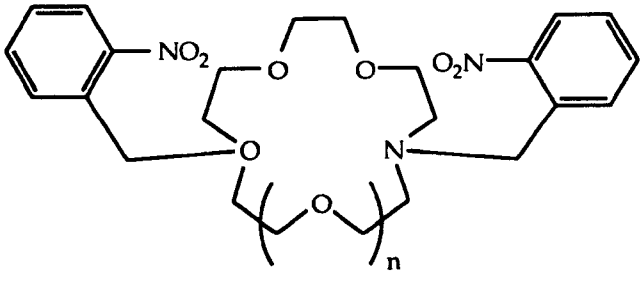

(33)

Table 1.5: Binding enhancements for Nitro-aromatic lariat ethers with various metal ions

Compound	Metal ion	ΔE (mV)	BEF
(26; n=1)	Li	310	1.7×10^5
	Na	170	7.5×10^2
	K	-	
(26; n=2)	Li	-	
	Na	70	15
	K	-	
(31; n=1)	Li	380	2.6×10^6
	Na	280	5.4×10^4
	K	200	2.4×10^3
(33; n=1)	Li	390	3.9×10^6
	Na	240	1.1×10^4
	K	190	1.6×10^3
(33; n=2)	Li	390	3.7×10^6
	Na	250	1.7×10^4
	K	210	3.5×10^3

If the results in Table 1.5 are examined they reveal that the order of binding enhancement is generally Li > Na > K. This reflects the differing charge to size ratios, lithium being the smallest ion and having the highest value. [15]-Crown-5 compounds however generally display selectivity towards sodium ions.[7] The inclusion of the reducible group has shifted the binding towards lithium. The sum is a levelling of the binding constants resulting in a loss of selectivity.

When the same system is studied with electron spin resonance (ESR) spectroscopy, seemingly contradictory results are obtained.[33] Compounds (**31**; n=1) and (**31**; n=2) were electrochemically reduced in the ESR cavity, in both the absence and presence of one equivalent of metal ion. For (**31**; n=1) only sodium ions induced large changes in the ESR spectrum and for (**31**; n=2), which has a larger macrocyclic ring, potassium ions induced a similar change. This would suggest that the ligand has retained the selectivity of the crown ether ring. This apparent conflict with the electrochemical results is due to the different quantities that are being measured. In the ESR experiments non-thermodynamic properties are being measured, such as coupling constants with the bound ion, e.g. ^{23}Na (which reflect geometry). In electrochemical experiments, shifts in the reduction potential of the ligand induced by the addition of metal ions are a measure of the ratio of the binding constants for the reduced and neutral ligands (which reflect reaction equilibria). If the neutral ligand binds as well as the reduced ligand no enhancement of binding and consequently no shift in reduction potential would be observed.

Coupling of the macrocyclic binding and electrochemical enhancement may be achieved if the chelating part of the molecule is changed for one which is more selective and the reducible group changed to one in which the effect of the charge is more directional.

Anthraquinone Based Switchable Podands, Lariats and Crowns

The anthraquinone molecule provides several advantages as an electrochemically switchable group;

- its anion is stable for months in water (provided oxygen is excluded),
- it undergoes discrete one or two electron reversible reductions,
- the charge in the reduced molecule is located on the carbonyl groups, providing highly directional charge donation.

Again it has been Gokel and co-workers who have made the most contributions to this area of research, although there has been a recent addition by Bethell *et al.*.[34] Anthraquinone based ionophores fall into four basic types; podands, lariats, crowns and cryptands. Each of these types displays differing electrochemical behaviour.

The lariat ether (34) displays lower binding enhancements with lithium ions than the model compound (35), despite the presence of the crown ring [2.4 x 10^3 for Li^+/(34); 7.7 x 10^3 for Li^+/(35)].[35] This is in contrast to the nitro aromatic counterpart (26), which displayed much higher enhancements than either the anisole (28) or podand (29) (30) models. This has been attributed to the poor geometric arrangement of the anthraquinone and crown ether parts of this compound. When a lithium ion is present it is complexed by the crown ether; this holds the ion at too great a distance from the anthraquinone for an appreciable interaction to take place upon electrochemical reduction. Compound (34) however does show an enhancement for sodium ions [2.3 x 10^2 for Na^+/(34)] due to a favourable geometrical arrangement (NB. this is a lower BEF than for Li^+). The ring to quinone distance is optimal for the larger sodium ion, enabling close ion pair contact. It is possible that this could be used as a method of discriminating between these metal ions.

The somewhat surprising result that the podand displayed higher enhancements than the crown compound led Gokel to develop the anthraquinone podands further, due in part to the ease with which podands can be made.[36] Compound (36; n=3) incorporates a

polyethylene glycol side arm to provide additional solvation. This raises the binding enhancement for Li^+ from 7.7×10^3 to 2.6×10^5 and that for Na^+ to 1.1×10^3 [adsorption only had been observed for (35)/Na^+]. The podand has this ability because the side arm is able to wrap around the metal ion whilst retaining close ion pair contact (Fig. 1.1). Electrochemically driven transport has been successfully achieved using both compounds (36; n=3) and (34). Neutral (36; n=3) displayed negligible transport of Li^+ across a model CH_2Cl_2 membrane, but when electrochemically reduced a transport rate for Li^+ of 2.2×10^{-7} mol/h was measured.[37] If a symmetrical transport cell is used in which there are two standard sets of electrodes, each controlled independently, coupled reduction and re-oxidation can be used. The advantage of this approach is that the ligand can be reduced, or switched to the "on state", near the source phase and then re-oxidised, or switched to the "off state", at the receiving phase. Thus transport can be driven across an electrochemical gradient. Using this approach (34) was demonstrated to transport sodium ions across a membrane.[38] Reduction of the ligand increased transport by a factor of *ca.* 2 and coupled reduction-oxidation increased it further by a factor of *ca.* 3; an overall increase by a factor of *ca.* 6. A revised figure of 1.3×10^{-4} mol/h was found for (36; n=3) in the neutral state and 1.4×10^{-3} mol/h in the reduced state, an increase by a factor of 10. These new figures were due to the extended equilibration times used in the second experiments. Coupled transport of lithium ions proved to be difficult due to possible disproportionation (equ. 1.3) and leaching of the reduced ligand/lithium complex into the aqueous phase.

$$L^{\bullet -} + LM^{\bullet} \longrightarrow L + LM^{-} \qquad \text{(equ. 1.3)}$$

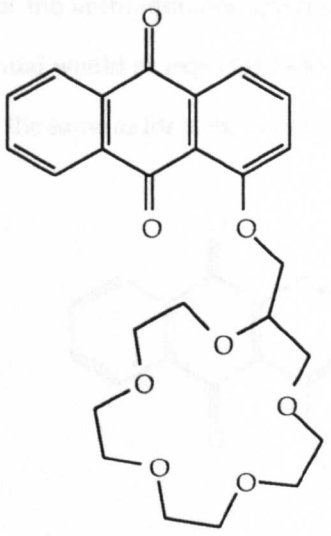

(34)

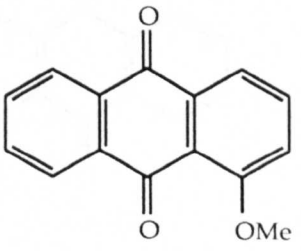

(35)

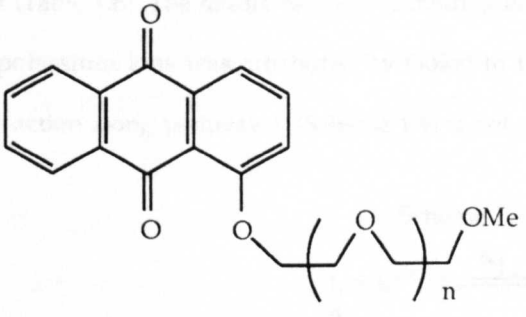

(36)

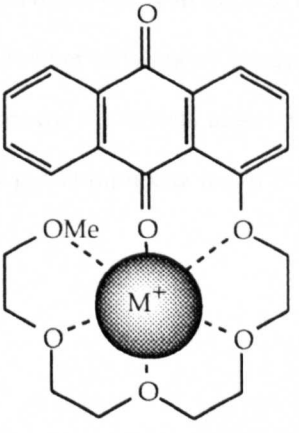

(Fig. 1.1) pseudo-crown complex

Gokel went on to develop this chemistry, producing a series of podands with varying chain lengths, (**36**; n=1,2,3,4), as well as a di-substituted podand (**37**).[39] Compound (**36**; n=1) is optimally suited to lithium ion binding, since it has four oxygens, including the quinone oxygen, which can solvate the ion in a tetrahedral array. Addition of further ethylen-oxy groups did not improve the enhancement as they were surplus to requirement and could not participate in binding. A levelling of the binding enhancements would therefore be expected for n=2, 3 and 4, and this is observed with an average shift of *ca.* 0.3V for all three compounds. In compound (**37**) four oxygens are available for solvation if only

one of the anthraquinone groups participates in binding, thus the same shift in reduction potential would be expected as for the mono-anthraquinone podands. The measured value is 0.3V, the same as for compounds (36).

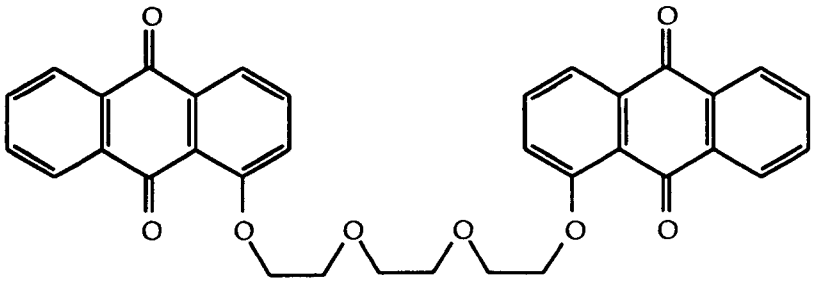

(37)

Sodium binding should be favoured by a larger ring. This is the case for (36; n=2), again a levelling of the binding enhancement is observed as further ethylenoxy groups are added (Table 1.6). The failure to observe binding enhancements for the radical anion of (36) with potassium ions was attributed by Gokel to the lack of pre-complexed metal (LM^+), thus reaction along pathway 1' (Scheme 1.4) is not observed.

Scheme 1.4

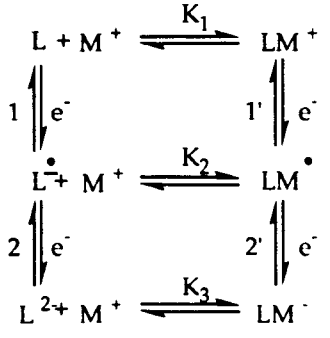

This was attributed to the poor complexing ability of the neutral ligand for potassium ions (potassium perchlorate is only slightly soluble in acetonitrile and requires solvation by the ligand to render it soluble). Reduction of the ligand causes an enhancement of binding for potassium, and this renders the potassium salt soluble; a shifted potential for the second peak can now be seen. This shift is due to the process 2'. If complexation is slow

on the CV timescale, as would be expected for a poor ligand, then reduction of the radical anion to the dianion would compete with complexation. This proved to be the case with the peak potential for the step 2' being completely inhibited at fast scan rates (1000 mVs^{-1}).

Table 1.6: Binding enhancements for one electron reduction of anthraquinone podands

	Li^+		Na^+		K^+	
Ligand	ΔE	BEF	ΔE	BEF	ΔE	BEF
(35)	0.23	7.7×10^3	Ads.[a]	–	None	–
(36; n=1)	0.30	1.2×10^5	0.05	7	None	–
(36; n=2)	0.29	8.0×10^4	0.13	1.6×10^2	None	–
(36; n=3)	0.30	1.2×10^5	0.13	1.6×10^2	None	–
(36; n=4)	0.30	1.2×10^5	0.14	2.3×10^2	None	–
(37)	0.30	1.2×10^5	0.14	2.3×10^2	None	–

a) adsorption

The levelling of the binding enhancement with increasing chain length seen in the podands is caused by the optimum size of the pseudo-cavity formed around the metal ion (Fig 1.1). This suggests that there is an optimum cavity size for binding specific metal ions as is known for unswitched ionophores. Fixing this cavity to that size may lead to increased selectivity for a particular ion. This could be achieved if the end of the poly-ethylene glycol chain were bonded to the anthraquinone, thus forming a crown ether type molecule. This was the next stage of development for electrochemically switchable ionophores, along with bibrachial podands, which serve as both acyclic models for the crowns and "bivalent" ionophores.

Gokel *et al.* prepared the bibrachial ligands **(38)** and **(39)** as developments of the mono-podands discussed above, and the anthraquinone crown ether compound **(40)** was prepared as a model for **(39)**.[40] It is interesting that the crown ether "model" proved to be a better ionophore than **(39)**, especially for sodium ions (Table 1.7); compound **(40)** was observed to leach sodium ions from the calomel reference electrode in both its neutral and

reduced forms. Anthraquinone crowns have been made previously by Vögtle[41] and by Akiyama *et al.* ,[42] yet neither of these two groups report the effect of metal ions on the redox chemistry. Vögtle prepared (**41**), as a chromoionophore, from the disodium or potassium salt of alizarin (1,2-dihydroxyanthraquinone) in xylene. This compound though is clearly not suitable for study as switchable ionophore due to the poor geometric arrangement of the crown and anthraquinone parts. Akiyama's compound (**42**) on the other hand is a good candidate for electrochemical switching. Its synthesis though is poorly developed with yields of only 8.9% (n=1) and 0.6% (n=2). Compound (**42**) was made by a similar route to (**41**), using the sodium salt of 1,8-dihydroxyanthraquinone in refluxing xylene.

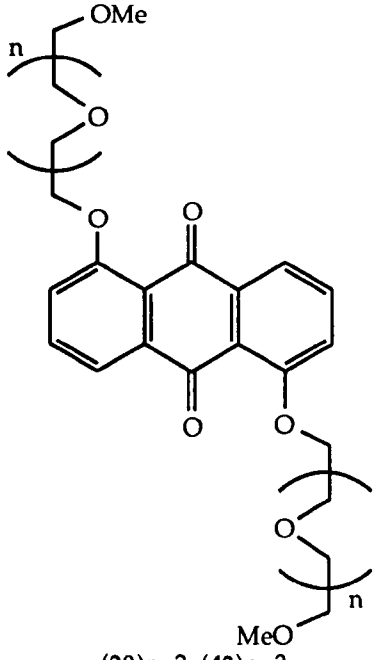

(38)n=2; (43)n=3

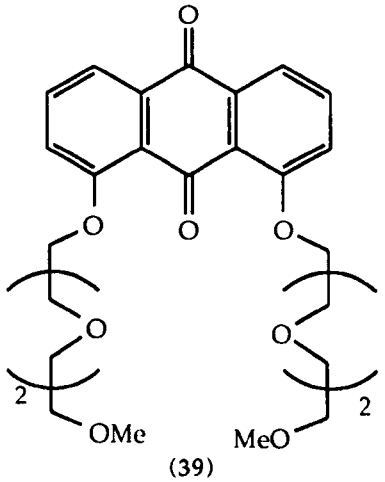

(39)

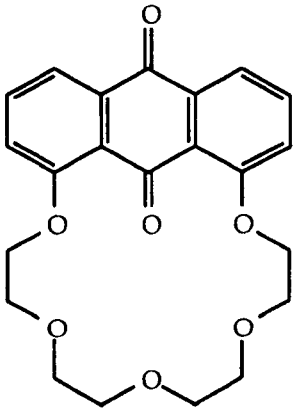

(40)

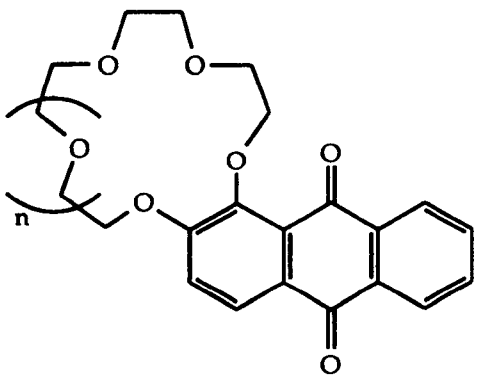

(41)

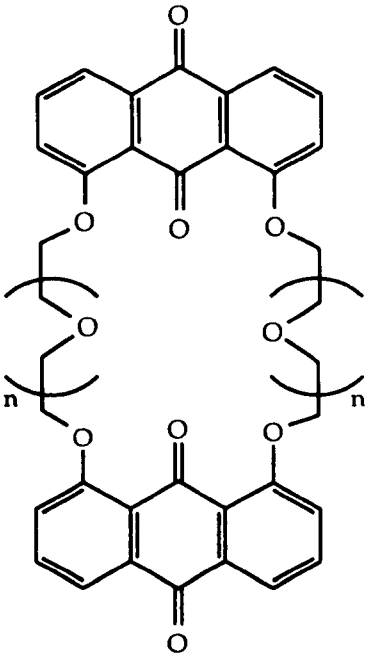

(42)

Table 1.7: Binding enhancements for anthraquinone bis-podands and crown ether type ionophores.

Ligand	M+	ΔE (V)	BEF
(39)	Li	0.39	3.92×10^6
	Na	0.14	232
	K	0.10	49
(38)	Li	0.46	5.97×10^7
	Na	0.21	3.55×10^3
	K	-	-
(40)	Li	0.41	8.53×10^6
	Na	0.22	5.24×10^3
	K	0.14	232

The bibrachial podands are especially interesting compounds since they can bind two metal ions simultaneously. This is easy to visualise for the *anti*-podand (38), which can bind a metal ion on either side of the anthraquinone, using one carbonyl group for each. This is confirmed in the X-ray crystal structure of the NaI complex of neutral (43), [analogous to (38) but with one extra ethylenoxy group in the side arm]. Syn-podand (39)

has also been shown, by ESR spectroscopy, to complex two metal ions simultaneously. This is somewhat more difficult to visualise, and may involve the metal ions in positions above and below the plane of the anthraquinone with the side arms wrapped around. This would provide a tetrahedral arrangement of oxygens to solvate each metal ion, with the carbonyl function as a shared donor. The anthraquinone crown, as noted earlier, is an especially good ionophore for sodium ions. Incorporation of the anthraquinone has rigidified the crown ring, this makes the crown less able to alter its shape in order to accommodate different metal ions, resulting in a higher selectivity towards sodium ions.

Further contributions from Gokel *et al.* dealing with anthraquinone podands and crown ethers have mostly been related to the synthetic aspects. In particular, the observation that polyethylene glycols can act as catalysts in the nucleophilic substitution of mono- and di-haloanthraquinones, compounds which are normally resistant to reaction with nucleophiles.[43,44,45] Amongst these reports though there is mentioned the synthesis of crown ethers (**44**) and (**45**) (analogous to (**40**) but with larger rings).[46]

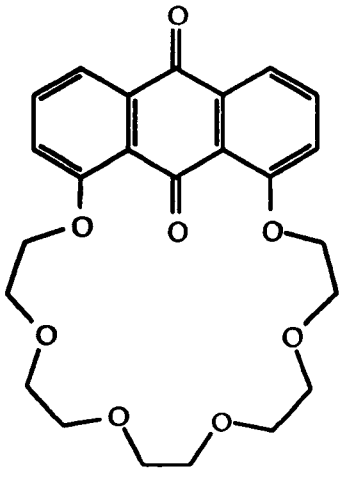

(**44**)

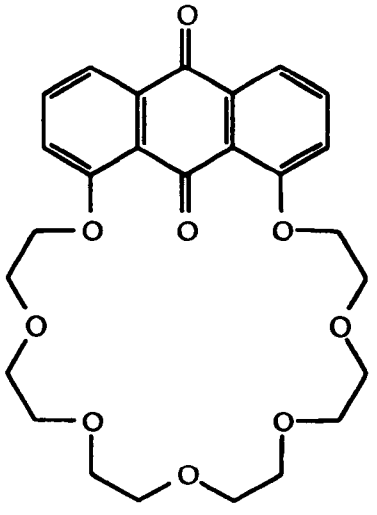

(**45**)

No electrochemical data for these compounds was reported. The electrochemical data for (**44**) and substituted anthraquinone (**46**) have been reported by Bethell and Costa.[34] Expanding the macro-ring has led to an increase in the binding enhancement seen for sodium and a decrease in that seen for lithium. The overall order of enhancements remains the same however, Li > Na > K > Rb ≈ Cs, reflecting the charge to size ratio (Table

1.8). Compound (44) shows the largest binding enhancement yet observed for both sodium and potassium ions. This is probably due to the improved ion fit in the macro-ring, which unlike simple crown ethers is crowded by the presence of the carbonyl group. The ring size must therefore be larger than in the correspondingly selective simple crown ether.

The compound (46) was made from 1,8-dichloro-4,5-dinitroanthraquinone (47), (see experimental section), by treatment with NH_2-$(CH_2CH_2O)_3CH_2CH_2NH_2$ in DMF. This surprisingly led to the replacement of the nitro groups. This compound displays decreased binding enhancements as compared to other anthraquinone crowns which is possibly due to intramolecular hydrogen bonds between the amine hydrogens and the carbonyl group. The compound (47) had been made in an attempt to produce (48). Compound (48) was expected to show much lower reduction potentials than the unsubstituted compound (40) due to the stabilising effect of the nitro groups on the radical anion and dianion. Reaction of (47) with anions derived from polyethylene glycols gives complex mixtures of products, in which both chloro and nitro groups are replaced.[47]

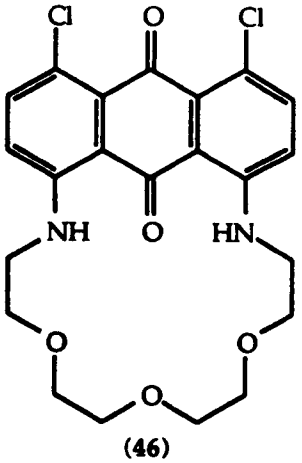

(46)

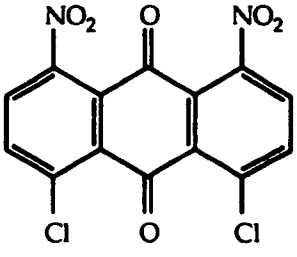

(47)

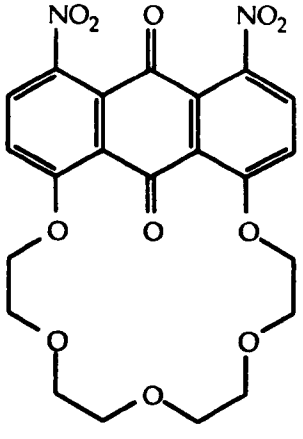

(48)

Table 1.8: Binding enhancements for compounds (40), (44) and (46) with group I metal ions.[34]

Compound	Metal ion	ΔE (V)	BEF
(40)	Li	0.4	5.8×10^6
	Na	0.23	7.8×10^3
	K	0.15	3.4×10^2
	Rb	0.11	7.3×10^1
	Cs	0.11	7.3×10^1
(44)	Li	0.34	5.6×10^5
	Na	0.26	2.5×10^4
	K	0.22	5.3×10^3
	Rb	0.15	3.4×10^2
	Cs	0.14	2.3×10^2
(46)	Na	0.07	1.5×10^1
	K	0.05	7.0×10^0

The final addition to the anthraquinone based ionophores is the anthraquinone cryptand (49). It was made from 1,8-bis(2-bromoethoxy)anthraquinone and 4,13-diaza-18-crown-6 (7) in 52% yield.[48] Its behaviour as an ionophore was studied in both the neutral and electrochemically reduced state (Table1.9).

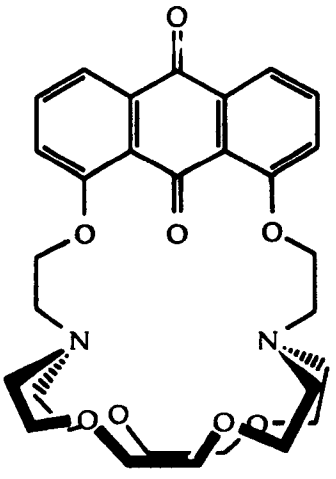

(49)

Table 1.9: Binding constants and enhancements for (49) with group I metal ions compared with [2.2.2] cryptand.

Ligand	Metal Ion	Log K_s	BEF
Cryptand [2.2.2]	Li^+	6.97	-
	Na^+	9.51	-
	K^+	10.5	-
Neutral (49)	Li^+	4.61	-
	Na^+	5.58	-
	K^+	6.22	-
(49) radical anion	Li^+	10.5	7.7×10^5
	Na^+	8.5	8.32×10^2
	K^+	9.1	7.59×10^2

Examination of Table 1.9 reveals that although the binding enhancement for potassium ion is lower than that for both sodium and lithium, the binding constant in the reduced state is close to that of cryptand [2.2.2]. In the neutral state however its binding constant is close to that of [18]-crown-6. This compound represents an efficient switchable ionophore despite the rather low enhancement seen upon reduction. The large enhancement seen for lithium ions though, causes a levelling of the binding, resulting in a loss of selectivity. Its behaviour with lithium ions is particularly unusual. In cyclic voltammetric experiments six waves can be distinguished corresponding to the six steps 1, 2, 1', 2', 1" and 2", as shown in Fig. 1.2. This would indicate the presence of a 1:2 ligand to metal ion complex. Both ESR experiments and CPK models suggest that the two lithium ions are inside the cavity of the cryptand and share the carbonyl donor. This is similar behaviour to that shown by the bibrachial podand (39) which can bind two sodium ions on either side of the carbonyl group. The significance of this lithium binding is dependant on the specific application of the switchable ionophore, since the naturally occurring levels of lithium salts in many circumstances is low. Competitive complexation experiments could clarify this.

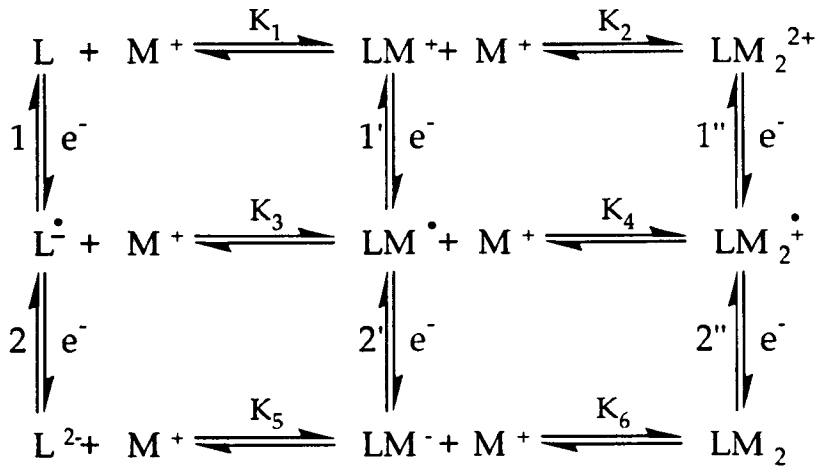

Fig. 1.2

Other Quinone Based ionophores

Quinone based systems have been reported by Sugihara *et al.* [49] Bock and Vögtle,[50] Wolf and Cooper,[51a] Kikuchi,[29] and Tsukube.[52] They are all lariat or fused crown type systems.

Sugihara *et al.* produced quinone compound (**50**; n=1,2) and the hydroquinone derivative (**51**; n=1,2). These were inter-converted chemically and binding constants measured for sodium and potassium ions [(**50**; n=2) Na^+ 1.8, K^+ 2.67: (**51**; n=2) Na^+ 2.39, K^+ 3.18]. They are structurally similar to the compounds produced by Wolf and Cooper, but are unsuitable as electrochemically switched ionophores. Compound (**50**) is susceptible to proton abstraction from the 3 and 5 positions when reduced to the radical anion. Compound (**51**) is fully protonated at the charge bearing oxygens, thus removing they potential for electrochemical enhancement of binding.

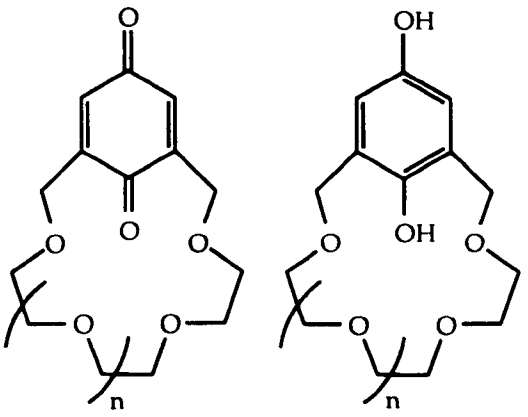

(50) (51)

Bock's compound is a lariat based on 1,4-naphthaquinone attached directly at the nitrogen to monoaza[15]crown-5, (52). It was studied by electron spin resonance spectroscopy; (52) was reduced by various group I metals and the hyperfine coupling constants, a, found. These displayed a dependence on the charge to size ratio, n^+/r_m^{n+}, of the metal used, (Fig. 1.3, no binding enhancements were reported).

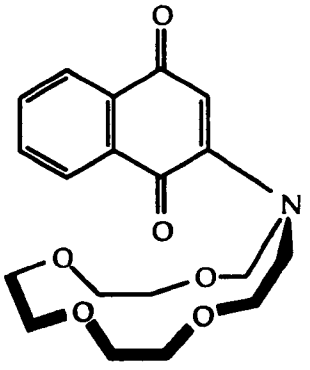

(52)

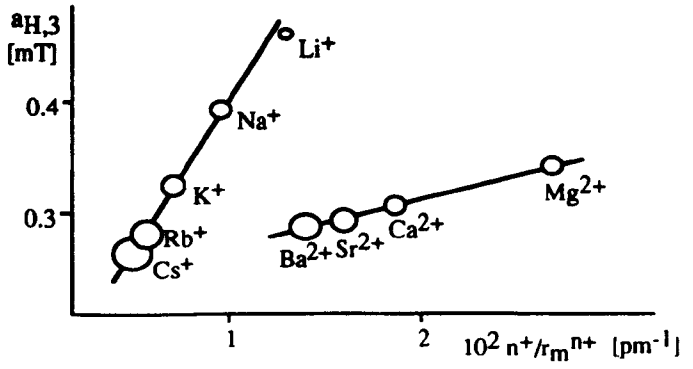

Fig. 1.3, Plot of ESR hyperfine coupling constants for (52) vs. charge density for group I and II metal ions

Wolf and Cooper produced (**53**; n=2), in which a simple quinone has been cyclised with a polyethylene glycol to produce a fused crown type molecule that resembles [18]crown-6. This was compared to an acyclic model (**54**; n=0), and again it was found that a proximal arrangement of the two parts of the molecule is required for a binding enhancement to be observed.[51a] An ion size selectivity was also observed for (**53**; n=2), the order of binding enhancements is $K^+ > Na^+ > Li^+$, (Table 1.10). Kikuchi *et al.* also produced (**53**) and (**54**), but with a variety of chain lengths [(**53**), n=1,2,3,4; (**54**), n=0,1,2].[29] They report essentially the same results as Wolf and Cooper, (Table 1.10), although their experiments were performed using acetonitrile instead of DMF as solvent. They also added metal salts to the ligand solutions in stoichiometric quantities, i.e. 1/2 and 1 equivalents, this is in contrast to the less conventional approach of Wolf and Cooper, who used metal salts in large excess, as they were both guest species and supporting electrolyte. These differences in experimental set-up may explain the different values found for the binding enhancements. Cooper *et al.* followed up their original paper some eight years later.[51b] In this they describe the synthesis and electrochemical behaviour of (**53**; n=1,2,3,4) as well as crystal structures for metal ion complexes of the dimethylhydroquinone derivatives (**55**). The crystal structures show that the quinone moiety can pivot relative to the crown ring in order to accommodate different sized cations.

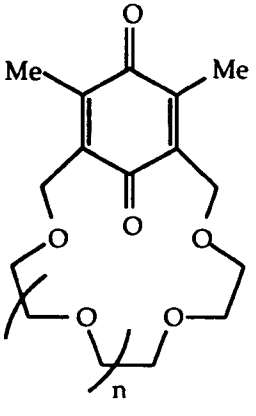

n= 1, 2, 3,4

(**53**)

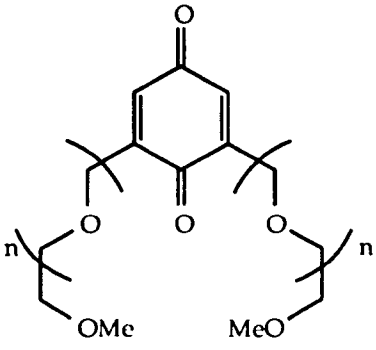

n= 0, 1, 2

(**54**)

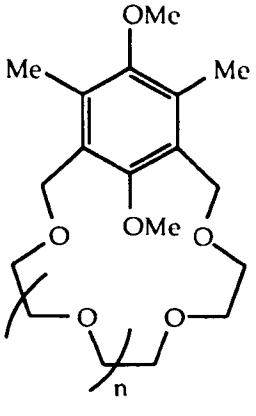

n= 1, 2, 3,4

(**55**)

Table 1.10

Compound	Cation	E_0 (V)	ΔE (mV)	BEF
(53) n=1	Free	-0.615,[a] -0.60[b]	–	–
	Li	-0.549[a]	66[a]	13[a]
	Na	-0.547,[a] -0.46[c]	68,[a] 180[d]	14,[a] 1200[b]
	K	-0.547,[a] -0.53[b]	68,[a] 100[b]	14,[a] 51[b]
	Rb	-0.548[a]	67[a]	13[a]
	Cs	-0.555[a]	60[a]	10[a]
(53) n=2	Free	-0.622,[a] -0.61	–	–
	Li	-0.570[a]	56[a]	7[a]
	Na	-0.496,[a] -0.42	130,[a] 180[b]	156,[a] 1200[b]
	K	-0.466,[a] -0.41	162,[a] 190[b]	542,[a] 1800[b]
	Rb	-0.488[a]	138[a]	213[a]
	Cs	-0.510[a]	117[a]	94[a]
(53) n=3	Free	-0.614,[a] -0.61[b]	–	–
	Li	-0.576[a]	38[a]	4[a]
	Na	-0.546,[a] -0.48[b]	68,[a]130[b]	14,[a] 166[b]
	K	-0.508,[a] -0.50[b]	106,[a] 110[b]	61,[a] 76[b]
	Rb	-0.500[a]	114[a]	84[a]
	Cs	-0.482[a]	132[a]	168[a]
(53) n=4	Free	-0.609,[a] -0.60[b]	–	–
	Li	-0.575[a]	33[a]	3[a]
	Na	-0.542,[a] -0.39[b]	67,[a] 210[b]	13,[a] 3800[b]
	K	-0.536,[a] -0.52[b]	74,[a] 80[b]	17,[a] 23[b]
	Rb	-0.522[a]	87[a]	29[a]
	Cs	-0.518[a]	91[a]	36[a]
(54) n=0	Free	-0.604,[a] -.066[b]	–	–
	Li	-0.574[a]	28[a]	3[a]
	Na	-0.592,[a] -0.65[b]	9,[a] 10[b]	1,[a] 2[b]
	K	-0.598,[a] -066[b]	4,[a] 0[b]	1,[a] 1[b]
	Rb	-0.599[a]	2[a]	1[a]
	Cs	-0.599[a]	2[a]	1[a]
(54) n=1	Free	-0.66[b]	–	–
	Na	-0.60[b]	60[b]	10[b]
	K	-0.65[b]	10[b]	2[b]
(54) n=2	Free	-0.65	–	–
	Na	-0.58	70[b]	15[b]
	K	-0.63	20[b]	2[b]

a) ref. 51b, Cooper *et al.* ; b) ref. 29, Kikuchi *et al.* ; c)Peak reduction potential, ref. 29 ; d) calculated from difference in peak reduction potentials, ref. 29.

The remaining quinone based system is the rather unusual double quinone system of Tsukube *et al.* (**56**; n=1,2,3), It was made by an oxidative coupling at the 5,5' positions of the aromatic rings of the open form. For the (**56**; n=2)/ M^+ interaction BEF's are Li^+, 25000; Na^+, 22; K^+, 3. Again a comparison to an acyclic model, (**57**), was made which displayed only ion pairing effects.

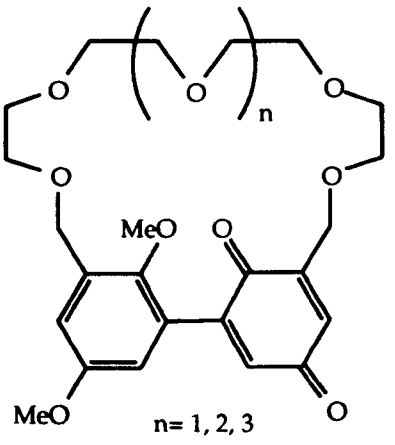

(56)

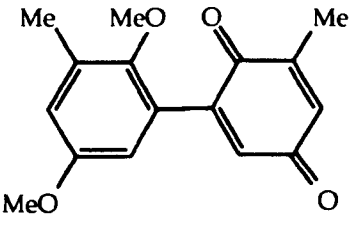

(57)

Chapter 2

Calixarenes

Calix[n]arenes form a class of macrocyclic compounds made up of, n, para-substituted phenols connected by methylene bridges ortho to the phenolic hydroxyl. The trivial name, coined for them by C. D. Gutsche, is derived from the chalice like structure of the tetramer (58; R=tBu), (Latin: calix = chalice, arene indicating the inclusion of aromatic groups).[53,54] This name has been adopted as the generic term for the whole family of oligomers due to the complexity of the official IUPAC name; the basic structure of the tetramer, including the hydroxyls, is termed pentacyclo[19.3.1.1^{3,7}1^{9,13}1^{15,19}]octacosa-1(25),3,5,7(28),9,11,13(27),15,17,19(26),21,23-dodecane-25,26,27,28-tetrol.[55] Figure 2.1 shows various representations of calix[4]arenes. The advantage offered by calixarenes to host-guest chemistry is that they provide an easily obtained base unit on to which more elaborate structures can be grafted.

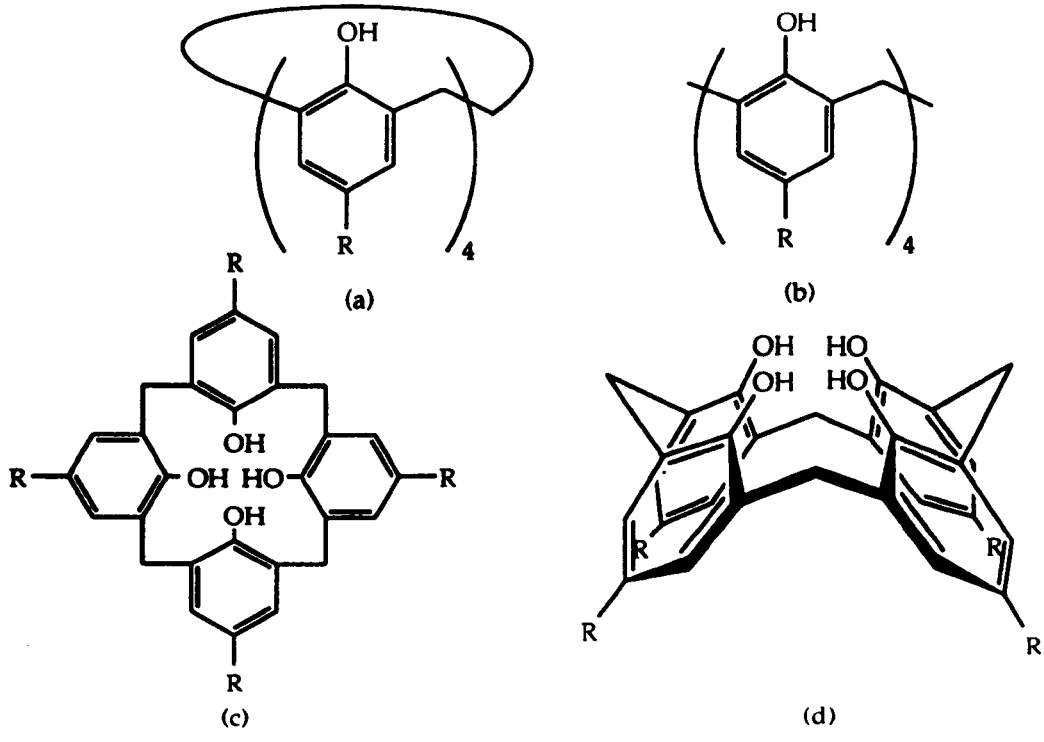

Figure 2.1 Various representations of calix[4]arene (58); [Forms (b) and (c) will be most frequently used to denote the calixarene structure.]

Synthesis of calixarenes

Calixarenes were originally produced by Zinke in 1942.[56,57] He produced a white crystalline material from the base catalysed condensation of *p-tert*-butylphenol and formaldehyde. He found an empirical formula of $C_{11}H_{14}O$ for this material, and attributed a cyclic tetrameric structure to the compound. This was despite finding a molecular weight of 1725 for the acetate, indicating an octameric structure. Zinke however felt this to be highly unlikely and discounted the idea. Further contributions were made by Hayes and Hunter, [58,59] Cornforth *et al.* [60,61] and Buriks *et al.* [62,63,64] all of which seemed to confirm the tetrameric structure assigned by Zinke. It was not until the early seventies though that Gutsche made a thorough investigation of all the reported preparations. He demonstrated that although some of the reported procedures did produce cyclic tetramers, others gave hexamers, octamers or mixtures of any or all of these.[65] Gutsche went on to develop convenient synthetic procedures for the series of calixarenes oligomers (n= 4, 6, 8).[66] Two monographs dealing with all aspects of calixarene chemistry have been written, one by C. D. Gutsche[67] and the other by V. Bohmer.[68]

Conformational isomers of calix[4]arenes

Calix[4]arenes can exist in any of four conformations, termed "cone", "partial cone", "1,3-alternate" and "1,2-alternate". These are depicted in Figure 2.2. In the free phenolic form, rotation of the phenol unit through the annulus of the ring as defined by the methylene bridges allows interconversion of the four forms. Variable temperature NMR experiments have found the rate constant for this rotation is be $150s^{-1}$ at room temperature.[69,70]

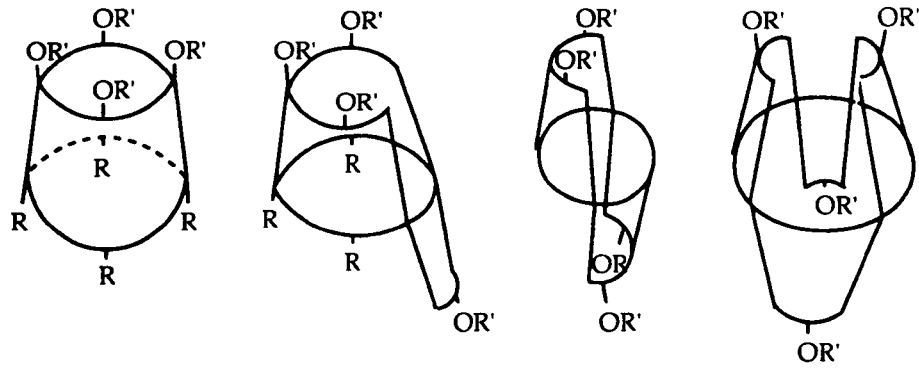

Figure 2.2 Representations of the four conformations of calix[4]arene.

Electronically neutral *para*-substituents have little effect on the rate of inversion as shown by both computational and variable temperature NMR studies.[71,72] Solvent polarity though has a greater effect. In solvents of low polarity intramolecular hydrogen bonds between the phenolic hydroxyl groups tends to hold the calixarene in the "cone" conformation. In more polar solvents, competitive hydrogen bonding with the solvent decreases this intramolecular bonding and leads to more rapid inversion.[71,73] The conformation can be frozen by substitution of the phenolic hydrogens by groups larger than ethyl,[74] or by connecting opposite phenyl groups.[75] In the case of the tetra-methyl ether the freedom of rotation is increased due to loss of the hydrogen bonding between the four hydroxyl units.[76] For several years prediction of which conformation would be found in any given substitution reaction was difficult. This was eventually solved by Shinkai *et al.*[77] who found that the metal ion of the base used in the synthesis has a profound effect on the outcome. Thus in the reaction of ethyl bromoacetate with (**58**; R=*t*-butyl), the "cone" conformation can be selected by use of sodium carbonate in acetone; potassium ions give predominately "cone" with some "partial cone" and caesium ions gives exclusively "partial cone". If the solvent or alkylating agent is changed, the distribution of isomers changes , but shows the same overall selectivity.[78] The "1,2-alternate" and "1,3-alternate" conformers are generally formed as by-products or via more elaborate syntheses.[79,80]

Calixarene based ionophores

Calixarene based ionophores fall into two main types. Those formed by functionalisation of the phenolic hydroxyls at the so called "lower rim" of the calixarene and those formed by functionalisation of the aryl groups at the so called "upper rim" of the calixarene.

"Lower Rim" Functionalisation

Examples of calixarene based ionophores derivatised at the "lower rim" have been provided by many groups, but most notably by McKervey *et al.*, Shinkai *et al.* and Ungaro *et al.*

Compound (59) was produced independently by Chang *et al.*,[81] McKervey *et al.*,[82] and Ungaro *et al.*[83] It has been shown to be a highly efficient ionophore for sodium ions and displays some selectivity for sodium over potassium ions. The corresponding methyl ester (60) as well as the corresponding compounds from (58; R=H), produced by McKervey,[82] is a less effective ionophore but displays a higher sodium selectivity in picrate extraction experiments (Table 2.1). Both compounds were formed in the "cone" conformation.

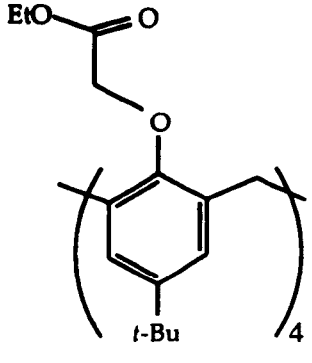

(59)

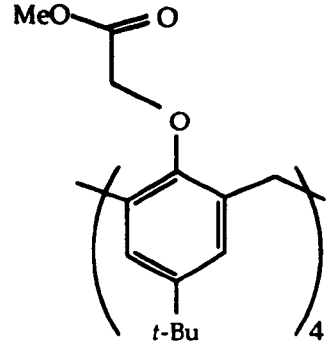

(60)

Table 2.1, Picrate salt extraction by "tetra esters"

Substituent		% Extraction of metal picrate into CH_2Cl_2 at 20°C				
R'	R	Li+	Na+	K+	Rb+	Cs+
Et	H	1.8	60.4	12.9	4.3	10.6
Et	*t*-Bu	15.0	94.6	49.1	23.6	48.9
Me	H	1.1	34.2	4.8	1.9	10.8
Me	*t*-Bu	6.7	85.7	22.3	9.8	25.5

Both IR data[84] and X-ray studies[85] on metal ion complexes have shown that the carbonyl group is the major donor and the ethereal oxygen plays only a minor role. As a consequence a plethora of similar designs have now been made in which the nature of the carbonyl group has been changed. Thus compounds (61) to (78) have been made by various groups in an attempt to alter the selectivity between group I, group II and transition metal ions, intra-group selectivity, and extraction efficiency (Table 2.2).

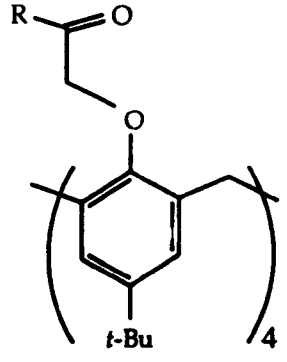

Table 2.2, Ketone, ester and amide derivatives of calix[4]arenes

Compound	R	Compound	R
(61)	OBu_n[a]	(70)	OH[a]
(62)	OBu_t[a]	(71)	Me[b]
(63)	OCH_2Ph[a]	(72)	1-Adamantyl[c]
(64)	OPh[a]	(73)	Bu_t[c]
(65)	OCH_2COPh[a]	(74)	Ph[c]
(66)	$O(CH_2)_2OMe$[a]	(75)	NEt_2[b]
(67)	$O(CH_2)_2SMe$[a]	(76)	NC_4H_8[b]
(68)	OCH_2CF_3[a]	(77)	NHOH[d]
(69)	$OCH_2C{\equiv}CH$[a]	(78)	$NH(CH_2)_2NMe_2$[d]

a) Ref 86; b) Ref 87; c) Ref 84; d) Ref 88

A second group of calixarene-based ionophores are the bridged calixarenes. Compound (79), produced by Ungaro in collaboration with Reinhoudt, has opposite phenolic oxygens linked by a polyethylene glycol chain, the remaining hydroxyl groups being substituted with either methyl or ethyl groups.[89,90] Although conformationally mobile in the free state these compounds adopt the "partial-cone" conformation upon complexation of metal ions. Compound (79) was reported to show an exceptionally high Na^+/K^+ selectivity (up to 1000 to 1). A second bridged calixarene is the calixspherand (80).[90] This compound behaves in a similar way to other spherands, i.e. it forms extremely strong NaBr complexes. Decomplexation can only be carried out by heating in a 1:4 methanol water mixture to 120°C in a sealed tube.

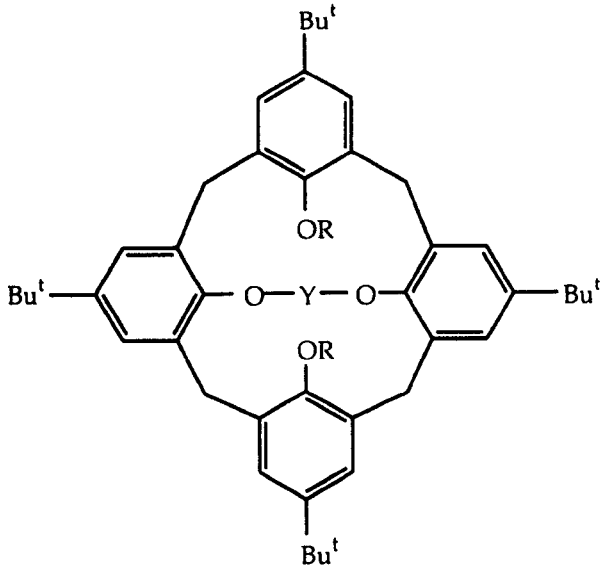

(79); R= Me, Et, Y= $CH_2(CH_2OCH_2)_3CH_2$

(80); R=Me,

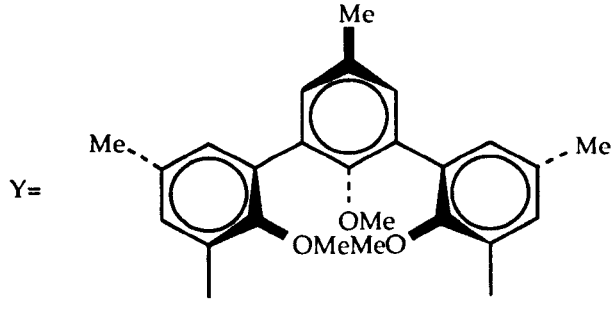

Examples of "lower rim" ionophores based on the calix[5] and calix[6]arenes are less common. This is in part due to the increased flexibility of these systems, making conformational freezing more difficult. Also synthetic procedures for these systems are less well developed. Examples of calix[5]arene based ionophores are the bridged calix[5]arenes (**81**; n=3,4,5), (**84**) and derivatives (**82**; n= 3,4) and (**83**). Metal extraction data for these compounds were not reported.[91]

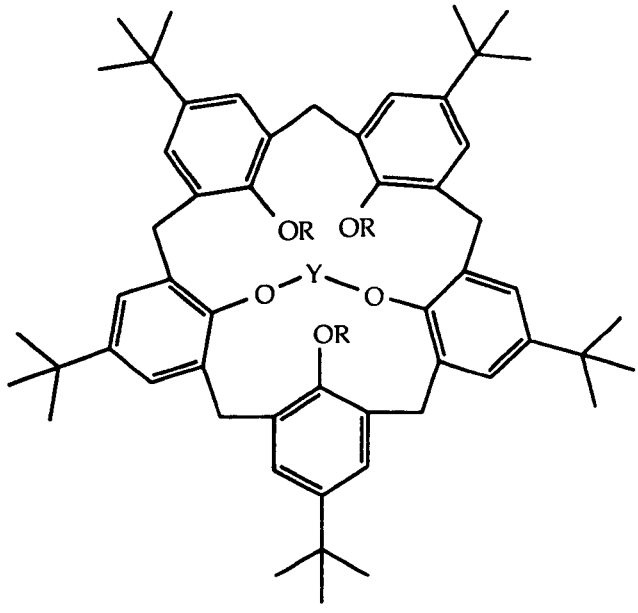

(**81**; n=3,4,5); R= H, Y= $CH_2(CH_2OCH_2)_nCH_2$

(**82**; n=3,4,); R= Me, Y= $CH_2(CH_2OCH_2)_nCH_2$

(**83**; n=3); R= CH_2CO_2Et, Y= $CH_2(CH_2OCH_2)_nCH_2$

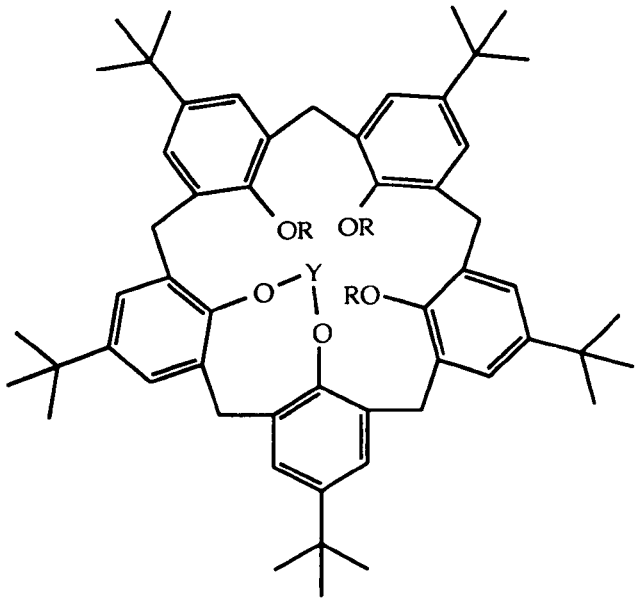

(84) R= H, Y= $CH_2(CH_2OCH_2)_4CH_2$

Shinkai has provided other examples of calix[6]arene based ionophores, namely compounds (85) [92,93] and (86) [94,95] both of which are selective for the UO_2^{2+} ion.

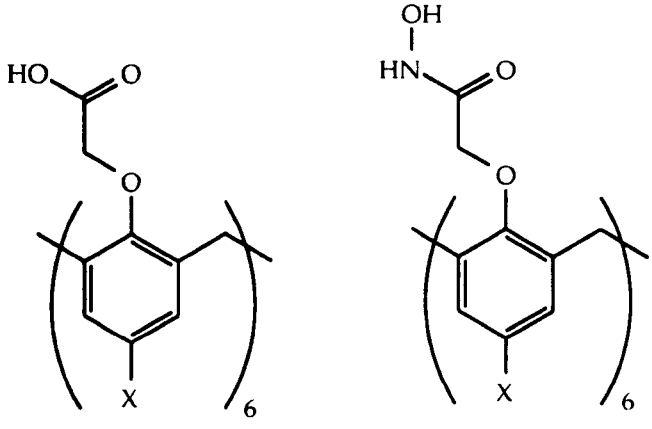

(85) (86)

X= H, ^tBu, SO_3Na

"Lower Rim" Chromoionophores

Modifications have been carried out on many types of calixarene based ionophores to render them capable of responding to the presence of a guest. This response could be a visible colour change or a change in the fluorescence spectrum.

Sutherland *et al.* produced compound (87) as a development of the calixcrown compound (79).[96] Introduction of an azo dye moiety into the calixarene made it capable of responding to the presence of group I metal ions by changing colour due to deprotonation of the phenolic residue. It retained the selectivity of the parent compound (79).

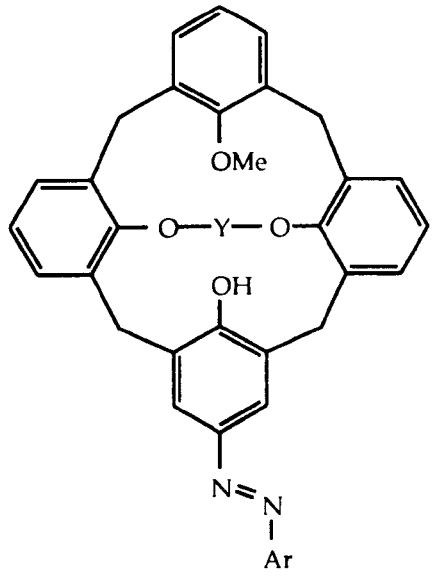

(87)

Y= $CH_2(CH_2OCH_2)_3CH_2$

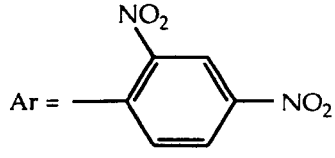

A similar design strategy was used by other groups to produce compounds (88),[97] (89),[98] (90)[99] and (91).[100] Compounds (88), (89), and (90) are all based on the tetra-ester compound (59). All the compounds display selectivity towards lithium ions.

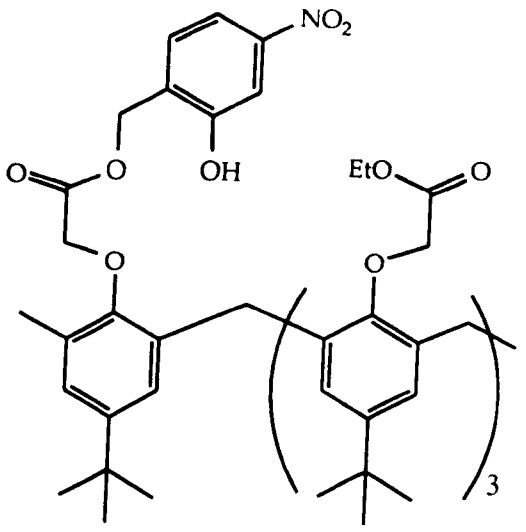

(88)

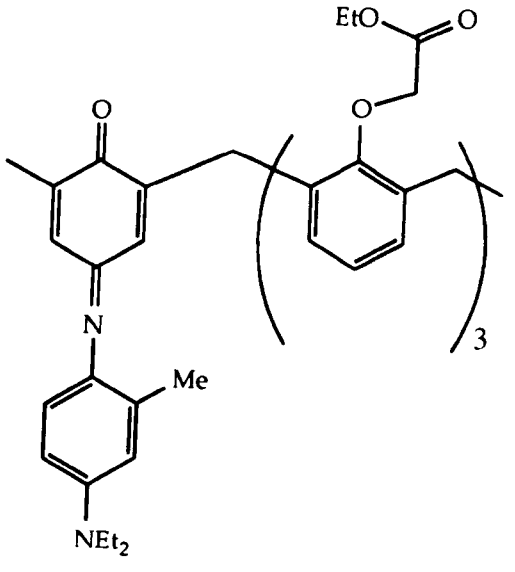

(89)

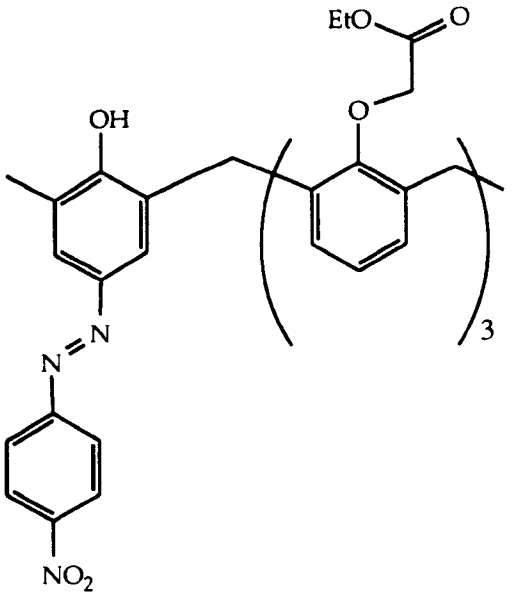

(90)

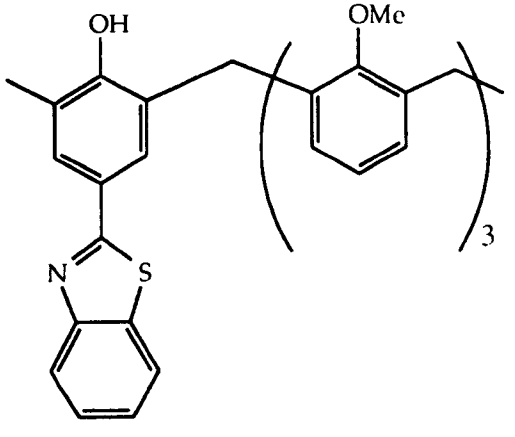

(91)

The second type of chromoionophores are those that use a change in fluorescence spectrum to indicate the presence of a guest.

Compounds (92)[101] and (93)[102], produced by Jin *et al.* and Pérez-Jiménez *et al.* respectively, show changes in fluorescence spectra upon complexation of sodium ions. In both cases a decrease in intensity is observed upon complexation. This is thought to be due to the

quenching of the fluorescence brought about by the proximity of the fluorescent moieties. A somewhat better design is compound (94),[103] which shows an increase in the intensity of the fluorescence spectrum upon complexation. In the free state the ligating side arms are free to rotate; this allows the nitro-aromatic moiety to interact with the pyrene moiety, quenching its fluorescence. Upon complexation the conformation of the side arms is locked, thereby separating the pyrene and nitro-aromatic moieties to a distance at which they cannot interact. All three of these compounds are based on the tetra ester compound (59) and would therefore be expected to show a similar selectivity.

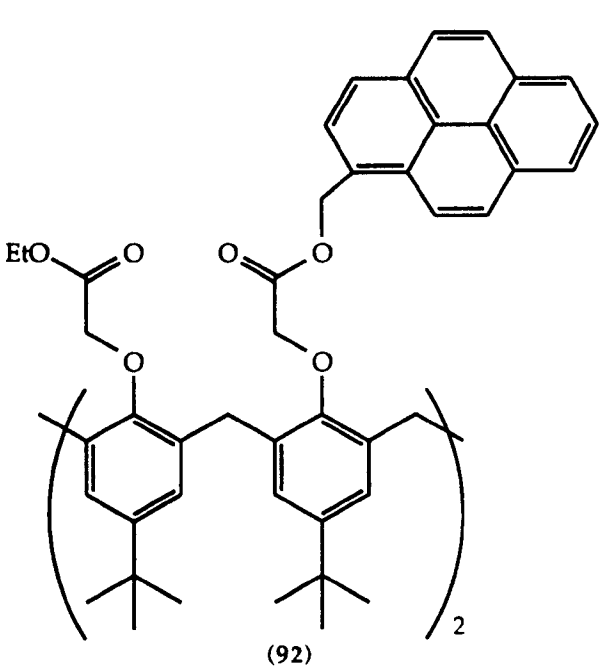

(92)

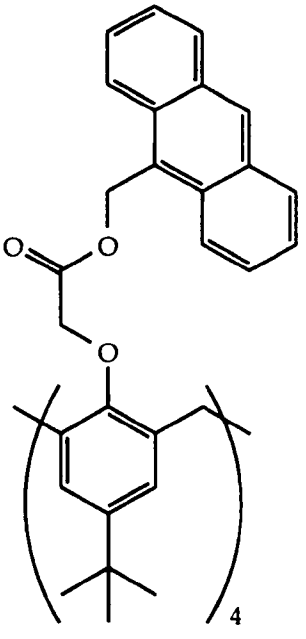

(93)

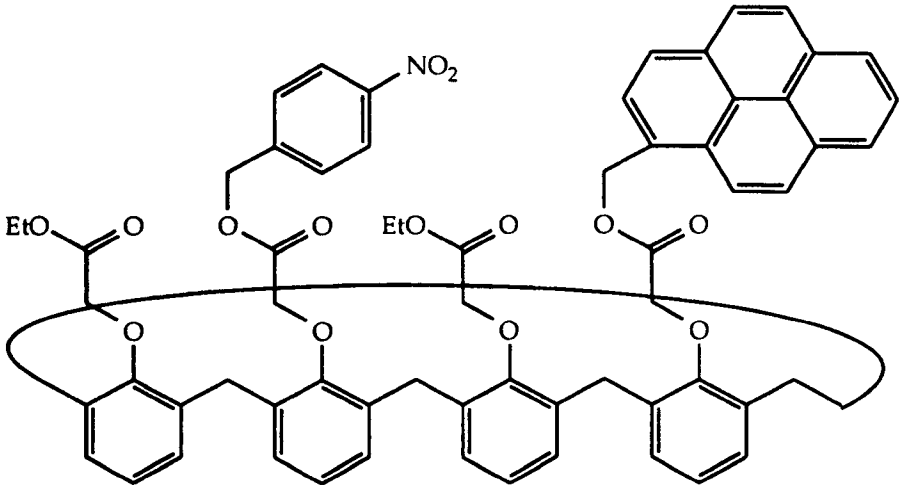

(94)

"Upper rim" ionophores

Functionalisation of the aromatic end or "upper rim" of the calixarene has also been carried out to form ionophores. The "upper rim" of the calixarene is larger than the "lower rim" and thus the cavities are larger. This gives them selectivity towards larger guests.

Two such examples of "upper rim" ionophores are the sulphonate (**95**)[104,105,106] and the diphenylphosphino compound (**96**).[107] Compound (**95**; n=4) has been used by Shinkai as an analytical reagent for cerium (III) ions.[104] Although it does not display any overall selectivity between lanthanide metal ions, it only gives a colouration with cerium ions. Compound (**95**; n=4, 6, 8) has also been studied as a host molecule for larger cations such as trimethylanilinium(chloride) and 1-adamantyltrimethylammonium(chloride).[105,106] Compound (**96**) was studied as an ionophore for both alkali and transition metal cations. It displayed some selectivity towards mercury, copper, cadmium and zinc ions.[107]

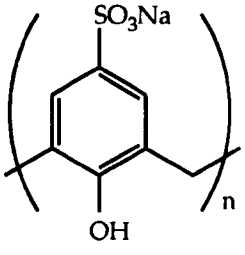

(**95**)

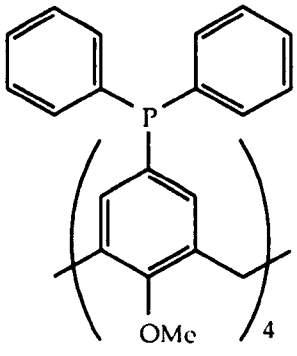

(**96**)

Calix[4]arene based switchable ionophores

This chapter has shown that calixarenes have proved to be a rich source of ionophores. To the best of our knowledge there are no examples of calixarene-based ionophores that incorporate an electrochemical switching group, such as those described in Chapter 1. With a view to expanding the range of switchable ionophores and improving their selectivity, the present investigation has been concerned with producing ionophores based on calix[4]arenes. Two basic designs for switchable ionophores were proposed; the first a lariat-like system; the second a "bridged" system. Incorporation of an anthraquinone or nitroaromatic moiety into either the side arm or the bridging moiety would provide the switching mechanism.

Chapter 3

Design and Synthesis of Electrochemically Switchable, Calixarene based, Ionophores

Ionophore Design

In Chapter 1 the advantages offered by switchable ionophores was demonstrated. Of the various mechanisms for switching, electrochemical switching is considered to be superior for the reasons given. The preceding chapter gave examples of how calix[n]arenes have been used as the building blocks for creating elaborate ionophores. It would seem appropriate therefore to combine these two areas of research in an attempt to produce a calixarene based ionophore which incorporated an electrochemical switch.

The electrochemically switched ionophores produced to date suffer from a lack of selectivity upon reduction. Compound (**49**) does display some selectivity between group I metal ions, but it can accommodate two lithium ions within its cavity.[48] This causes problems when the compound is reduced. Production of calixarene based ionophores (which are known to be highly selective towards sodium or potassium ions)[82,84,85] incorporating a switching moiety may redress this problem. With this aim in mind several designs were made and the syntheses of two of these were undertaken. Design (**A**) is based on compound (**59**).

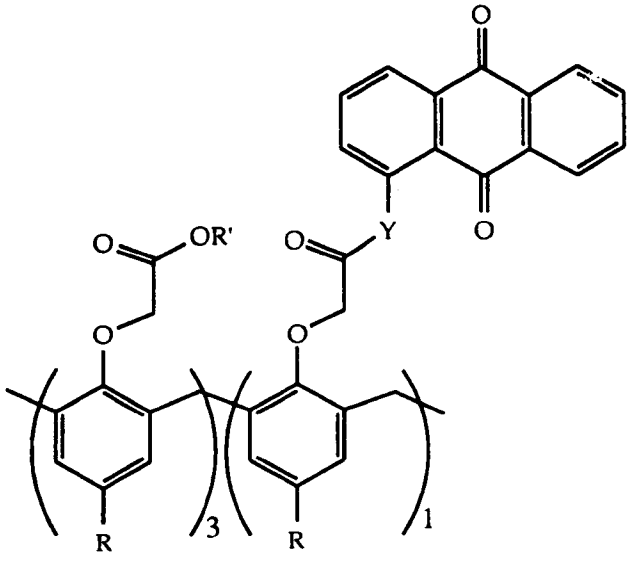

(**A**)

It was hoped that replacement of one of the ester moieties with an electrochemically switchable group, such as an anthraquinone or nitro-aromatic, would render the compound capable of acting as an electrochemically switchable ionophore. It was envisaged that the synthesis of this compound would prove straightforward. The linkage Y will depend on the synthetic route and could be O, NH or NMe, where R is H or ^{t}Bu, R' is Me or Et.

Design (**B**) is essentially new, but bears similarities to compounds (**49**), (**79**) and (**80**). Again the nature of the linkage would be chosen for synthetic ease. This compound would fill the gap left by Gokel *et al.* in the anthraquinone based ionophores described earlier. The cavity should be ideally suited to potassium ions and yet be too small to accommodate two lithium ions, the major drawback of compound (**49**). Another advantage offered by this design is that the group R' can be varied in an attempt to alter selectivity. Thus R' could be a simple ether, an ester, an amide or a thioester. Design (**C**) is similar to both (**B**) and (**53**), but the cavity is larger than that in design (**B**) due to the increased flexibility of the linkages to the capping group. The linkage X can be varied as can the substituent W. Variation of the substituent W can be used as a method for controlling the reduction potential. Electron withdrawing groups such as nitro, chloro or cyano can greatly reduce the potential at which the quinone is reduced. This increases the stability and lowers the energy costs for reduction. The effect of introducing such electron withdrawing groups can be seen for compounds such as chloranil (**97**), tetracyanoquinodimethane, TCNQ (**98**) and dicyanodichloroquinone, DDQ (**99**), all of which have low reduction potentials. The reduction potential for the step $O \rightarrow R^{\bullet -}$, in acetonitrile with tetrabutylammonium perchlorate as supporting electrolyte, are: chloranil...-0·2V; TCNQ...0·09V; DDQ...0.23V versus Ag/Ag^{+}.[108] This compares with a value of ≈-0.9V for a typical oxy-anthraquinone derivative.[109]

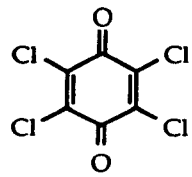

(**97**)

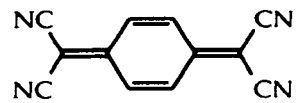

(**98**)

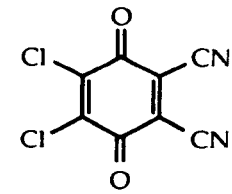

(**99**)

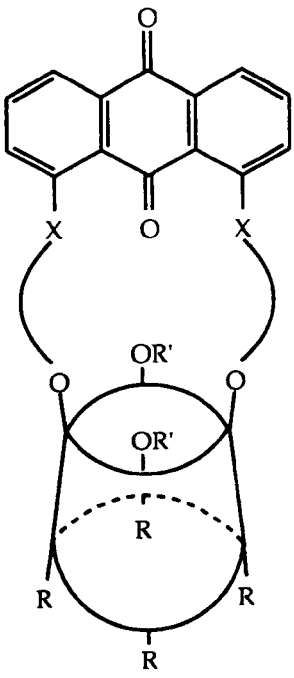

(B)

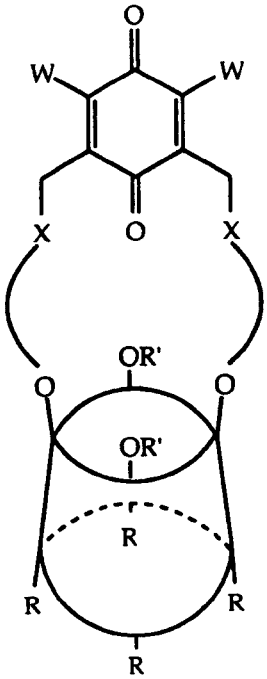

(C)

Synthesis of Type A Compounds

It was foreseen that the synthesis of compounds of type A would be straightforward. According to Scheme 3.1; tetra-alkylation of *p-tert*-butylcalix[4]arene to give the tetra-ester (**59**) is known to proceed in good yield and gives the "cone" conformation exclusively .[84] Subsequent hydrolysis of one ester group would give the mono-acid-tri-ester (**100**). Conversion of this into the corresponding acid chloride and reaction with either an alcohol or an amine would give the target molecule (**101**). For electrochemical switching purposes the switching moiety is generally an aromatic compound such as anthraquinone or a nitroaromatic. Phenolic derivatives must be ruled out as the switching moieties due to the ease with which phenolic esters can be hydrolysed.

Thus in Scheme 3.1 step (i) was carried out by treating *p-tert*-butylcalix[4]arene (**58**) with ethylbromoacetate and potassium carbonate in acetone. This gave the product (**59**) in 70% yield.

Subsequent hydrolysis of a single ester group, step (ii), proved to be somewhat more difficult. Initial attempts where made using sodium hydroxide in ethanol/water. Using exactly one equivalent of base per equivalent of tetra-ester, one ester group could be hydrolysed, as demonstrated by the product's $[M+Na]^+$ signal at m/z 988 in FAB MS. The mono-acid produced could not, however be separated from the tetra-ester (**59**), by either recrystallisation or chromatography. Chromatography led to almost complete loss of both the tetra-ester and the mono-acid. This was believed to be due to complexation of sodium ions, present as impurities on the adsorbent. Further problems were caused by complexation of sodium ions by unreacted tetra-ester, preventing further reaction.[110] To solve this problem the hydroxide counter ion was changed from sodium to tetraethylammonium. This ion is too large to be accommodated in the cavity of the tetra-ester and is not complexed. This approach proved to be successful in that mono hydrolysis could be achieved, but the problems of incomplete reaction and purification remained. The reason for incomplete hydrolysis of the ester function, even with the non-complexing tetraethylammonium ion, is that under these conditions the hydrolysis is subject to second order kinetics and is therefore

slow towards the end of the reaction. The reaction is usually driven to completion by the addition of excess base, thus giving pseudo-first order reaction conditions. With this particular reaction excess base would lead to hydrolysis of multiple ester groups.

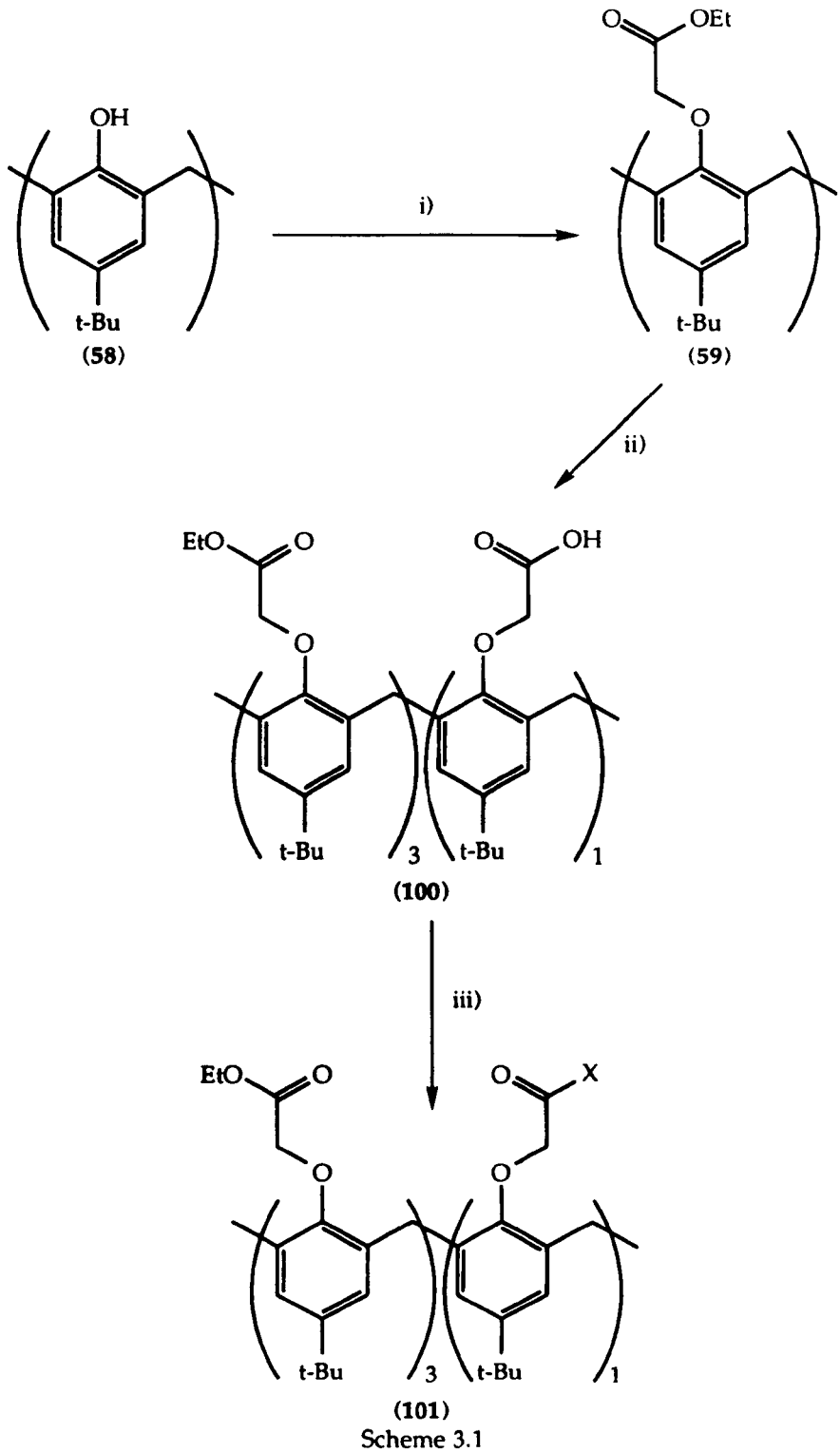

Scheme 3.1

An alternative synthesis was devised for the mono-acid to overcome these problems, and this is shown in Scheme 3.2. It involves total hydrolysis of the tetra ester (**59**) and then tri-methylation of the tetra-acid (**102**) with diazomethane. The tetra-acid was produced in 82% yield by hydrolysis of the tetra-ester with tetraethylammonium hydroxide, the analyses of this compound agreed with those in the literature[111,112] in all aspects except for the NMR spectrum which was very unusual. The compound gave very broad resonances at δ 6·9, 4·6 and 1·2 and a sharp doublet at 3·3ppm; a suitable interpretation for this pattern could not be found. The tetra-acid was also produced independently by acid hydrolysis of the tetra-*tert*-butyl ester (**62**) this gave an identical NMR spectrum. Given that the analyses for (**102**) were correct in all aspects, conversion to the trimethyl ether was attempted using diazomethane. This failed to give the trimethyl-ester mono-acid (**103**), but instead gave a mixture of mono-, di-, tri-, tetra- esters along with unreacted tetra-acid (as shown by FAB MS). The mixture of esters could not be separated.

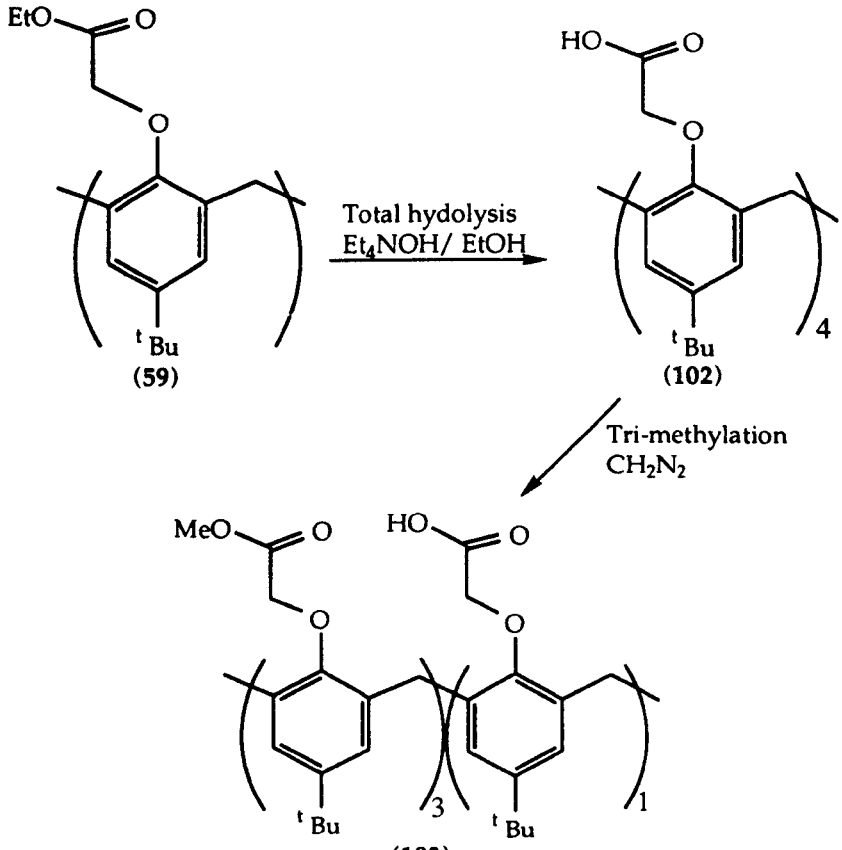

Scheme 3.2

At this point a report appeared in the literature from M.A. McKervey *et al.* which claimed that mono-hydrolysis of the tetra-ester could be achieved by treating the ester with a catalytic amount of trifluoroacetic acid, in chloroform.[112] This reaction was attempted and it gave the desired product, with multiple hydrolyses not being a problem. In our hands however the reaction proved to be somewhat capricious, with both the timescale and the yield of the reaction being different on each run. Part of the problem stems from McKervey's vagueness about the exact reaction conditions in the original publication. The reaction is somewhat unusual, hydrolysis is believed to proceed via a complexed hydroxonium ion. It therefore relies on adventitious water molecules in the solvent. A more detailed study was carried out therefore into the effect of the water, ethanol and trifluoroacetic concentrations upon the yield of mono-acid. It was found that the optimum conditions were 3g of tetra-ester in 300ml $CHCl_3$, 0.1ml TFA, 5% ethanol v/v and 5% water v/v. The timescale for complete reaction remained indeterminate, but the reaction could be followed quite conveniently by NMR. The reaction was generally taken to *ca* 95% conversion and the mono-acid used in the next stage without further purification.

Step (iii) of Scheme 3.1 was carried out by initial treatment of the mono-acid with an excess of thionyl chloride to produce the corresponding acid chloride (**101**; X= Cl). The excess thionyl chloride was removed and the yellow oily product taken up in dry toluene and added to a toluene solution of the appropriate amine, containing triethylamine. This furnished the amide in *ca* 50% yield, from the tetra-ester, after chromatography. Thus two amides were produced from the amines, 1-aminoanthraquinone (**104**) and 2-nitroaniline (**105**) to give (**106**) and (**107**) respectively. Attempts to make an N-methyl derivative, (**108**), by the same method, using 1-methylaminoanthraquinone (**109**) failed. This was probably due to both 1-methylaminoanthraquinone being a secondary amine and the strong hydrogen bond between the amino hydrogen and the quinone oxygen. This hydrogen bond is also present in other 1-substituted anthraquinones and is sufficiently strong to completely suppress the OH stretch in the infra-red spectrum of 1-hydroxyanthraquinone (**110**)

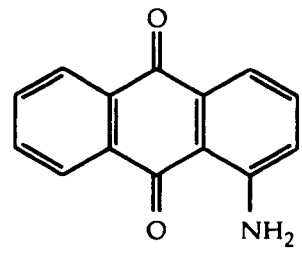

(104)

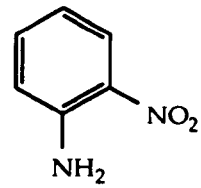

(105)

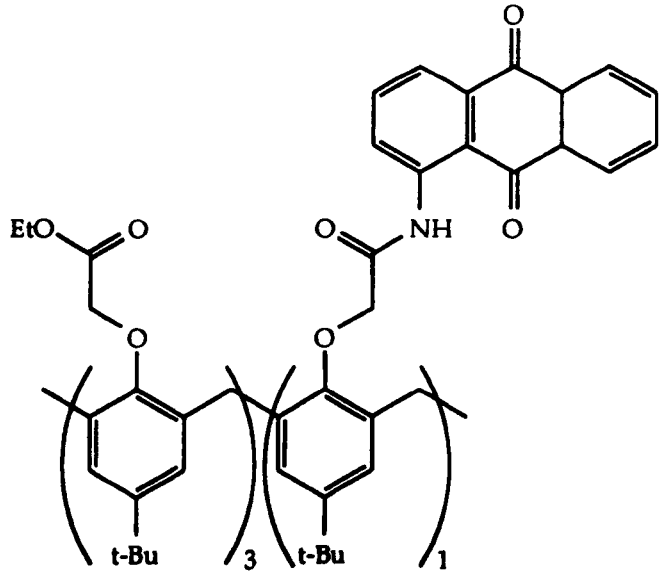

(106)

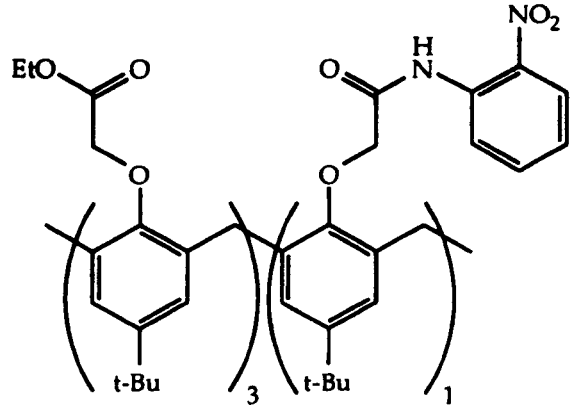

(107)

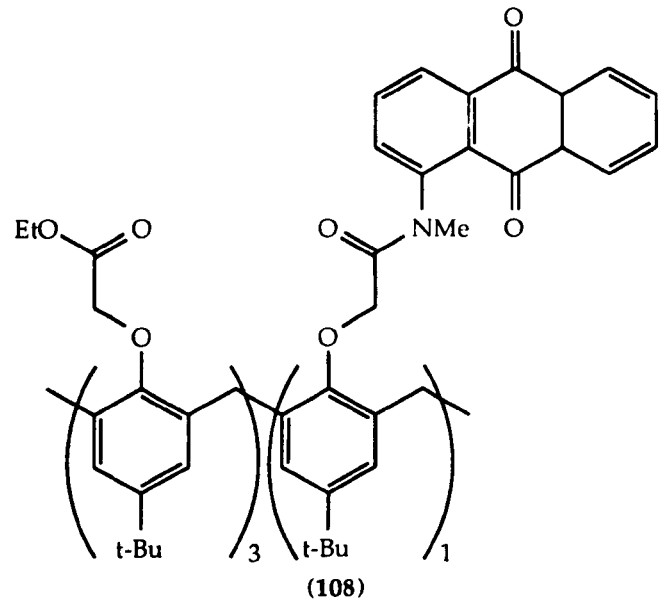

(108)

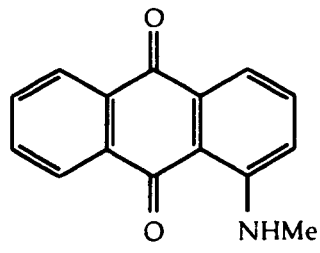

(109)

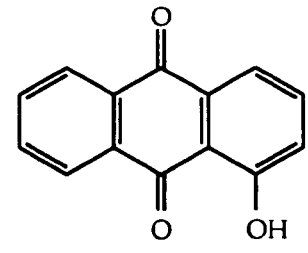

(110)

Synthesis of Compounds of Type B & C

Synthesis of bridged compounds of types B and C can be envisaged to proceed via a common intermediate. Adding suitable side arms to the calix[4]arene would give a compound onto which a variety of bridging units could be added. This would give the convergent synthesis. The alternative synthesis of bridged calixarenes is to make a complete bridging unit and add this to the calixarene. The disadvantage with this approach is that if a different bridge is desired a separate bridging unit must be made.

Thus compound (113) was designed as the initial target molecule. This compound has two acid functions on the arms which could be used to make amide or ester linkages, the

remaining hydroxyls on the calixarene being substituted with methyl groups. The methyl groups have two functions, the ionophore will be pH independent and intramolecular proton transfer to the radical anion would not be possible. Thus synthesis of compound (113) was undertaken as in Scheme 3.3.

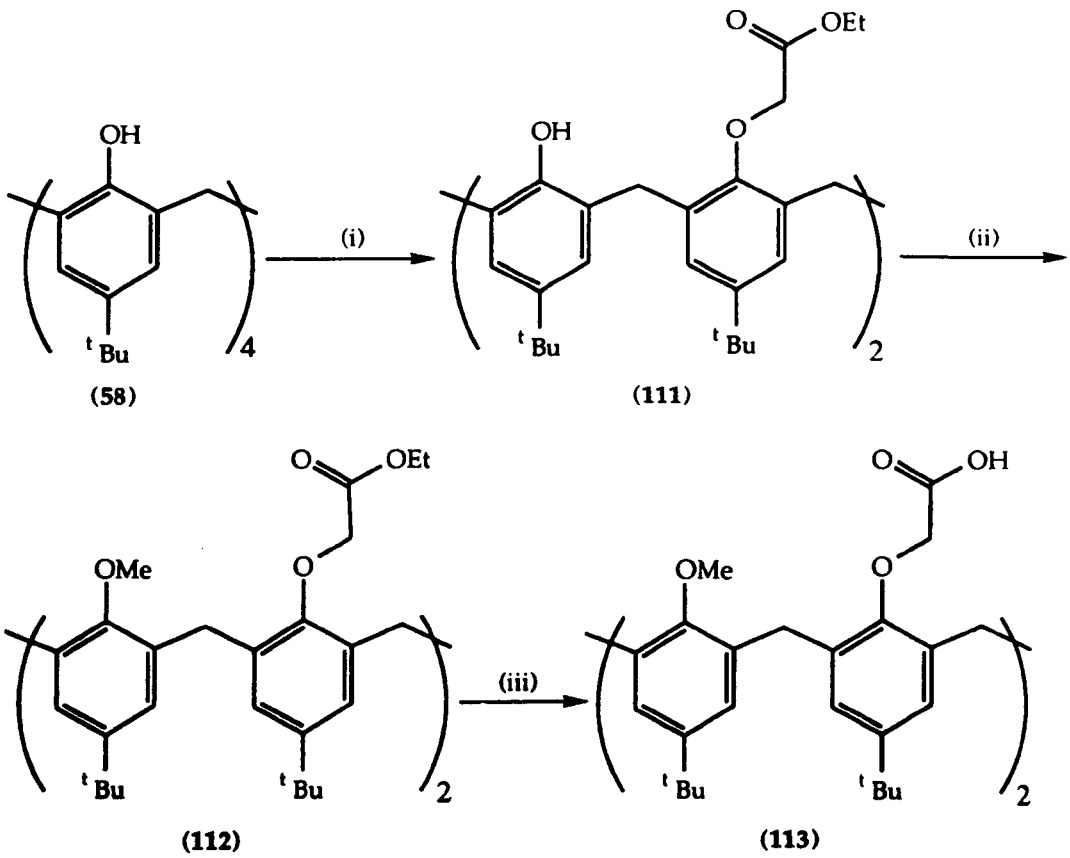

Scheme 3.3

Dialkylation of p-t-butylcalix[4]arene, step (i), was carried out according to literature methods, using between two and three equivalents of both base and alkylating agent.[114,115,116] This reaction always gives the 1,3-disubstituted product as opposed to a random substitution of the phenols, even in the presence of a slight excess of alkylating agent. This somewhat unusual result can be explained by considering the unique arrangement of the hydroxyl groups in calix[4]arenes. The cyclic arrangement of the hydroxyls leads to a high degree of hydrogen bonding, [see Fig 3.1(a)]. This decreases the pKa for the first deprotonation,[117] subsequent alkylation of the anion leaves three

hydroxyls. The central hydroxyl, (*), is now bonded to two others lowering its pKa, [Fig 3.1(b)]. Alkylation of this phenolate anion leaves only two remaining phenolic hydroxyls. These hydroxyls bond across the calixarene; this both raises the pKa and causes the structure to distort. In this distorted structure the two substituted phenolic units are almost parallel and the free phenolic units are almost coplanar and orthogonal to the substituted aryl units, [Fig. 3.1(c)]. Reaction at the remaining hydroxyl sites is now greatly reduced due to these steric and chemical effects.[118,119]

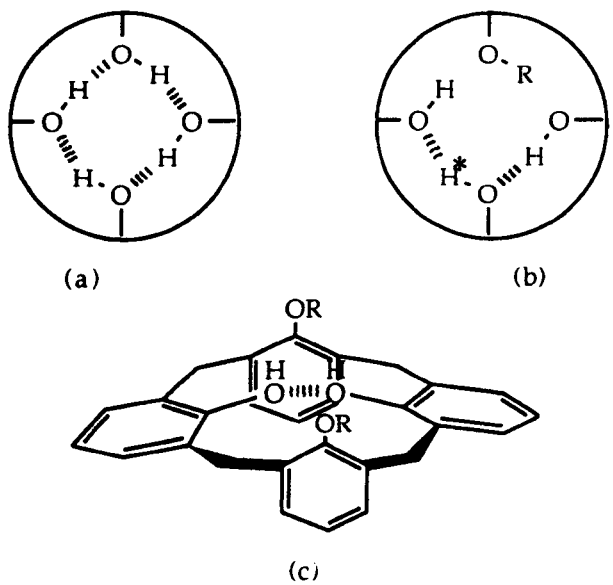

Fig 3.1 Hydrogen bonding effects in calix[4]arenes, the dashed lines represent the hydrogen bonds

Thus compound (111) was produced by treating (58) with ethyl bromoacetate and potassium carbonate in acetone.[114] This gave the dialkyated product in 68% yield. Further substitution of the hydroxyls to give (112) required a stronger base. Sodium hydride was chosen since the presence of the ester functions precludes the use of either oxygen or nitrogen derived bases. Many attempts were made to carry out this reaction using different solvents, reaction times, stoichiometries and alkylating agents. All failed to give the desired product. The problem with this approach appeared to be deprotonation of the activated methylene group in the side arm $ArO\underline{CH_2}CO_2Et$. Mass spectrometry showed the presence of

mono, di, tri, tetra, penta, and hexa methylated compounds as well as some unreacted ester (**111**). The position of these substitutions is unknown, however since separation of the different compounds could not be achieved. The failure of this synthetic route led to the simple revision of reversing the order of the alkylations, with methylation preceding reaction with ethyl bromoacetate. (Scheme 3.4)

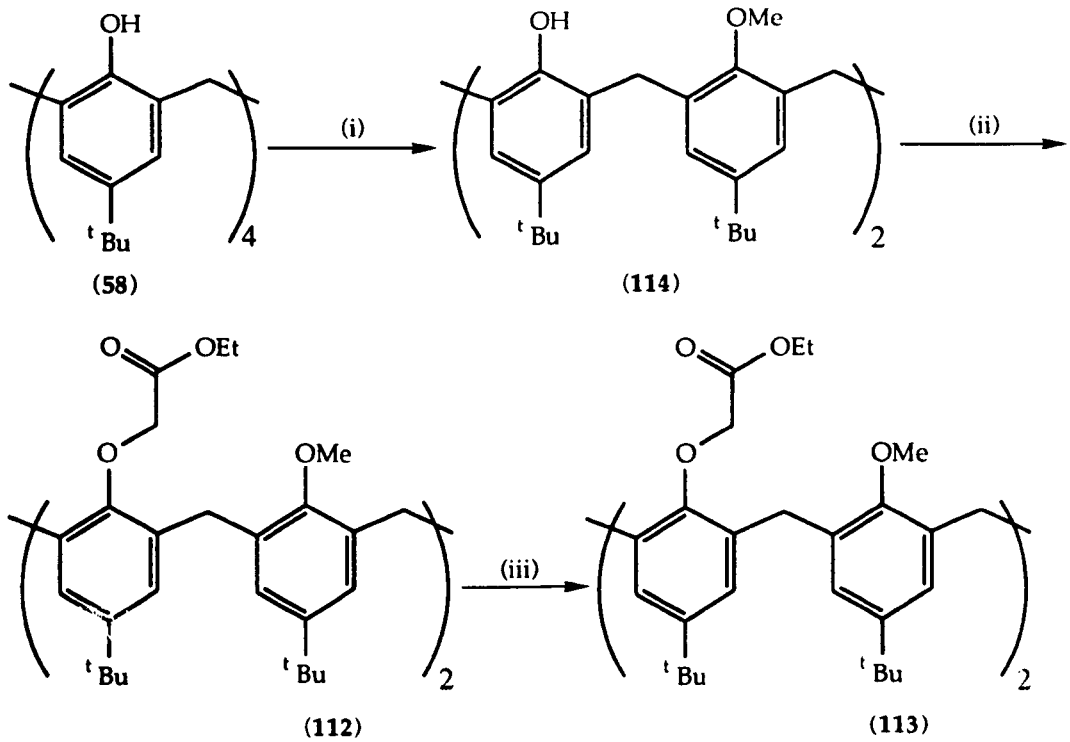

Scheme 3.4

Thus step (i) can be achieved by treatment of (**58**) with MeI and K_2CO_3 in acetone, as for (**111**), or by using diazomethane[76] to give (**114**) in 80% yield. Further alkylation of this compound though proved to be difficult. Deprotonation takes place, as indicated by the consumption of sodium hydride, but no alkylation takes place. This is probably due to the extreme distortion from the "cone" conformation found in compound (**114**) preventing the hydroxyl anions from reacting with the substrate.[76] This second failure led to yet a further revision of the synthetic route, as outlined in Scheme 3.5

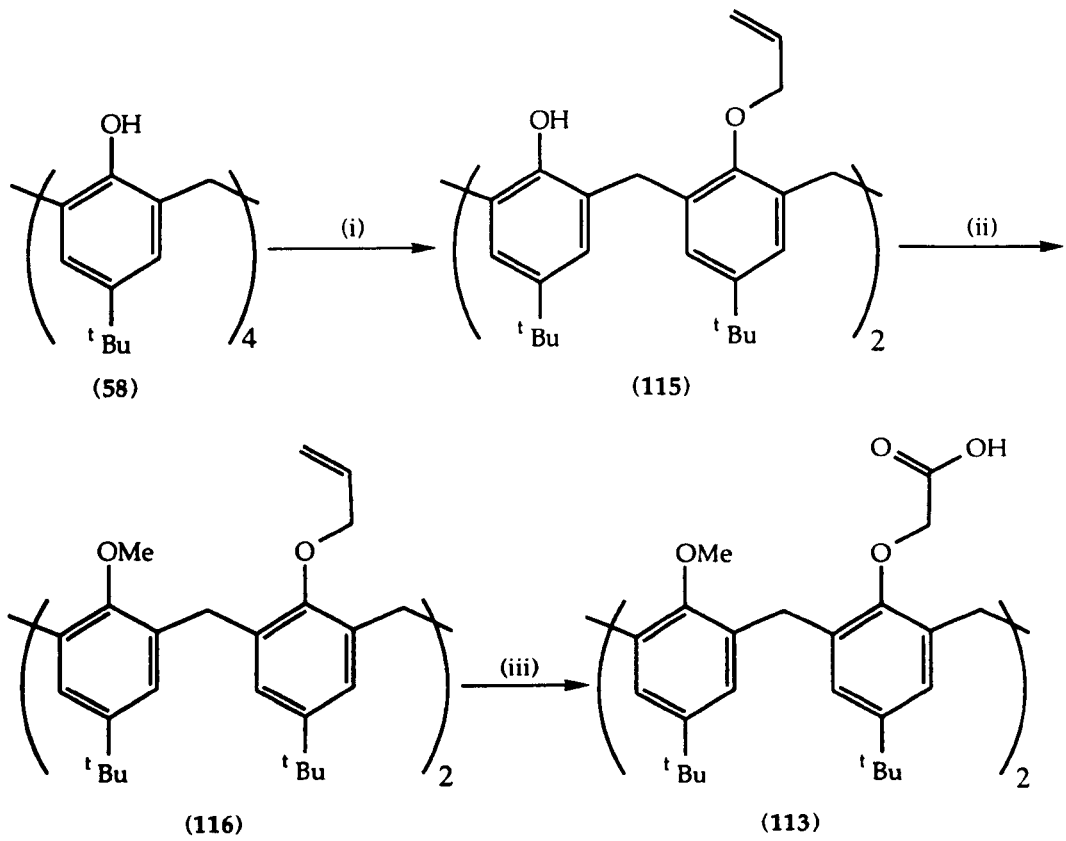

Scheme 3.5

The bis(allyl) ether (**115**) should be amenable to further alkylation as it contains no activated carbons and the allyl group should help to prevent the severe distortion from ideal cone geometry that is seen for the di-methyl ether (**114**). Further functionalisation of the compound could be achieved by ozonolysis of the terminal double bond. Alkylation of *p-tert*-butylcalix[4]arene (step i) to the bis(allyl) ether (**115**) proceeds smoothly in 85% yield, using the conditions for di-alkylation given earlier. The compound appears to have the distorted cone conformation as shown by the pair of doublets δ 3·34 and 4·3 ppm. Subsequent methylation with methyliodide and sodium hydride in THF also proceeds smoothly to give the dimethyl-diallylether (**116**) in 85% yield. The NMR spectrum of this compound was unusual since all the resonances were broadened; this was attributed to conformational movement of the compound on the NMR timescale. This explanation was confirmed by variable temperature NMR experiments, changing the temperature altered the shape of the resonances but no coalescence of peaks could be seen in the temperature

range 223-323K. Lowering the temperature complicated the spectrum with more resonances appearing, raising the temperature only broadened the peaks. The general pattern of the spectrum though suggested that it existed preferentially in the cone conformation.

Production of the di-acid-di-methyl ether compound (**113**) was attempted by treatment with ozone and oxidative work-up with hydrogen peroxide. A reaction did take place, as indicated by the disappearance of the di-allyl compound, but little information about the isolated product could be discerned as the NMR now only showed very broad overlapping peaks. A small $[M]^+$ was observed in the FAB MS and the IR spectrum was indicative of a carboxylic acid. Elemental analysis though was poor. Potassium permanganate was also used as an oxidant but this did not improve the procedure. The compound was further reacted, despite these poor results, by initial treatment with thionyl chloride and then 1,8-diaminoanthraquinone in an attempt to bridge the calixarene. Only intractable mixtures could be isolated, with FAB MS showing no signs of the desired product (**117**).

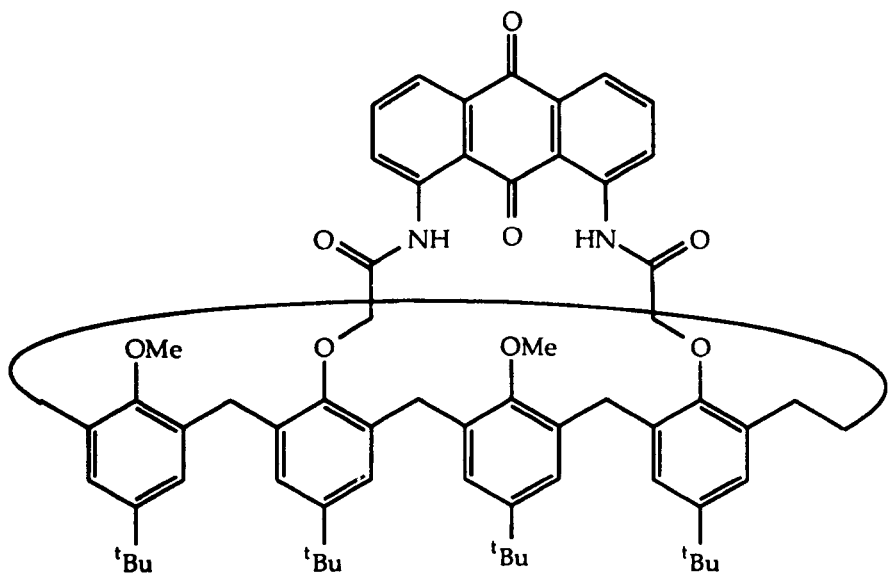

(**117**)

Alternatively the dimethyl-diallylether, however, can be treated with a reducing agent to produce the alcohol (**118**). Deprotonation of this alcohol and reaction with a suitable capping moiety would also give a bridged calixarene but with an ether linkage.

Thus according to Scheme 3.6 the diallyl-dimethyl ether (116) was prepared as for Scheme 3.5. Ozonolysis of the double bonds and reductive work-up with sodium borohyride gave the alcohol, in 62% yield. Again, however, the NMR spectrum of the product had only broad overlapping peaks which gave no structural information. The compound did, however, give good mass and infra-red spectral data.

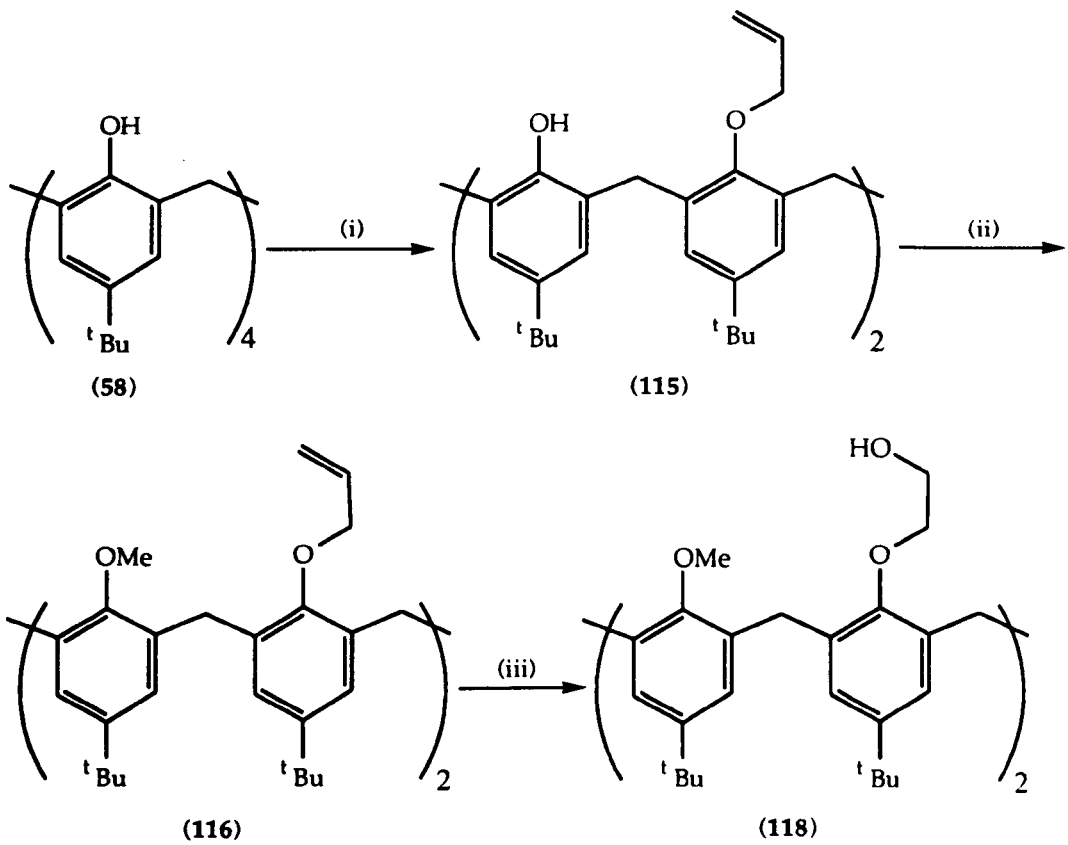

Scheme 3.6

The compounds chosen for the capping reaction were 1,8-dichloroanthraquinone, 1,8-dichloro-4,5-dinitroanthraquinone(47) and 2,6-dibromo-3,5-bis(bromomethyl)-1,4-benzoquinone (119); details of the preparation of (47) and (119) can be found in the experimental section. Reaction of the di-alcohol (118) with 1,8-dichloroanthraquinone in THF in the presence of sodium hydride, when carried out on a small scale, gave the desired compound (120) in low yield (<5%). Sufficient material was isolated by chromatography to obtain a FAB MS only. All attempts to scale up the preparation to a gram scale failed. We

had however demonstrated that compound (120) could be made and that only a suitable preparative method needed to be devised.

1,8-Dichloro-4,5-dinitroanthraquinone(47) and 2,6-dibromo-3,5-bis(bromomethyl)-1,4-benzoquinone (119) were never used as a capping moieties. The failure of (47) to give clean reactions with glycolic anions[47] and the failure of the previous attempts to cap the di-alcohol led us to abandon this route to capped calixarenes. 2,6-Dibromo-3,5-bis(bromomethyl)-1,4-benzoquinone (119) was never used as a capping moiety due to time constraints.

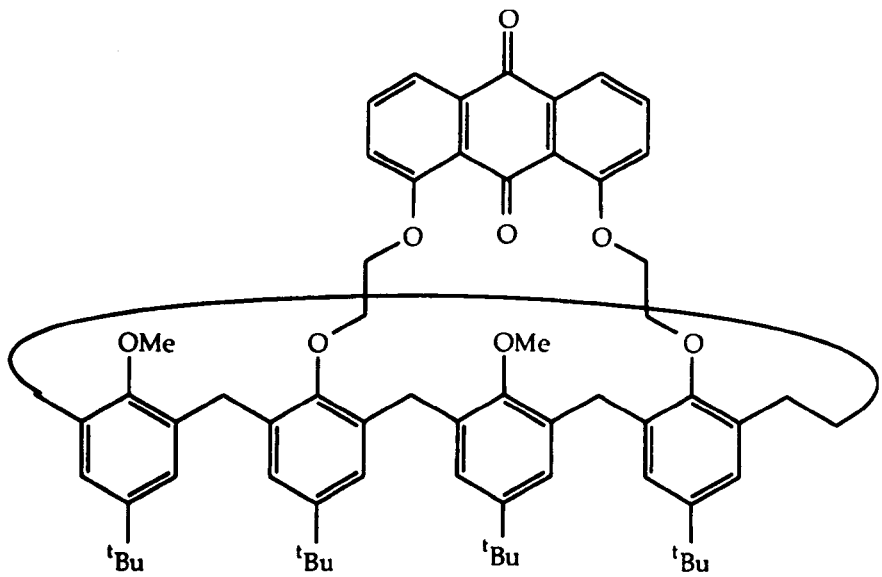

(120)

Gokel *et al.* had used this methodology previously to produce the podand (36), bibrachial podands (38) and (39) and the crown ether analogues (40), (44) and (45). All these reactions however are unusual since they involve anions derived from poly-ethylene glycols. When 1,8-dichloro anthraquinone is reacted with anions derived from simple alcohols, such as propanol, only very small amounts of product were observed, with almost complete recovery of the starting material.[43-46] Gokel *et al.* tried this methodology to produce the cryptand (49) using the diaza-crown (121), but this failed to give the desired product. Compound (49) was, however, made by the reaction of 1,8-di(2'-

bromoethoxy)anthraquinone (122) with crown ether (7). Compound (122) being made from 1,8-dihydroxyanthraquinone and 1,2-dibromoethane. The use of a hydroxyanthraquinone as the nucleophile in this last reaction is unusual because anions derived from hydroxyanthraquinones are generally only weakly nucleophilic due to the close ion pairing with the counter ion. The addition of 18-crown-6 as a sequestrant for the counter ion does not improve the reaction.[39,42] Gokel overcame the problem by using caesium carbonate as the base and DMF as solvent, the dicaesium salt of 1,8-dihydroxyanthraquinone is soluble in DMF and the ion pairing loose due to the large ionic radius of caesium.

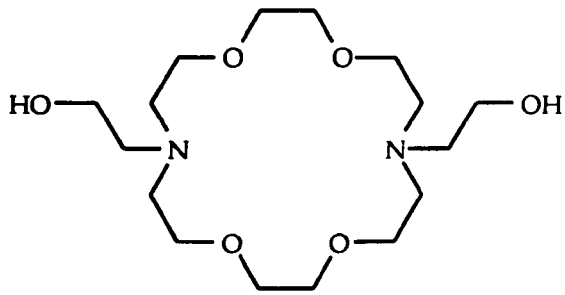

(121)

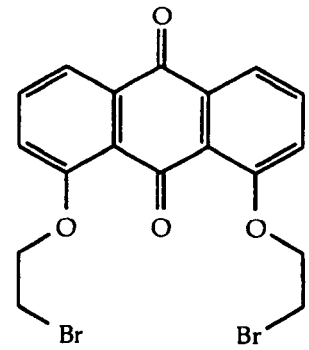

(122)

Gokel *et al.* also found that poly-ethylene glycols were also good leaving groups in nucleophilic aromatic substitution reactions and can be used as catalysts.[43-45] This approach would be impracticable for our purposes. For catalysis the optimum chain length is three ethylenoxy units, this would cause steric problems when the large calix[4]arene derivative approached the substituted anthraquinone. We chose therefore to attempt to bridge *p-tert*-butylcalix[4]arene (58) with 1,8 di(2'-bromoethoxy)anthraquinone (122), as in Scheme 3.7. Thus *p-tert*-butylcalix[4]arene (58) was treated with 1,8-di(2'-bromoethoxy)anthraquinone (122) in butyronitrile in the presence of sodium carbonate and sodium iodide. This gave the capped calixarene (123) in 36% yield. The NMR spectrum of the crude material did indicate a higher yield, but purification of the compound proved to be difficult. The main impurities were unreacted calix[4]arene and multiply bridged bis-calixarenes (124) and (125), the latter were detected by FAB MS having masses 1882.4 and

2174·7 respectively, and were not isolated as separate compounds. The unreacted *p-tert*-butylcalix[4]arene could be removed easily by exploiting its low solubility in dichloromethane. Removal of the polymeric compounds however required multiple recrystallisations, with the desired product remaining in the mother liquors. This is an inherently poor purification technique which resulted in a low yield of pure product (123).

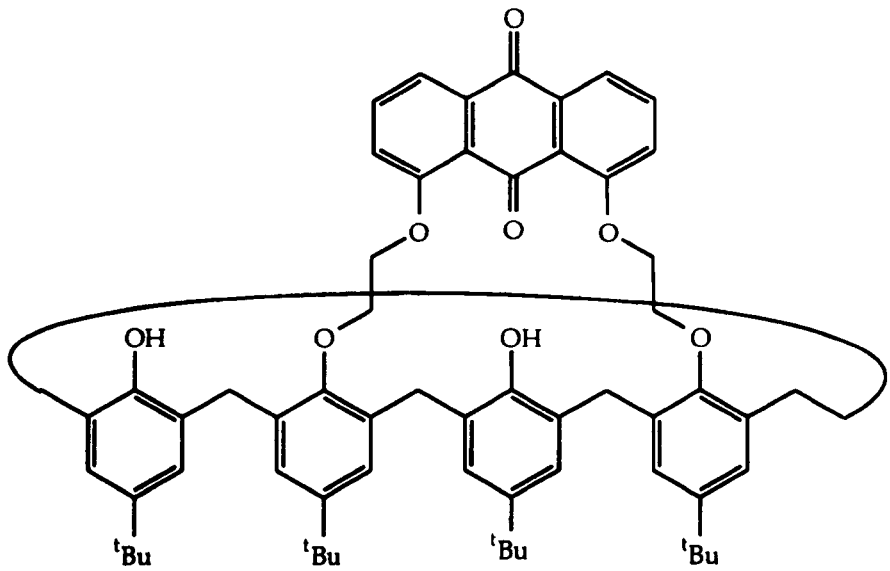

(123)

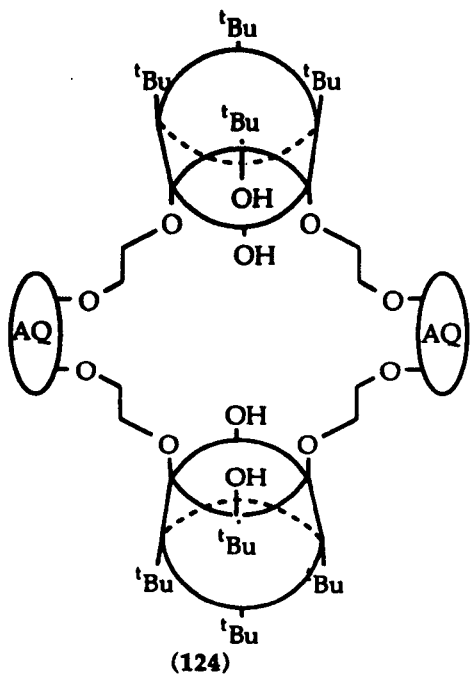

(124)

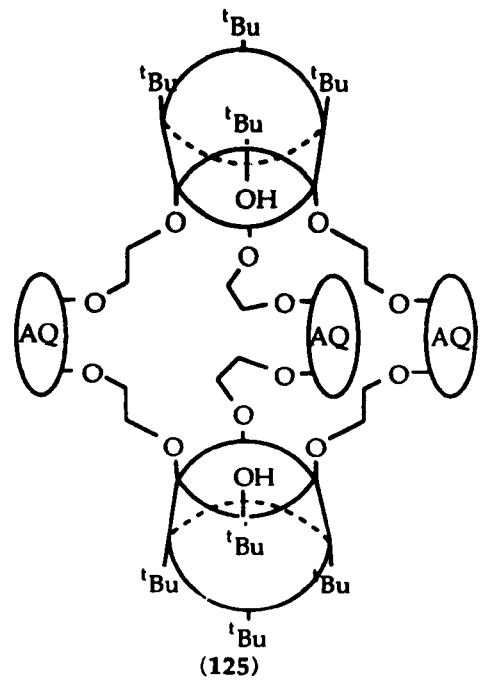

(125)

AQ= Anthraquinone

After conducting preliminary electrochemical measurements on (**123**) good quality single crystals were obtained from the electrochemical cell after the solution was left standing for 48hrs. These were submitted for X-ray analysis but the structure could not be resolved due to the low number of reflections. The unit cell dimensions were found to be: a 13·346Å; b 21·188Å; c 22·194Å; α 90°; β 101·79; γ 90°; space group $P2_1/a$; monoclinic. Although the yield for this reaction is low the starting materials are readily available and low in cost; there is also some recovery of unreacted *p-tert*-butylcalix[4]arene (**58**). When the reaction is carried out in the presence of potassium salts the results are slightly different. The yield of mono-bridged product is lower and that of the polymeric compounds higher. There is also a third compound produced, the doubly bridged compound (**126**). There are only a few examples of 1,2-bridged calixarenes and these were produced by more elaborate procedures.[120,121]

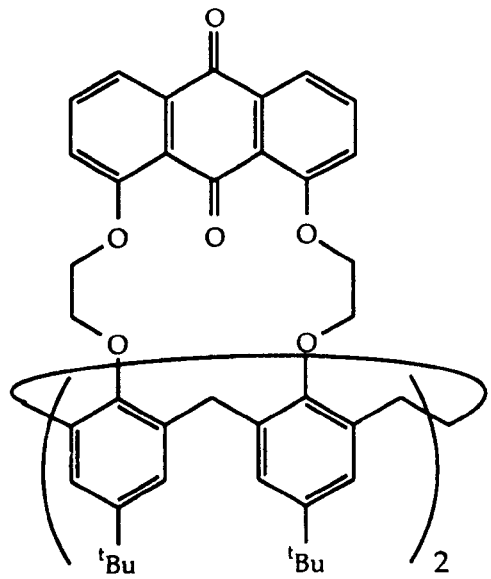

(**126**)

This is rather unusual as molecular modelling (see Chapter 5) of the target compound (**120**) suggest that the cavity is ideally suited to potassium ions; therefore one would expect that potassium ions would direct the synthesis towards the mono-bridged product via a templating effect. The reason for this apparent conflict may be that the transition state is large, as the active alkylating compound is the halogen exchanged iodo- (**122**). Potassium ions would be too large to allow the reaction between the bridging moiety

and the phenoxide ions in the 1 and 3 positions since they would hold the reactive centres at too great a distance for reaction. The smaller sodium ion however would allow the reactive centres to move closer together. Synthesis of compound (126) could be improved by changing the stoichiometry of the reaction so as the bridging unit (122) is in a two-fold excess over the calixarene and by using potassium ions as the template.

Compound (123) was further fuctionalised at the remaining two hydroxyls by treatment with sodium hydride in THF and then reaction with an alkylating agent. Thus compound (120) was made in 50% yield by treatment with dimethyl sulphate; compound (127) in 71% yield by treatment with ethyl bromoacetate and compound (128) in 25% yield by treatment with N,N-diethyl-2-chloroacetamide.

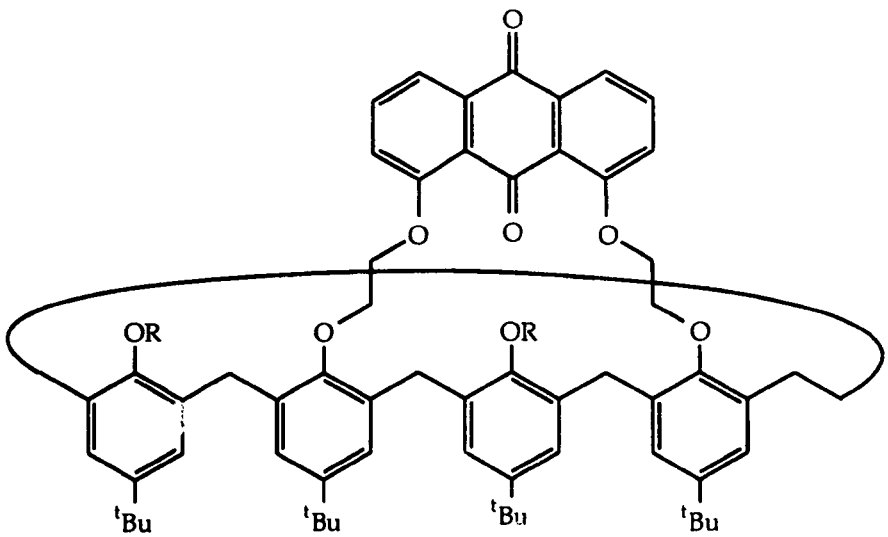

(120) R= Me
(127) R= CH_2CO_2Et
(128) R= CH_2CONEt_2

So far we have produced seven new calixarene compounds which contain electrochemically switchable moieties, namely compounds (106), (107), (120), (123), (126), (127) and (128). The electrochemical properties of compounds(106), (107), (120), (127) and (128) will be discussed in the next chapter. The free phenolic residues in compound in (123) make this compound unsuitable as a switchable ionophore due the possible proton transfers to the reduced anthraquinone. The low yield of compound (126) meant that an insufficient quantity of this compound was available for electrochemical testing with the available equipment.

Chapter 4

Cyclic Voltammetry

In Chapter One the concepts which led to the development of electrochemically enhanced ionophores were described along with a brief explanation of the mechanism by which this enhancement occurs. As mentioned in Chapter 1 the enhancement of binding can be quite easily measured by cyclic voltammetry.

In a cyclic voltammetric experiment the potential between the reference and working electrodes in a three electrode cell (Fig 4.1) is swept through a set range at a constant rate (usually in the range 50-1000mVs^{-1}). Current is measured between the working and counter electrodes. The direction of the sweep is reversed at a vertex and usually returns to the start potential; hence the name "cyclic". A typical potential sweep is shown in Figure 4.2.

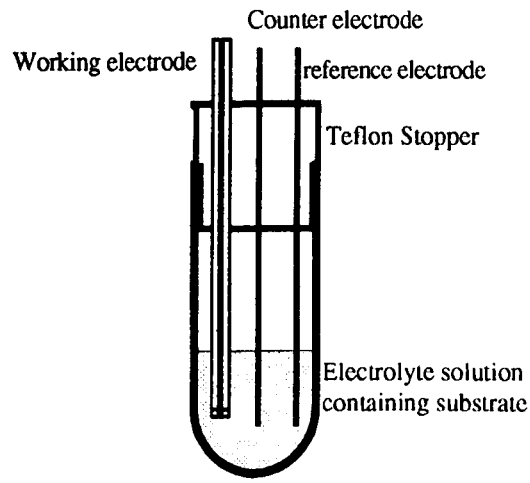

Figure 4.1: Three electrode electrochemical cell.

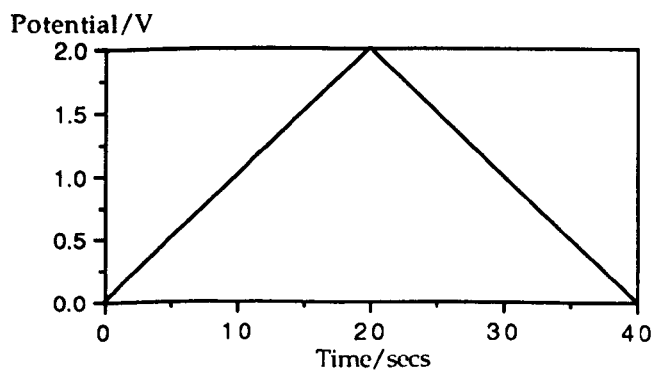

Figure 4.2: Typical sweep for a cyclic voltammetric experiment, 100mVs-1.

Detailed descriptions of both the theories of and methods involved in cyclic voltammetric experiments can be found in many texts.[122,123] For the present investigation experiments were carried out using acetonitrile as solvent, which contained 0·1 molar tetraethylammonium perchlorate as supporting electrolyte. The working electrode was a platinum disc, the counter electrode either a platinum foil flag or a stainless steel needle (which conveniently served to de-oxygenate the solution) and the reference electrode a silver wire. The use of a silver wire as a reference electrode is somewhat unconventional as the usual reference is a Ag/Ag^+ electrode. The silver wire was used to avoid any potential complications due to complexation of silver ions by the ligand. This pseudo-reference electrode was calibrated by comparing the reduction potential of chloranil (97) as measured against the silver wire with that measured against a Ag/Ag^+ reference.[108] These potentials matched to within 10mV. Ligand concentrations were of the order 1-5 mmolar. A similar experimental set-up has been used by Gokel and Echegoyen *et al.* in the testing of their reducible ionophores.

If an enhancement of the ionophores binding for metal ions takes place upon reduction this manifests itself as a shift in the peak potential to a less anodic value. This can occur in two ways: either there is a separate peak, the height of which is related to the amount of metal ion added and the ligand/ion binding ratio;[28,30-40] or there is a gradual shift in the potential as a function of added metal ion.[50,52] The former is the more common of the two and it is this behaviour which is discussed. There are two possible explanations for the phenomenon. The first is that the shifted potential is the reduction potential of the ligand/M^+ complex which is more cathodic than that of the free ligand due to assisted electron transfer to the organic species by the chelated ion. This corresponds to reaction along path 1' and assumes that the equilibrium K' lies to the right and is fast (Fig 4.3).

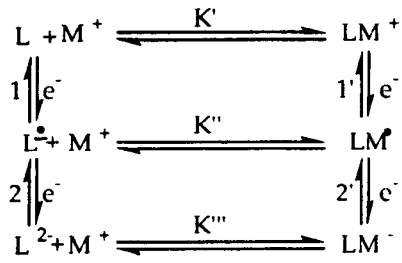

Figure 4.3; Reaction pathways for an anthraquinone based, switchable ligand.

The alternative interpretation of the phenomenon is that reduction takes place along path 1 and is followed by rapid ion complexation along path (equilibrium constant K"). The effect of this is to remove the species $L^{\bullet -}$ which disturbs the Nernst equilibrium such that more ligand is reduced; this raises the observed current leading to an earlier peak potential (an EC process). This is a view supported by the work of Parker and Tilset, who demonstrated that for the reaction of electrochemically generated cation radicals with nucleophiles (according to Scheme 4.1) pre-peaks are observed if the overall rate for reaction as in Scheme 4.1 is greater than or equal to 10^6 $M^{-1}s^{-1}$ at a sweep rate of $100mVs^{-1}$.[124]

$$A + Nu \underset{k_{-en}}{\overset{k_{en}}{\rightleftharpoons}} [\text{encounter complex}] \xrightarrow{k_p} Ar{-}Nu^+$$

Scheme 4.1

k_{en} = rate of encounter complex formation; k_{-en}= rate of loss of encounter complex; k_p= rate of product formation

If equation 1.2 is used to determine the binding enhancement the order of the complexation and electron transfer steps is not specified as it is dependent only upon the magnitude of the shift.

$$K^2/K^1 = \exp\left\{-\frac{F}{RT}\left(E^{o1} - E^{o2}\right)\right\} \qquad \text{(equ. 1.2)}$$

K^1: binding constant for neutral ligand

K^2: binding constant for reduced ligand

E^{o1}: redox potential for free ligand

E^{o2}: redox potential for the complex

Chemically, however the order of these events is important. If complexation precedes electron transfer the ligand can be considered to reasonably good at binding metal ions. If complexation takes place after electron transfer, then in the neutral state the ionophore is rather poor. The latter behaviour is more akin to a truly switchable ionophore, i.e. it has an on and off state. Transport of complexed metal ions in this case, however will be diffusion limited. If complexation takes place before reduction transport

will be limited by decomplexation rates. Physically, very little can be done to speed decomplexation rates, yet there are many things which will speed diffusion, e.g. stirring of both the membrane and receiving phases or reducing the transport distance, e.g. placing the ligand in a PVC membrane. Gokel and Echegoyen *et al.* have consistently interpreted their data based on the assumption that the shifted peak is solely due to the LM^+ complex. They performed a computer simulation of the cyclic voltammetric behaviour of a theoretical system in which they altered the values of K' and K'' and the binding enhancement and compared the results with experimental data for compounds (**26**;n=1) and (**31**;n=1).[125] They found that only when K' was large ($>10^4\ M^{-1}$) did the simulation show two distinct peaks. In the range $10^4 > K' > 1$ the behaviour was intermediate, with the peaks slowly merging at lower values of K'. When $K' < 1$ the simulation predicted that only one peak would be present, the position of which would slowly move to a more anodic value with increasing metal ion concentration, reaching a maximum when the metal ion was in a 50 fold excess over the ligand. The simulation also predicts that in the range $10^4 > K_1 > 1$ the value of the binding enhancement calculated from the shift in the peak potential is very much lower than the "real" enhancement as predicted by the simulation. There is, however, a flaw with the simulation, since it assumes that all chemical and electrochemical homo- and heterogeneous processes are fast on the experimental time-scale. This is an unreasonable assumption for two reasons. Firstly electron transfer to anthraquinones and nitroaromatics is slow as shown by the difference of greater than 59mV between the peak reduction and oxidation potentials. Chemical processes can also be slow, as shown by Gokel's own experiments; with compound (**36**) there are two competing reaction pathways for species $L^{\bullet -}$. Complexation followed by electron transfer (K'' then 2') to give LM^- or electron transfer (2) to give L^{2-} (Fig 4.1). Gokel found that he could completely suppress the peak for electron transfer 2' by increasing the scan rate to $1000mVs^{-1}$; this is not a particularly fast scan rate and therefore implies that the complexation step is a slow one. Wolf and Cooper *et al.* on the other hand have performed similar experiments on benzoquinone derived crown ether compound (**53**) with DMF as solvent. They observed only one peak which shifted as a function of $[M^+]$. According to Gokel *et al.* this would correspond to the case in which $K' < 1$;

yet the compounds were sufficiently good ionophores that Cooper *et al.* were able to obtain crystal structures of the related (**55**)/metal ion complexes.[51b] Further studies have predicted that if pre-complexation occurs the potential can be shifted to more anodic values.[126] Finally Gokel *et al.* have shown by ESR experiments that for compound (**26**;n=1), although the order of binding enhancements from CV experiments is $Li^+ > Na^+ > K^+$, the compound is selective for sodium ions.[33] Clearly the interpretation of the data from cyclic voltammetric experiments must be treated with some caution. We have chosen therefore to interpret our electrochemical results using equation 1.2 to evaluate the binding enhancement. Simple two phase extraction experiments can be used to determine the binding constant of the unreduced ligand and therefore the binding constant of the reduced ligand can be calculated.

Electrochemistry of Type A Compounds

Initial measurements were made on both compounds (**106**) and (**107**) to determine if the presence of the calixarene moiety had any influence on the electrochemistry.

Electrochemistry of compound (106)

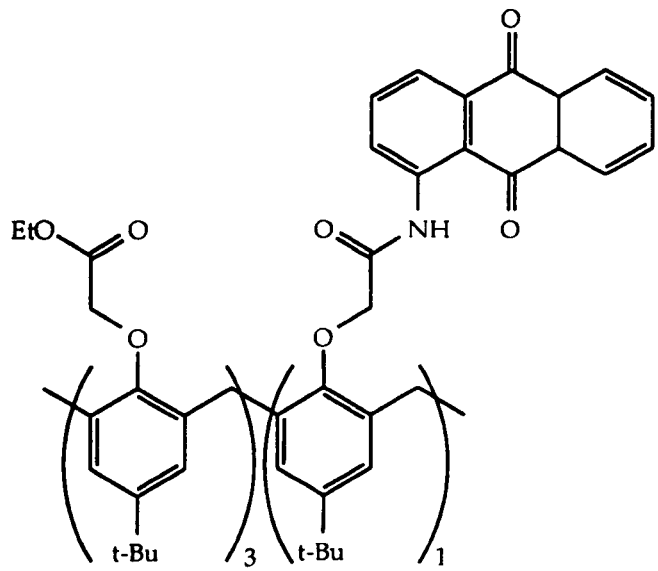

(106)

Compound (**106**) displayed the normal electrochemical behaviour of an anthraquinone derivative. There were two discrete electron transfers, to form $AQ^{\bullet -}$ and AQ^{2-}, both of which were reversible. These transfers were slow as indicated by the large difference between the reduction and oxidation peak potentials ($\Delta E_p > 59mV$). A typical CV plot is shown in Figure 4.4(a).

The peak potentials vs. the pseudo Ag/Ag^+ are;

$AQ \rightarrow AQ^{\bullet -}$ $\quad E_p^{R_1}$ -815mV

$AQ^{\bullet -} \rightarrow AQ^{2-}$ $\quad E_p^{R_2}$ -1419mV

$AQ^{2-} \rightarrow AQ^{\bullet -}$ $\quad E_p^{O_2}$ -1237mV

$AQ^{\bullet -} \rightarrow AQ$ $\quad E_p^{O_1}$ -743mV.

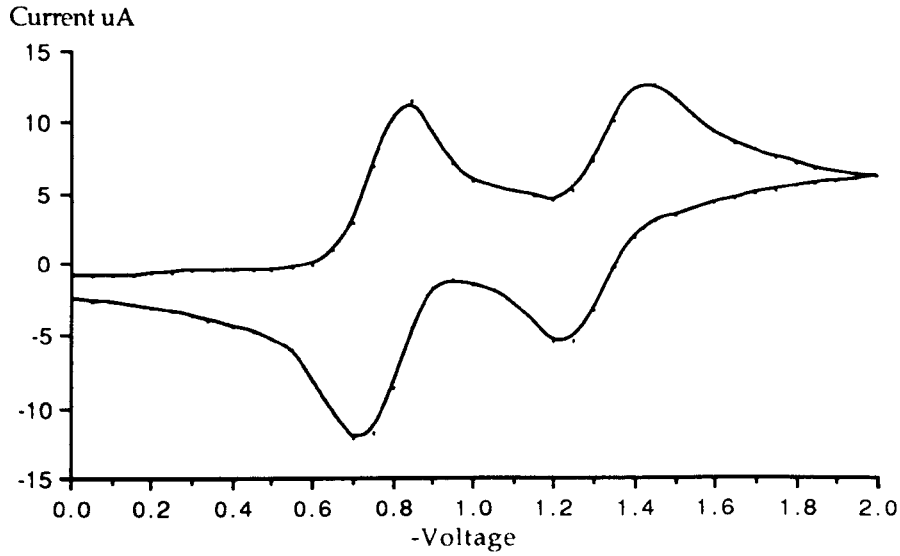

*Figure 4.4(a): Cyclic voltammogram of compound (**106**), sweep rate 100mVs-1.*

Upon the addition of sodium perchlorate the voltammogram changed very little. There was a small shift of 10mV in the peak potential of the first reduction wave and a larger shift of *ca.* 100mV in the second wave (see Figs 4.4(b) and 4.4(c)).

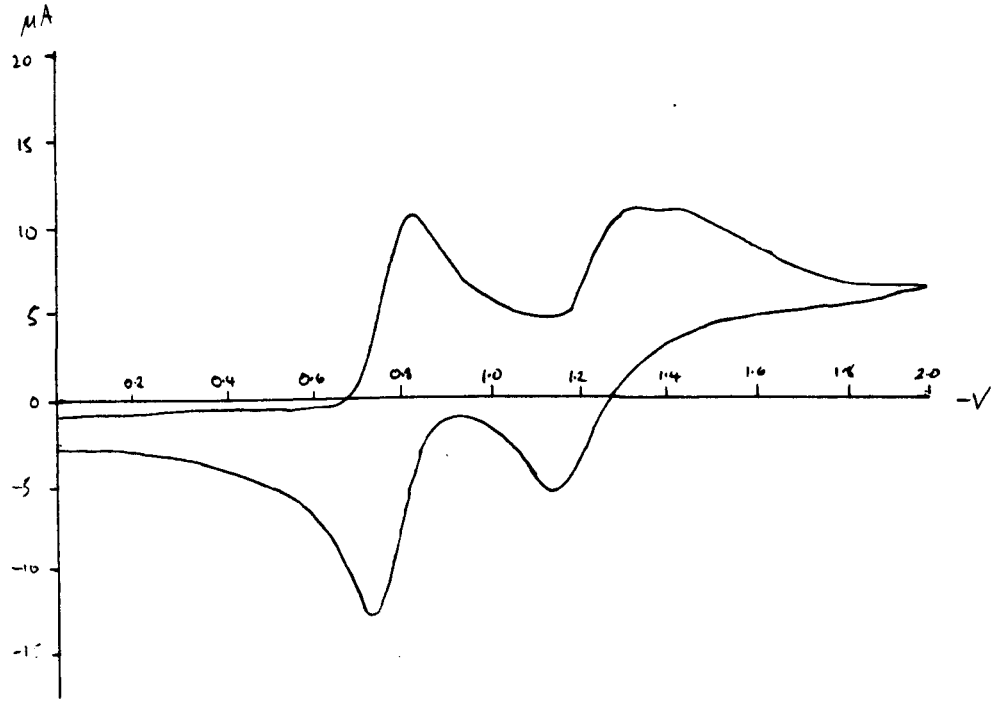

*Fig 4.4(b) CV of compound (**106**) with 0.5≡ $NaClO_4$, sweep rate 100mVs^{-1}.*

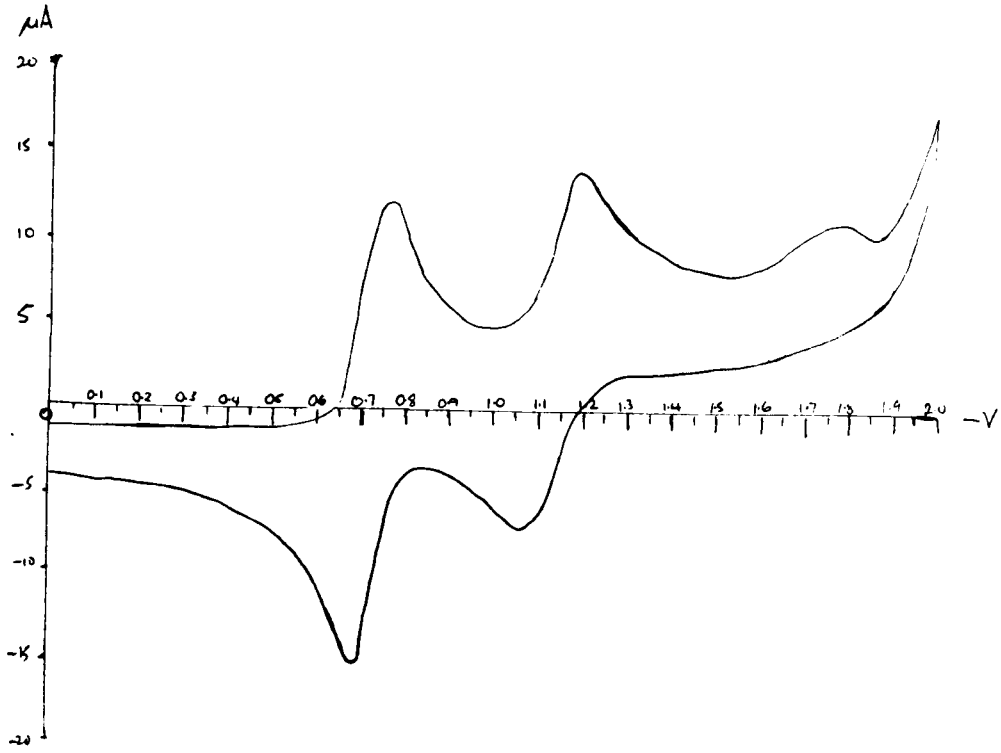

Fig 4.4(c) CV of compound (106) with 1≡ $NaClO_4$, sweep rate 100mVs^{-1}.

The small peak at ≈ -1.75V in Figure 4.4(c) is associated with a possible proton transfer from a hydrated sodium ion and is irreversible. If the cell is kept rigorously anhydrous it is not present. For binding enhancement purposes only the first reduction is important as ion pairing effects are more important for the more highly charged AQ^{2-} anion. This was confirmed by the comparison of compound (106) with the calixarene free, model compound, N-acetyl-1-aminoanthraquinone (129).

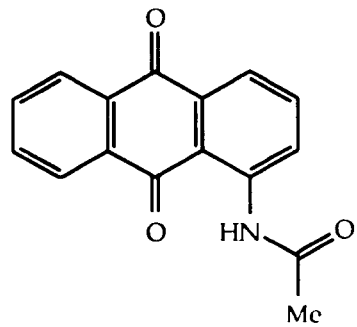

(129)

Compound (129) displayed similar behaviour to (106) upon the addition of metal salts. Cyclic voltammograms are shown in Figures 4.5(a), 4.5(b) and 4.5(c).

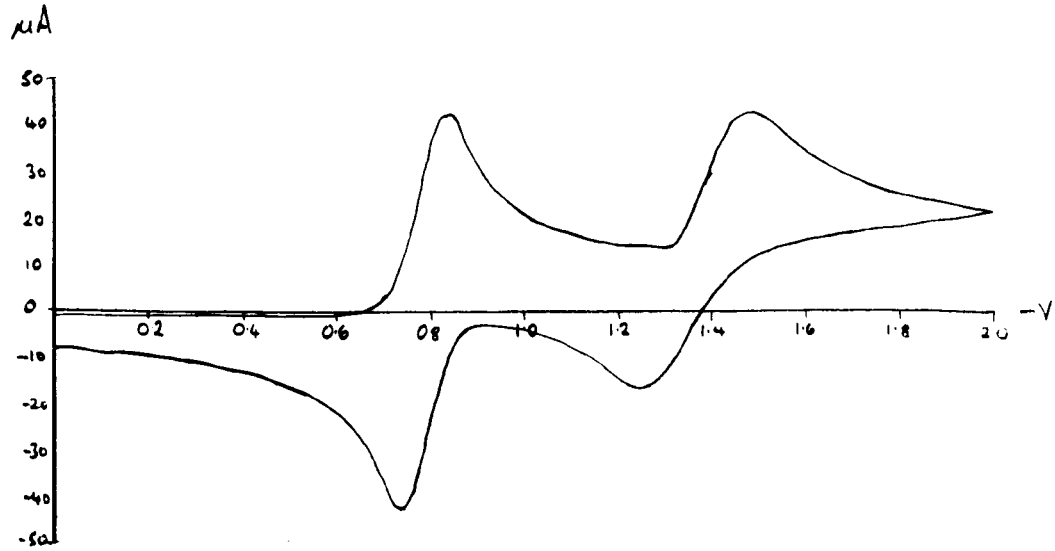

Fig 4.5(a): Cyclic voltammogram of compound (129), sweep rate 100mVs^{-1}.

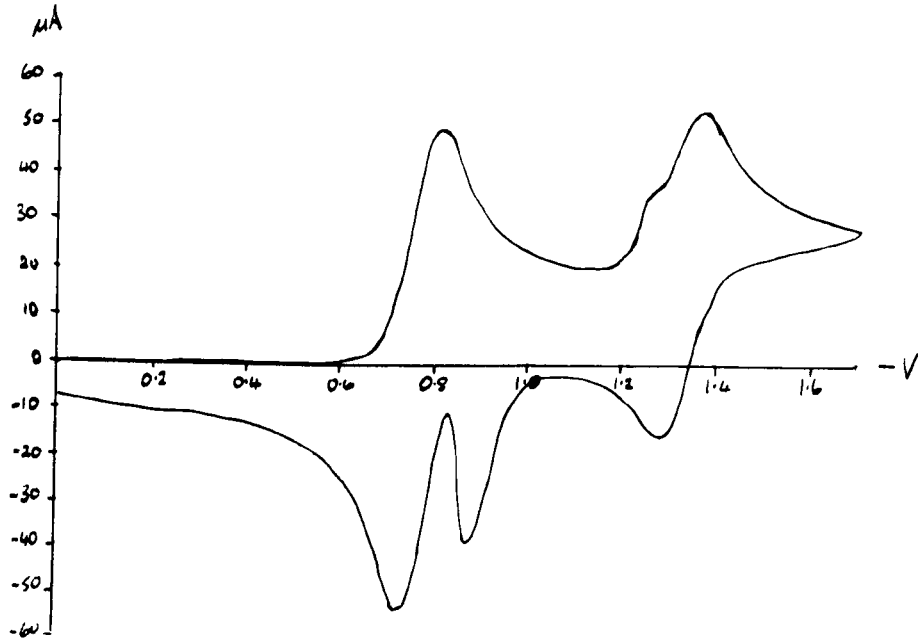

Fig 4.5(b): CV of compound (129) with 0.5≡ $NaClO_4$, sweep rate 100mVs^{-1}.

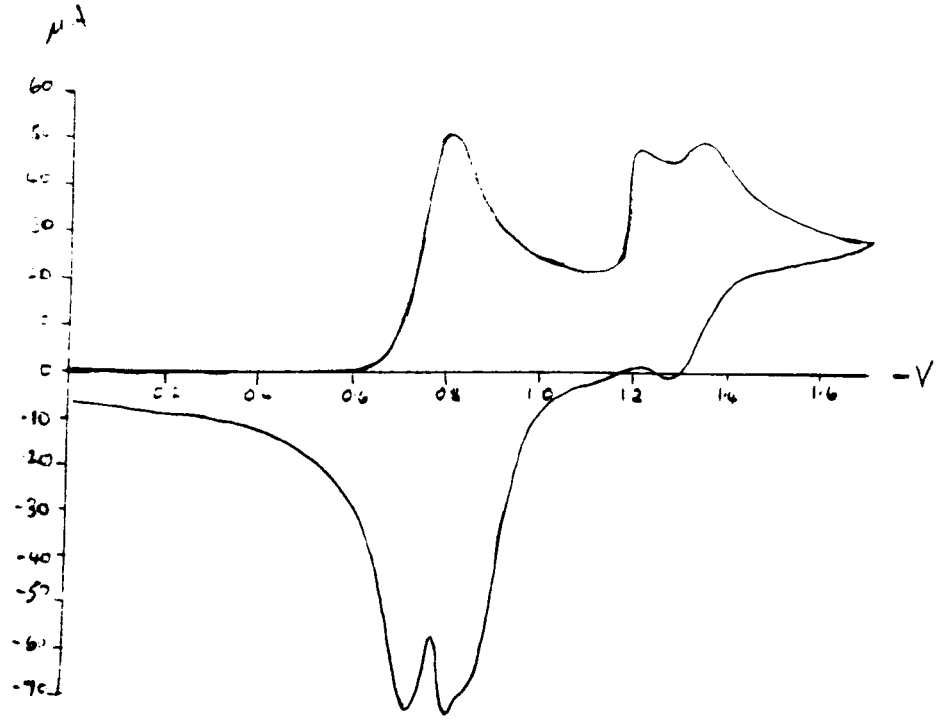

Figure 4.5(c): CV of compound (129) with 1≡ $NaClO_4$, sweep rate 100mVs^{-1}.

One difference is that upon reduction to the AQ^{2-} anion in the presence of metal ions there is adsorption onto the electrode surface. This is indicated by both the steepness of the reduction wave at ≈ -1.2V and the large desorption peak at ≈ -0.8V on the reverse scan. The current associated with this peak is larger than for the forward peak indicating that adsorption continues until the scan is reversed. A second difference is that when sodium ions are added to compound (129) the peak associated with the proton transfer from the hydrated ion is evident immediately; the sweep was reversed at -1.7V when metal ions were added to prevent this reaction. With compound (106) this peak only appears when more than one equivalent of sodium ions is present, indicating that the sodium ions are being bound by the ionophoric cavity of the calixarene derivative.

The shift in the second reduction wave of (106) is therefore associated with ion pairing only as (129) does not have any groups which could ligate metal ions. It is possible that proton transfer from the amide function or hydrogen bonding could "quench" the charge on the anthraquinone. This was ruled out by examination of a second model compound N-acetyl-1-methylaminoanthraquinone (130). This compound behaved in an analogous fashion to (129), demonstrating that proton transfer is not an important effect in this

system. Cyclic voltammograms for **(130)** in the absence of added metal ions and with 0.5 and 1 equivalents of sodium perchlorate added are shown in Figures 4.6(a), 4.6(b) and 4.6(c).

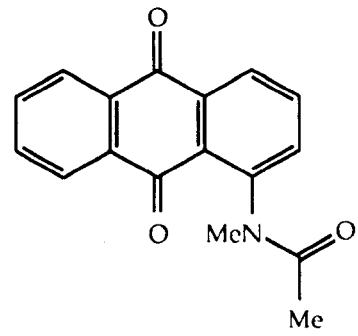

(130)

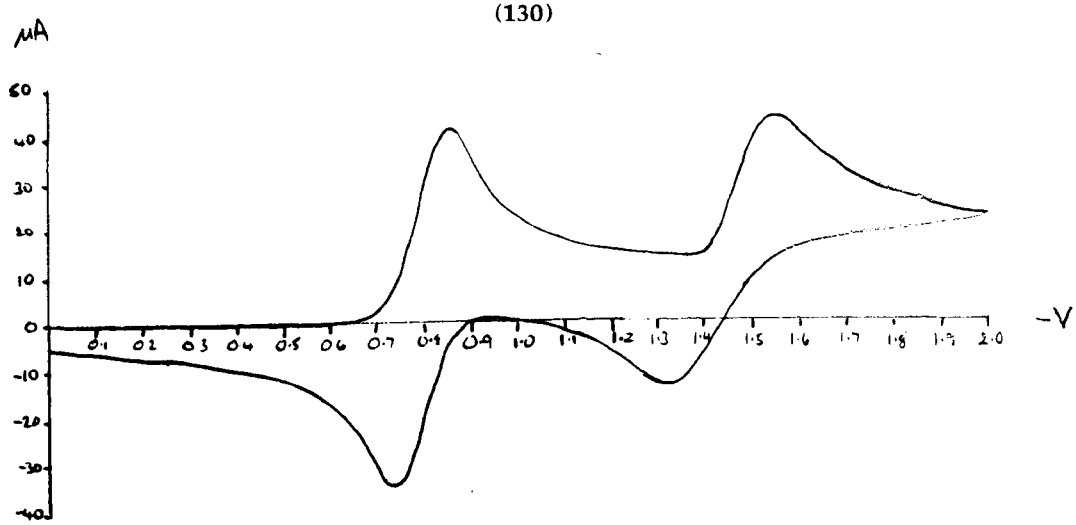

Figure 4.6(a): Cyclic voltammogram of (130), sweep rate 100mVs^{-1}

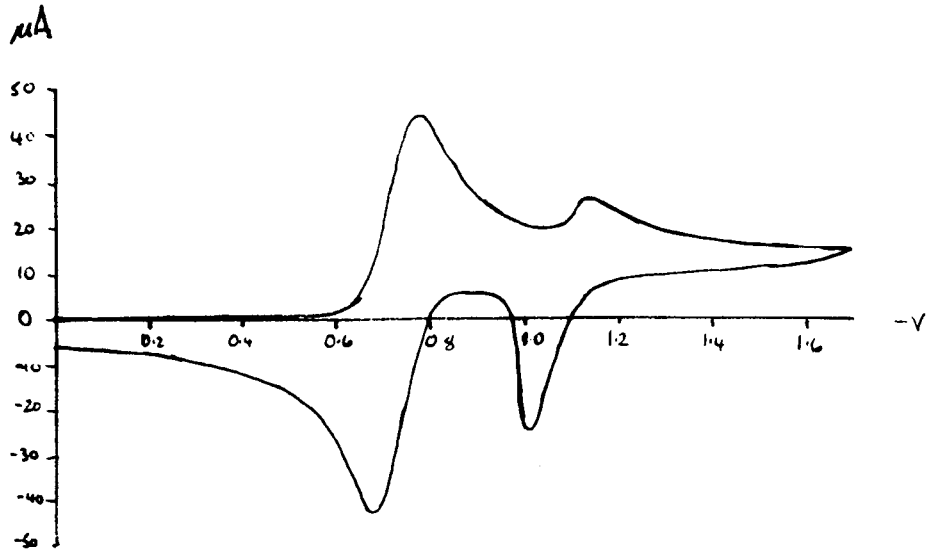

Figure 4.6(b): Cyclic voltammogram of (130) with 0.5≡ $NaClO_4$, sweep rate 100mVs^{-1}

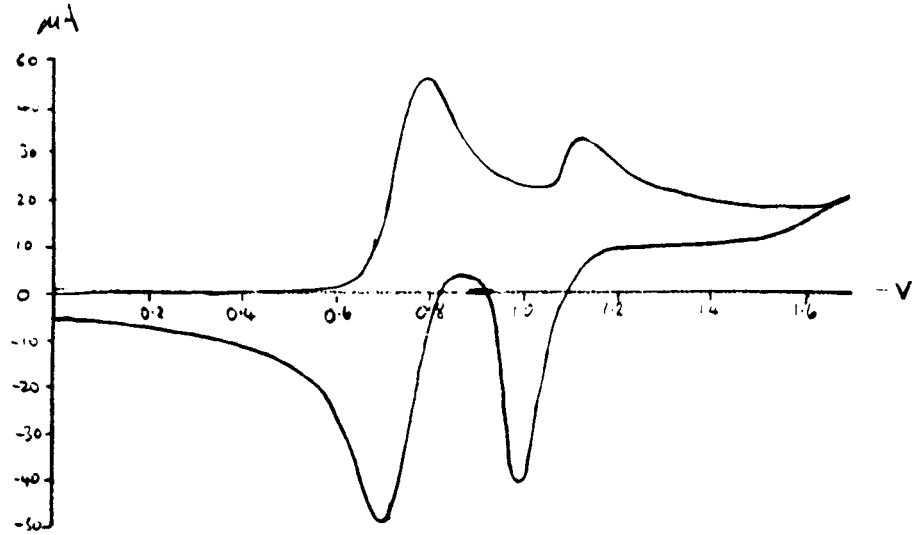

Figure 4.16(c): Cyclic Voltammogram of (130) with 1≡ $NaClO_4$, sweep rate 100mVs^{-1}.

As compound (106) is based on compound (59) it would be expected to show similar selectivities.[84] Its failure to show any significant effects in its electrochemical behaviour upon addition of sodium ions precluded any further testing of this compound with other metal ions. It was, however demonstrated qualitatively that (106) was capable of metal ion extraction by performing picrate extractions. After shaking a chloroform solution of (106) with an aqueous solution of sodium picrate, a depletion of the picrate anion was evident in the aqueous layer; indicating that the sodium ion had been taken up. This confirmed that (106) was complexing metal ions as suggested in the cyclic voltammetric observations. Measurement of the amount of picrate in the organic solution was difficult as both the picrate anion and compound (106) absorb in similar regions in the UV. Extensive molecular modelling of compound (106) was performed in an attempt to find the reason for its failure to act as a switchable ionophore, this is discussed in Chapter 5.

Electrochemistry of compound (107)

Due to the failure of compound (106) as an efficient switchable ionophore electrochemical measurements on compound (107) were limited to obtaining a CV in the absence of metal ions and with half an equivalent of sodium perchlorate. These are shown in Figures 4.7(a) and 4.7(b).

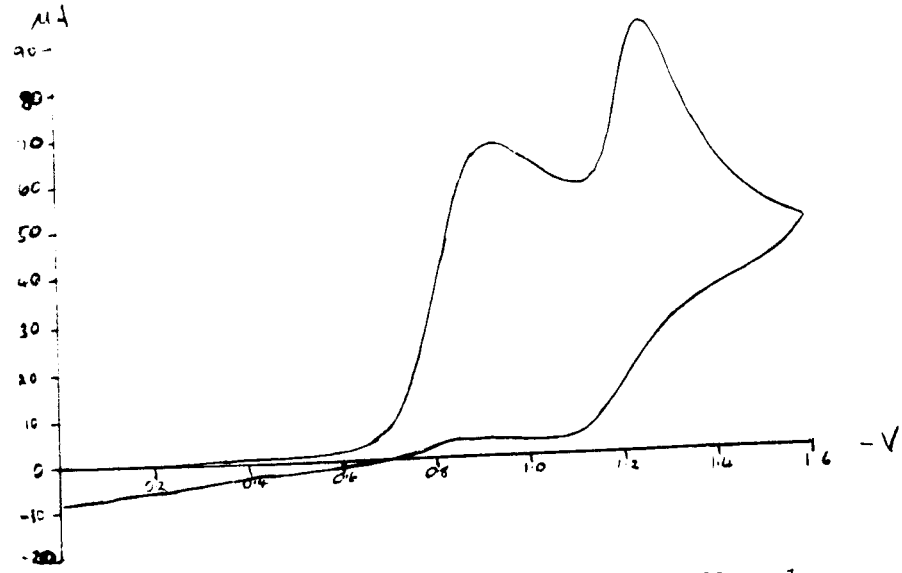

Figure 4.7(a): Cyclic voltammogram of (107), sweep rate 100mVs^{-1}

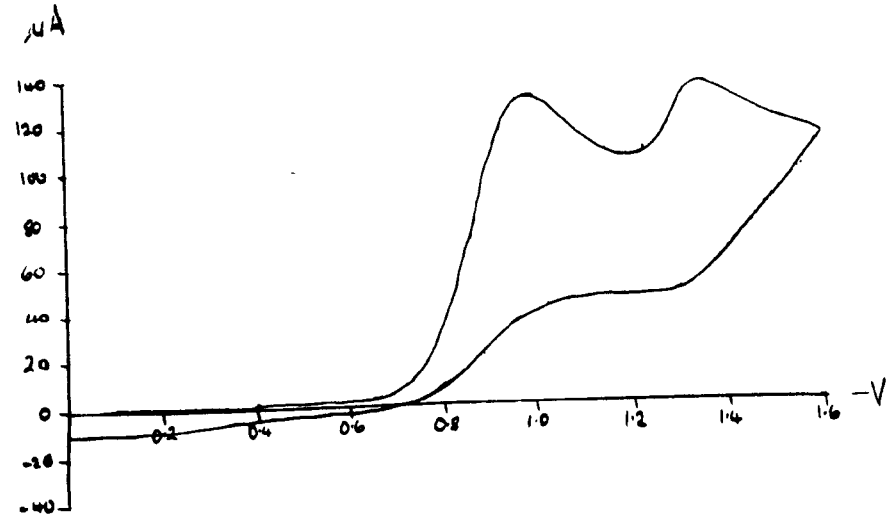

Figure 4.7(b): Cyclic voltammogram of compound (107) in the presence of 1≡ $NaClO_4$

It is evident that not only is there no detectable shift in the reduction potential of the compound upon the addition of metal ions but the reduction is also irreversible. This precluded any further testing of this compound.

Electrochemistry of Type B Compounds

The electrochemical behaviour of the ionophores (**120**), (**127**) and (**128**) in the absence of added metal ions were obtained [as for compounds (**106**) and (**107**)]. To these were added Group One metal perchlorates in 0.5, 1, and 2 molar equivalents. Here, however potentials are reported versus a silver/silver chloride reference electrode, in which the AgCl was electro-deposited onto a silver wire. This means that silver ions do not need to be added to the electrolyte solution.

Electrochemistry of compound (120)

The electrochemical behaviour of compound (**120**), in the absence of added metal ions, is similar to that of compound (**49**).[48] It displays a reversible reduction to the radical anion and a pseudo-reversible reduction to the dianion. Its cyclic voltammogram is displayed in Figure 4.8. The small peak at -0.887mV was thought to be due to sodium impurities present in the solvent or electrolyte or on the glass. This was later confirmed upon the addition sodium ions. Peak potentials are listed in Table 4.1.

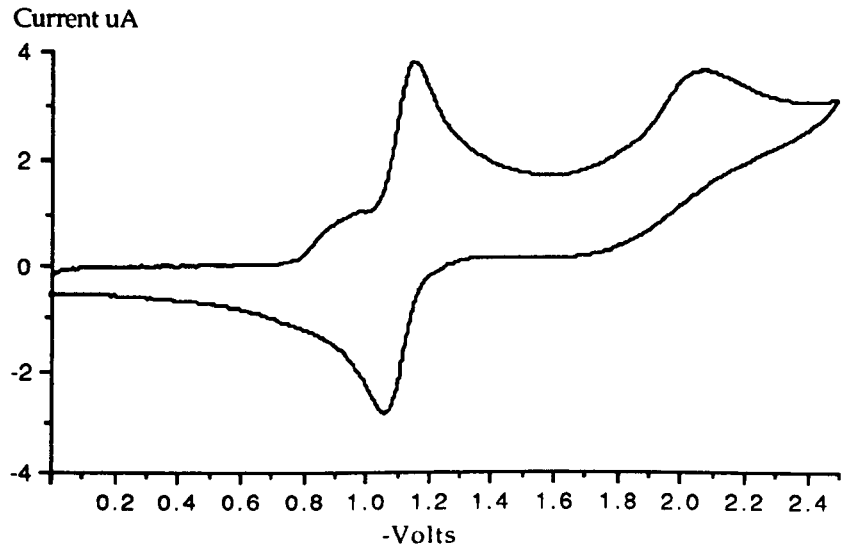

*Figure 4.8: CV of compound (**120**) in the absence of metal salts, sweep rate 200mVs^{-1}*

Table 4.1: Peak potentials for (120)

$E_p^{R_1}$	$E_p^{O_1}$	$E_p^{R_2}$	$E_p^{O_2}$
-1.154	-1.064	-1.991	*ca.* -1.6

Superscript R and O refer to reduction and oxidation peaks; all values are in volts relative to Ag/AgCl

Upon the addition of lithium perchlorate the CV changes dramatically; there is a large shift in both the first and second reduction potentials. At half an equivalent of added metal ion four distinct peaks can be seen, Figure 4.9(a). The first is for the reduction of the LM^+ complex, the second uncomplexed ligand, the third is for the reduction of the $LM^\bullet$ species and the fourth for the uncomplexed ligand. There is small peak between the first and second peaks and this is due to the sodium ions present. The current associated with this peak has increased over that in the free ligand and this is probably due to additional sodium ion present in the lithium salt. Atomic absorption was performed on the lithium perchlorate and the level of sodium determined at 0.04% w/w. This would appear to suggest that the ligand has a slight preference for sodium over lithium ions. On the reverse sweep the currents are lower, suggesting that some adsorption to the electrode has taken place.

When one equivalent of lithium ions is present the CV displays peaks for the complex only, Figure 4.9(b). The small peak due to sodium ions is most likely masked by the lithium ion peak due to the increased current. A second feature of this CV is that the reductions are now fully reversible. This is because the charge on the ligand when it is reduced to the dianion is now balanced by the positive charge of the metal ion. The compound is now much less basic and therefore less likely to pick up a proton from water impurities. This was difficult to test, as to maintain an anhydrous cell required us to add a small quantity of alumina to the cell; the alumina, however contained significant quantities of sodium ions. This reversible behaviour could be maintained for several cycles, but was destroyed by eventual adsorption. Conditioning of the working electrode at between -4 and -5V restored the previous electrochemical behaviour. Increasing the metal ion ratio to two led to irreversible adsorption, with electrode conditioning having no effect on subsequent behaviour. Peak potentials are listed in Table 4.2.

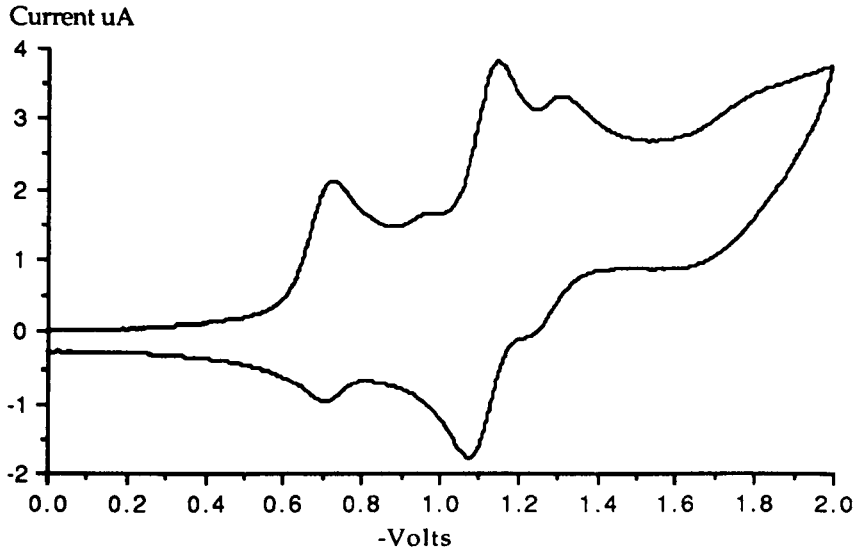

Figure 4.9(a): CV of (120) with 0.5≡ $LiClO_4$

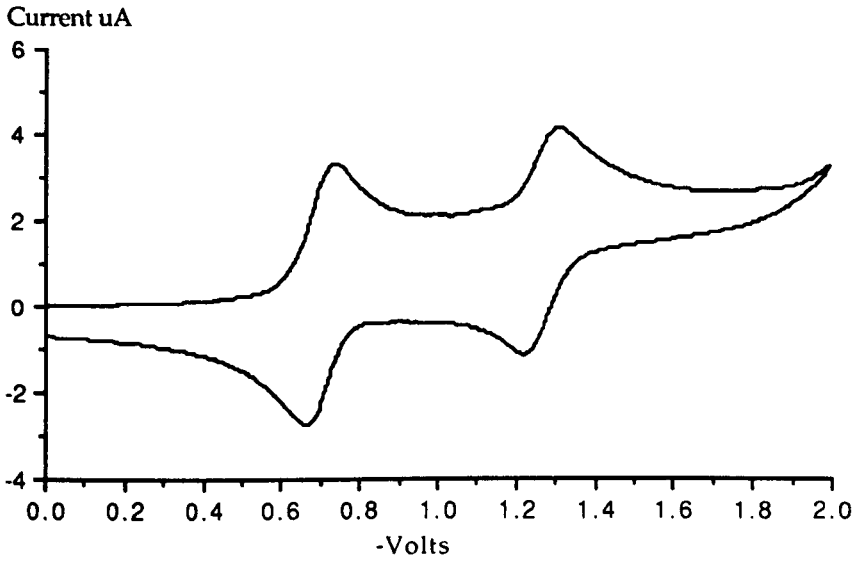

Figure 4.9(b): CV of (120) with 1≡ $LiClO_4$

Table 4.2: Peak potentials vs. Ag/AgCl for (120) with added lithium perchlorate

≡ $LiClO_4$	$E_p^{R_1}$	$E_p^{O_1}$	$E_p^{R_2}$	$E_p^{O_2}$	$E_p^{R_{1'}}$	$E_p^{O_{1'}}$	$E_p^{R_{2'}}$	$E_p^{O_{2'}}$
0.5	-1.151	-1.075	*ca.* -1.9	*ca.* -1.6	-0.725	-0.714 [a]	-1.308	-1.200
1	-	-	-	-	-0.739	-0.665	-1.312	-1.224
2	adsorption only							

Superscript R and O refer to reduction and oxidation peaks, R' and O' are the shifted potentials; a) some adsorption

Addition of sodium perchlorate had a similar effect to that of lithium, except that the shift in potential was not as great. At half an equivalent of sodium ions three peaks are visible with only a small hump indicating reduction of the free ligand to the dianion. When one equivalent of sodium ions is present only peaks for the complexed ligand can be seen. These are shown in Figures 4.10(a) and (b).

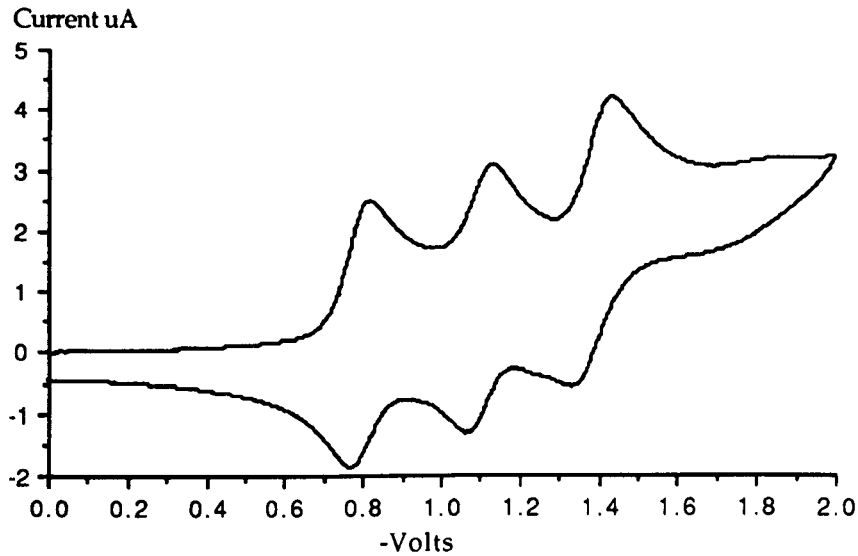

Figure 4.10(a): CV of (120) with 0.5≡ $NaClO_4$, sweep rate 200mVs^{-1}

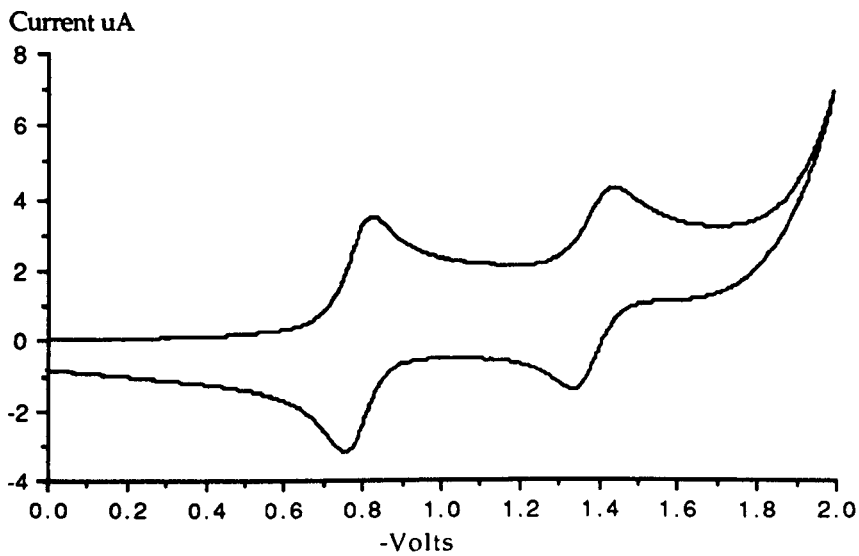

Figure 4.10(b): CV of (120) with 1≡ $NaClO_4$, sweep rate 200mVs^{-1}

When more than one equivalent was added the second reduction is suppressed and a new reaction takes place at high potential that is irreversible [Figure 4.10(c)]. If the sweep is reversed at a lower potential this reaction can be avoided, adsorption still takes place however after multiple scans. Conditioning potentials as high as -6V were subsequently required to clean the working electrode. Peak potentials are summarised in Table 4.3.

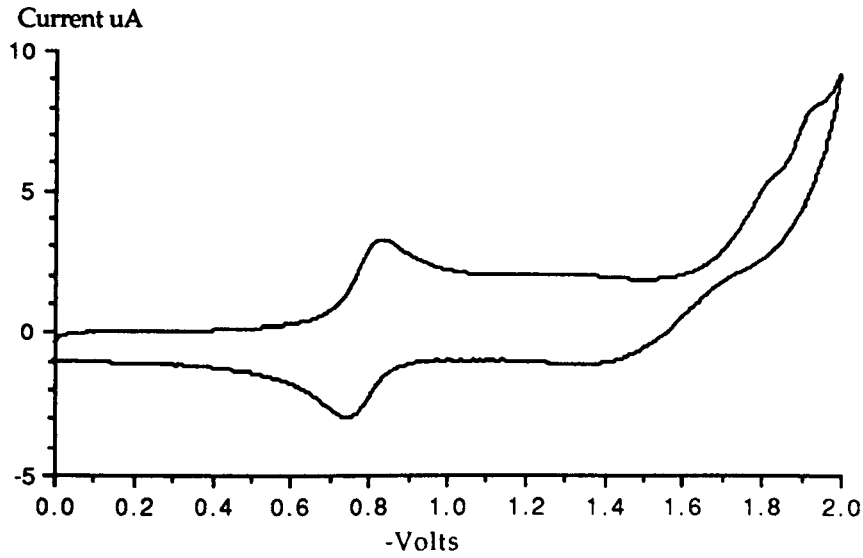

Figure 4.10(c): CV of (120) with 2≡ NaClO4, sweep rate 200mVs^{-1}

Table 4.3: Peak potentials vs. Ag/AgCl for (120) with added sodium perchlorate

≡$NaClO_4$	$E_p^{R_1}$	$E_p^{O_1}$	$E_p^{R_2}$	$E_p^{O_2}$	$E_p^{R_{1'}}$	$E_p^{O_{1'}}$	$E_p^{R_{2'}}$	$E_p^{O_{2'}}$
0.5	-1.132	-1.066	*ca.* -1.9	*ca.* -1.6	-0.820	-0.772	-1.434	-1.335
1	-	-	-	-	-0.829	-0.759	-1.443	-1.336
2	-	-	-	-	-0.841	-0.750	*ca.* -1.9	-

Superscript R and O refer to reduction and oxidation peaks, R' and O' are the shifted potentials.

The behaviour of compound (120) with potassium ions is somewhat different. With half an equivalent of potassium perchlorate present there are two new peaks present in the cyclic voltammogram, Figure 4.11(a). The first is rather broad and poorly resolved and its associated current less than that for the free ligand. This suggests that complexation is incomplete. The second peak, however is of an equal intensity to that of the free ligand, thus complexation continues to take place after reduction. When one equivalent of

potassium ions is present only two peaks remain, those for the complexed ligand, Figure 4.11(b). The first peak, however is still rather broad and has a shoulder in the tail region. Variable sweep rate experiments were then performed and two peaks were resolved at a sweep rate of $5Vs^{-1}$ (Figure 4.12). This confirmed that rapid complexation was taking place after reduction as at this sweep rate reduction of the ligand competes with complexation. Peak potentials are given in Table 4.4.

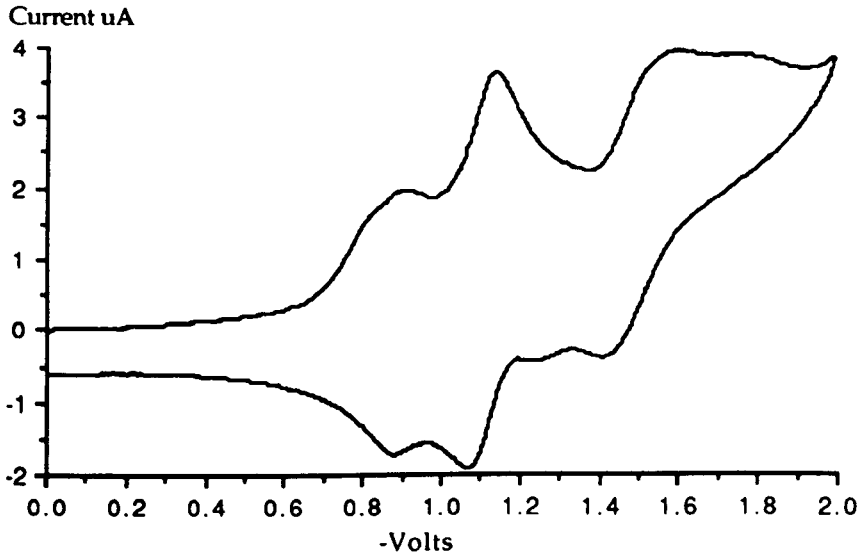

Figure 4.11(a): CV of (120) with 0.5≡ $KClO_4$, sweep rate $200mVs^{-1}$

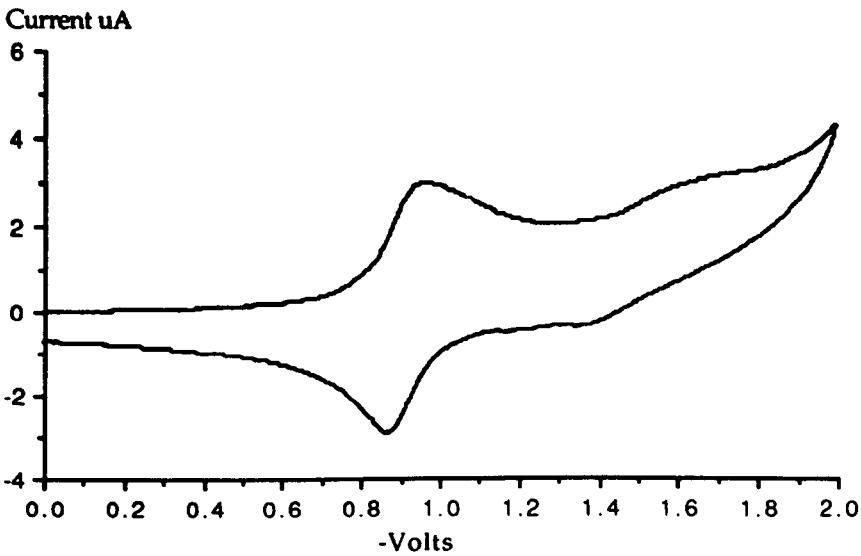

Figure 4.11(b): CV of (120) with 1≡ $KClO_4$, sweep rate $200mVs^{-1}$

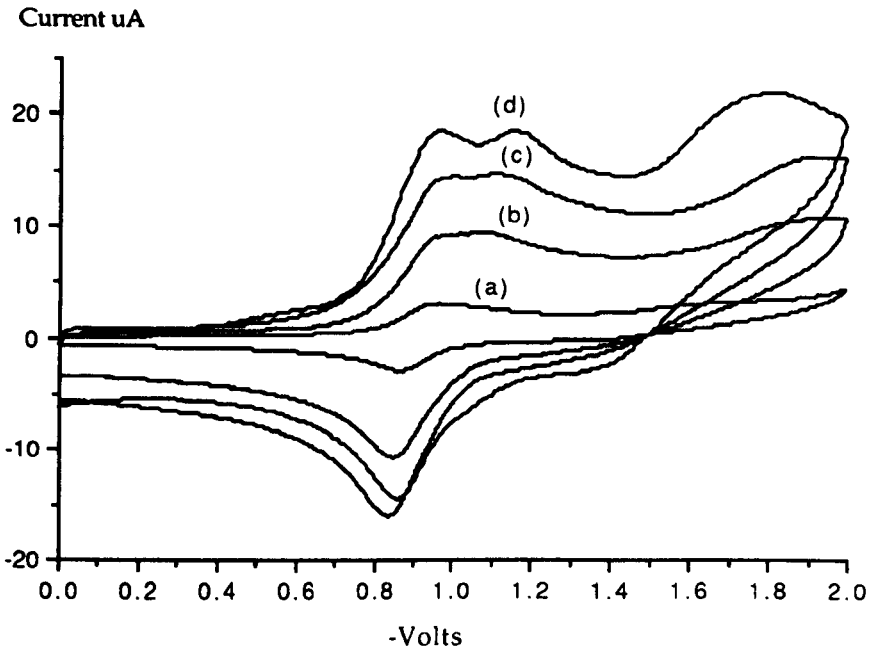

Figure 4.12: Sweep rate dependence on the peak potentials for the (120)/$KClO_4$ interaction; (a) 200mVs^{-1}, (b) 1Vs^{-1}, (c) 4Vs^{-1} (d) 5Vs^{-1}

Table 4.4: Peak potentials vs. Ag/AgCl for (120) with added potassium perchlorate

≡$KClO_4$	$E_p^{R_1}$	$E_p^{O_1}$	$E_p^{R_2}$	$E_p^{O_2}$	$E_p^{R_1'}$	$E_p^{O_1'}$	$E_p^{R_2'}$	$E_p^{O_2'}$
0.5	-1.142	-1.067	*ca.* -1.8	*ca.* -1.5	-0.918	-0.879	-1.598	-1.413
1	-	-	-	-	-0.968	-0.866	*ca.* -1.6	*ca.* -1.4
2	-	-	-	-	-0.992	-0.839	-	-

Superscript R and O refer to reduction and oxidation peaks, R' and O' are the shifted potentials.

When two equivalents of potassium are present the second reduction peak is inhibited but the first peak is unchanged. There is, however, eventual adsorption after multiple scans. Electrode conditioning restored the original behaviour.

The addition of rubidium or caesium perchlorates had little effect on the electrochemical behaviour of (120). Rubidium ions shifted the second peak to a lower potential but had no significant effect, other than ion pairing, upon the first reduction. Caesium ions also had only an ion pairing effect on the on the first reduction and appeared to inhibit the second reduction. Both these ions led to adsorption when greater than one equivalence of metal ion was present. Peak potentials are given in Table 4.5

Table 4.5: Peak potentials vs. Ag/AgCl for (120) with added metal perchlorate

M^+	≡	$E_p^{R_1}$	$E_p^{O_1}$	$E_p^{R_2}$	$E_p^{O_2}$	$E_p^{R_{1'}}$	$E_p^{O_{1'}}$	$E_p^{R_{2'}}$	$E_p^{O_{2'}}$
Rb	0.5	-1.133	-1.066	-	-	-1.133	-0.924	-1.568	-1.444
	1	-	-	-	-	-1.123	-0.902	-	-
	2	-	-	-	-	-1.125	-0.892	-	-
Cs	0.5	-1.133	-1.054	-	-	-1.133	-1.054	-	-
	1				adsorption only				
	2				adsorption only				

Superscript R and O refer to reduction and oxidation peaks, R' and O' are the shifted potentials.

As the system displayed a degree of irreversibility binding enhancements will be calculated using the values of the peak potential at one equivalent of metal, as these were the most reproducible. Only shifts in the first peak will be considered as these are not due solely to ion pairing. The shifts in peak potentials are summarised in Table 4.6

Table 4.6: Summary of the shifts in the peak potentials for (120)

M^+	ΔE	BEF
Li^+	0.415	1.044×10^7
Na^+	0.325	3.138×10^5
K^+	0.186	1.398×10^3
Rb^+	0.021	2
Cs^+	0.021	2

The large enhancement seen for lithium ion is analogous to those reported previously[34,36,39,40,48] and is due in part to the strong electrostatic interaction between the radical anion and the highly surface charge dense lithium ion. Solvation effects also play a role in this enhancement as lithium ions are poorly solvated in acetonitrile, thus assisting complexation. That the ligand could still scavenge sodium ions in the presence of a *ca.* 2000 fold excess of lithium ions indicates that despite this large enhancement for lithium the ligand would prefer to complex sodium ions. With sodium ions there is also a substantial enhancement of binding upon reduction by a factor of more than 300,000, this is the largest enhancement yet reported for sodium ions. This is due to the excellent complementarity of the cavity and ion sizes. Again with potassium ions there is a large binding enhancement upon reduction by a factor of 1400, this too is the largest enhancement yet recorded for

potassium ions. Rubidium and caesium ions show no enhancement of binding upon reduction of the ligand indicating that these ions are too large to fit into the ionophoric cavity.

Electrochemistry of compound (127)

As with other compounds of this type[48] (127) displayed pseudo-reversible reduction behaviour. The CV of this compound is shown in Figure 4.12.

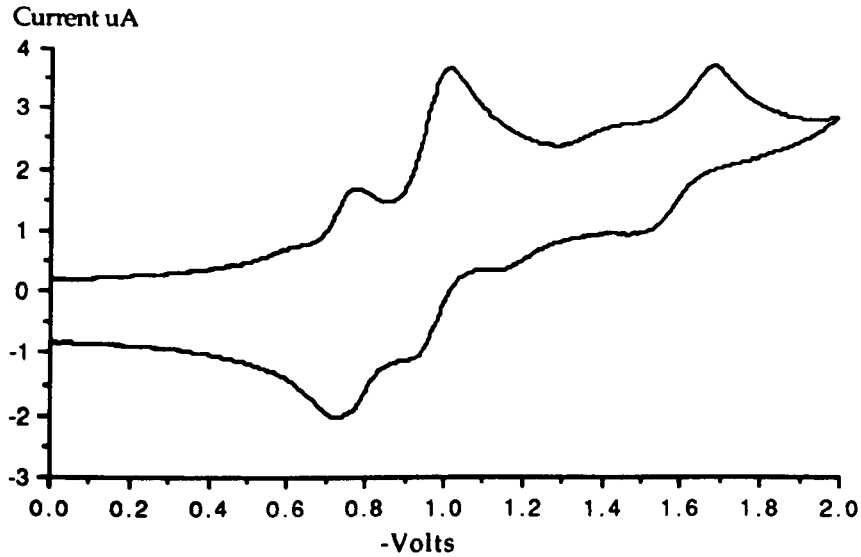

Figure 4.12: CV of compound (127), sweep rate 200mVs^{-1}

As with compound (120) the small peak at -778mV was believed to be due to sodium impurities present in the solvent or electrolyte or on the glass. This was later confirmed when sodium ions were added. The assignment of the peaks is in Table 4.7.

Table 4.7: Peak potentials for (127)

Potential/V	Assignment
-0.778	$LM^+ \rightarrow LM^{\cdot}$ (Na^+ impurity)
-1.014	$L \rightarrow L^{\pm\cdot}$
Shoulder at ca. -1.500	$LM^{\cdot} \rightarrow LM^-$ (Na^+ impurity)
-1.689	$L^{\pm\cdot} \rightarrow L^{2-}$
-1.484	$L^{2-} \rightarrow L^{\pm\cdot}$
Shoulder at ca. -1.15	$LM^- \rightarrow LM^{\cdot}$ (Na^+ impurity)
-0.908	$L^{\pm\cdot} \rightarrow L$
-0.708	$LH^- \rightarrow L$

It appears that when the dianion is formed that it is partially hydrated to form LH^-, this reaction does not reach completion on the experimental time-scale and consequently there is a small peak associated with the reaction $L^{2-} \rightarrow L^{\bullet-}$. Re-oxidation of the $LM^{\bullet}$ species is not directly observed as it is masked by the re-oxidation of LH^-. It is felt that this is not an important phenomenon as binding enhancements can only realistically be calculated using the first reduction wave. This is because ion pairing effects are much larger for the anthraquinone dianion. This view is supported by our own work [cf. compounds (**106**) and (**107**)] and that of Wolf and Cooper.[51a,b] Any binding enhancements based on shifts in the second reduction wave must be treated with some caution.

Addition of lithium ions had a dramatic effect on the electrochemical behaviour. The CV's for the addition of 0.5, and 1 equivalents of lithium perchlorate are shown in Figure 4.13(a) and (b). In the presence of half an equivalent of lithium perchlorate five peaks can be seen. These are assigned to reduction of the lithium complex, the sodium complex, the free ligand, the lithium/ligand complex $LM^{\bullet}$ to LM- and the free ligand to the dianion respectively. As with compound (**120**) complexation of lithium ions appears to be incomplete, as indicated by the lower current of the peak associated with the complex. The oxidation wave is also at the same potential as the reduction wave, indicating adsorption. There is a rather large peak associated with the sodium complex, suggesting a strong preference for sodium ions by the ligand. Increasing the lithium ion/ligand ratio to one increases the current associated with the Li^+ complex, reduction of both the free ligand and the sodium complex can still be seen however. This confirms that this ligand does indeed prefer sodium over lithium ions.

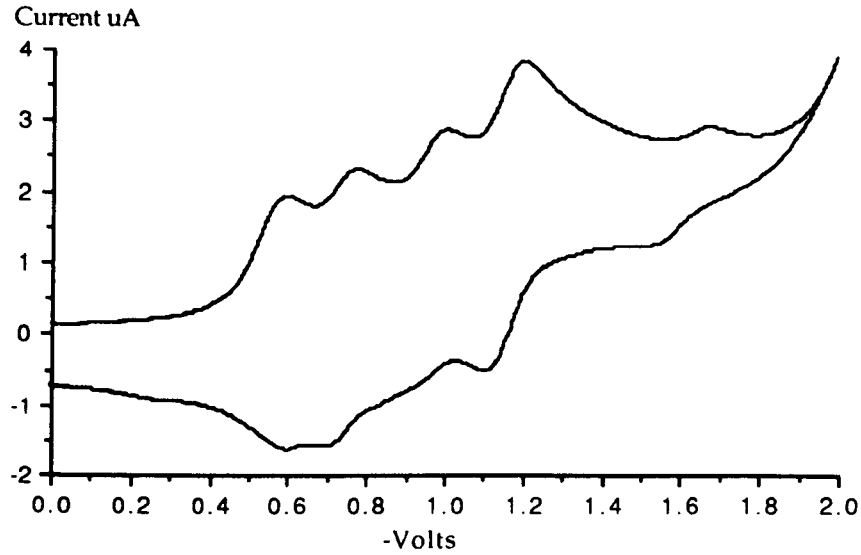

Figure 4.13(a): CV of (127) with 0.5≡$LiClO_4$, sweep rate 200mVs^{-1}

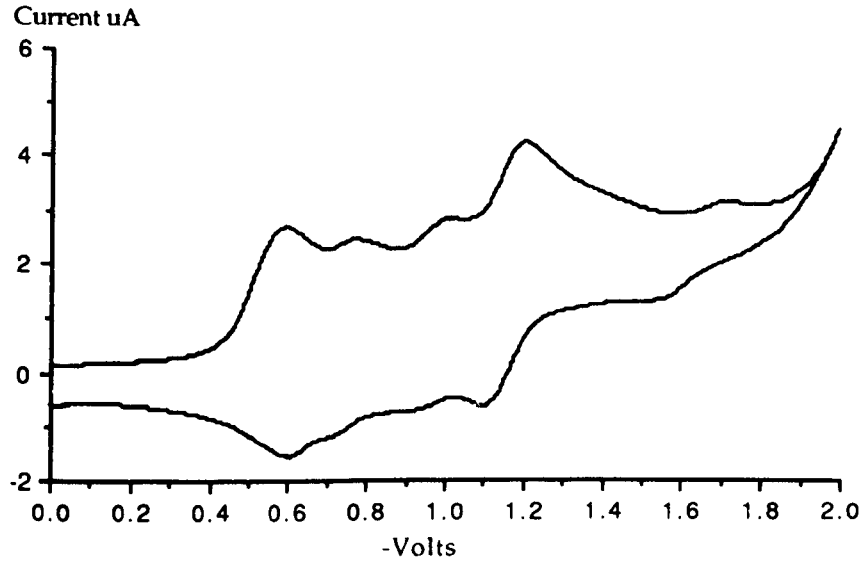

Figure 4.13(b): CV of (127) with 1≡$LiClO_4$, sweep rate 200mVs^{-1}

When an excess of lithium was added to the cell only irreversible adsorption was observed. The peak potentials (excluding those assigned to sodium) are given in Table 4.8.

Table 4.8:Peak potentials for (127) in the presence of lithium perchlorate.

≡$LiClO_4$	$E_p^{R_1}$	$E_p^{O_1}$	$E_p^{R_2}$	$E_p^{O_2}$	$E_p^{R_{1'}}$	$E_p^{O_{1'}}$	$E_p^{R_{2'}}$	$E_p^{O_{2'}}$
0.5	-1.005	a	-1.655	*ca.* -1.5	-0.608	-0.598	-1.200	-1.098
1	-1.024	a	-1.715	*ca.* -1.5	-0.598	-0.598	-1.206	-1.098
2	adsorption only							

Superscript R and O refer to reduction and oxidation peaks, R' and O' are the shifted potentials; (a) no peak could be discerned.

Upon the addition of sodium perchlorate to the solution a new peak for the sodium complex can be seen along with a broadening of the second reduction wave. The shift is not as great as that for lithium, but complexation does appear to be complete as with half an equivalent of sodium ions present the current values for the complex and the free ligand are equal. Increasing the numberof equivalents to one leads to the observation of reduction waves for the complex only. Cyclic voltammograms are shown in Figures 4.14(a) and (b).

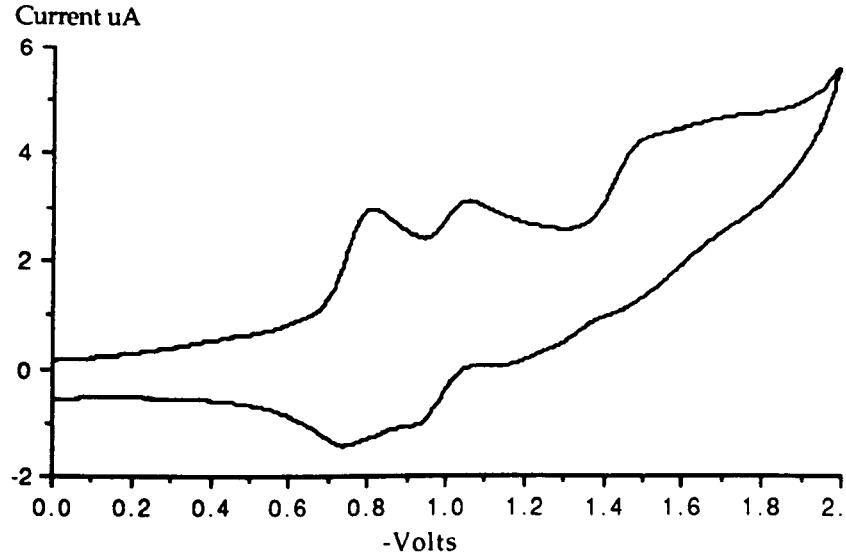

Figure 4.13(a): CV of (127) with 0.5 ≡ $NaClO_4$, sweep rate 200mVs^{-1}

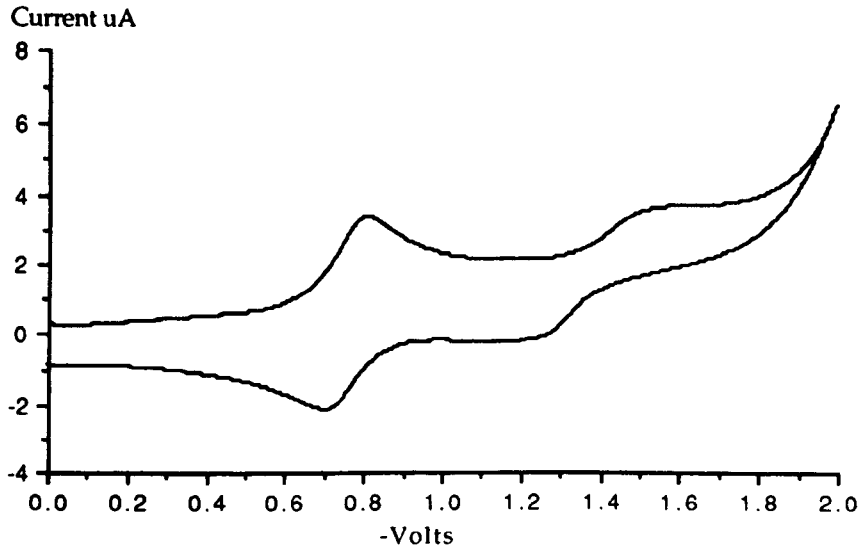

Figure 4.13(a): CV of (127) with 1 ≡ $NaClO_4$, sweep rate 200mVs^{-1}

As with lithium, increasing the sodium ion ratio to two led to adsorption only. Peak potentials are given in Table 4.9.

Table 4.9:Peak potentials for (127) in the presence of sodium perchlorate.

≡$NaClO_4$	$E_p^{R_1}$	$E_p^{O_1}$	$E_p^{R_2}$	$E_p^{O_2}$	$E_p^{R_{1'}}$	$E_p^{O_{1'}}$	$E_p^{R_{2'}}$	$E_p^{O_{2'}}$
0.5	-1.062	-0.906	*ca.* -1.7	a	-0.816	-0.740	*ca.* -1.5	a
1	-	-	-	-	-0.812	-0.705	-1.56	-1.200
2	adsorption only							

Superscript R and O refer to reduction and oxidation peaks, R' and O' are the shifted potentials; (a) no peak could be discerned.

Addition of potassium perchlorate shifted the potentials to a much lesser degree than for either sodium or lithium. At half an equivalent of added metal ion it is difficult to discern a peak associated with the potassium ion as there are three overlapping peaks for the sodium complex, the potassium complex and the free ligand. The second reduction wave is broadened slightly. Increasing the amount of potassium to one equivalent led to the observation of one peak with a large shoulder at a less cathodic value; this shoulder corresponds to the sodium complex. As with both lithium and sodium, only adsorption was observed when two equivalents of metal ion were added. Cyclic voltammograms for 0.5 and 1 equivalent of added metal ion are shown in Figures 4.14(a) and (b). Peak potentials are given in Table 4.10

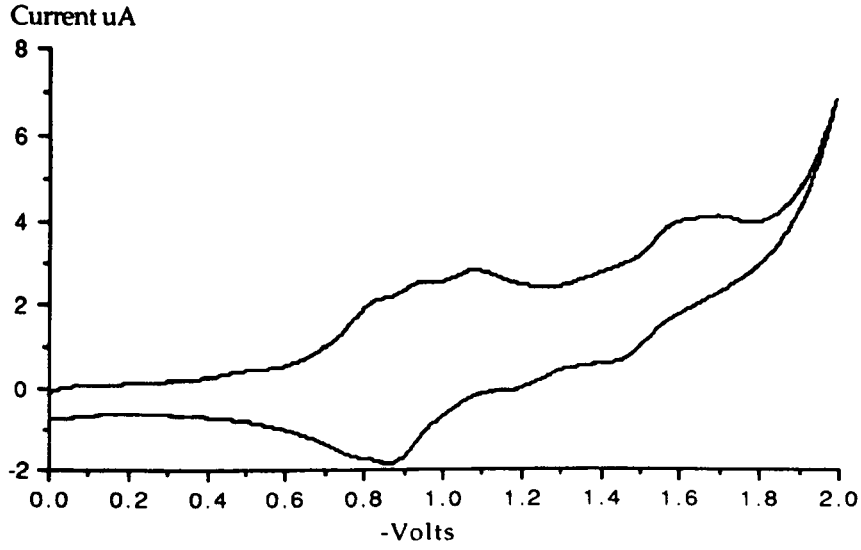

Figure 4.14(a): CV of (127) with 0.5 ≡ $KClO_4$, sweep rate 200mVs^{-1}

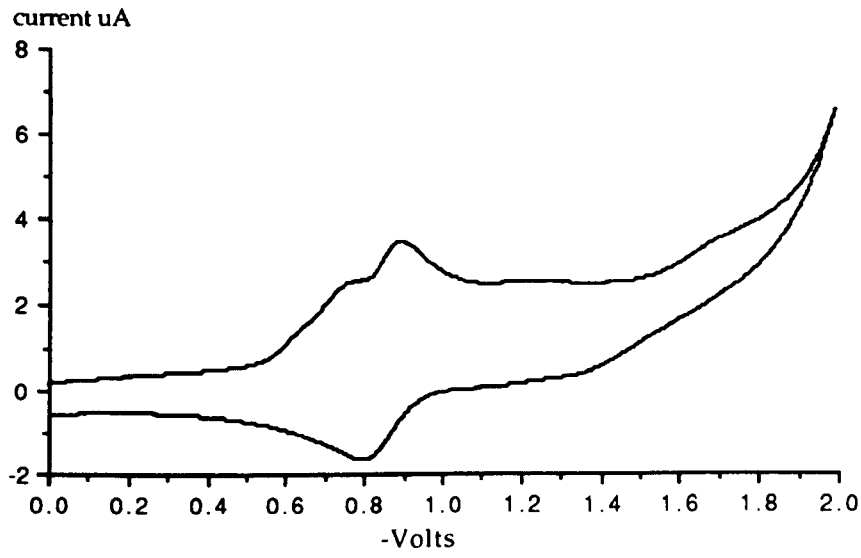

Figure 4.14(b): CV of (127) with 1 ≡ $KClO_4$, sweep rate 200mvs^{-1}

Table 4.10:Peak potentials for (127) in the presence of potassium perchlorate.

≡$KClO_4$	$E_p^{R_1}$	$E_p^{O_1}$	$E_p^{R_2}$	$E_p^{O_2}$	$E_p^{R_{1'}}$	$E_p^{O_{1'}}$	$E_p^{R_{2'}}$	$E_p^{O_{2'}}$
0.5	-1.09	a	*ca.* -1.7	a	*ca.* -0.95	-0.862	*ca.* -1.6	*ca.* -1.4
1	-	-	-	-	-0.895	-0.801	a	a
2	adsorption only							

Superscript R and O refer to reduction and oxidation peaks, R' and O' are the shifted potentials; (a) no peak could be discerned.

Addition of either rubidium or caesium perchlorates had no effect on the reduction potential and at greater than one equivalent led to adsorption. The potential shifts and binding enhancement factors are summarised in Table 4.11.

Table 4.11: Summary of the shifts in the peak potentials for (127)

M^+	ΔE	BEF
Li^+	0.416	1.077×10^7
Na^+	0.202	2.599×10^3
K^+	0.119	1.027×10^2
Rb^+	-	-
Cs^+	-	-

As with compound (120) there is a considerable binding enhancement for lithium ions. This appears not to be significant however given the compound's strong preference for sodium ions for which there is also a large binding enhancement. The enhancement for potassium ions is relatively small in comparison to that for sodium and here too the ligand

seemed to be able to scavenge sodium ions even in the presence of a large excess of potassium. This reflects the excellent "fit" of sodium ions to the cavity size. Simple extraction experiments could not be performed to assess this selectivity however, as insuffcient material remained after electrochemical measurements. For both rubidium and caesium ions there was no enhancement of binding, demonstrating that these ions are too large to be accommodated by the ionophoric cavity.

Electrochemistry of compound (128)

Compound (128) behaved in an analogous manner to both (120) and (127) in the absence of added metal ions. Its cyclic voltammogram is shown in Figure 4.15; peak potentials are given in Table 4.12.

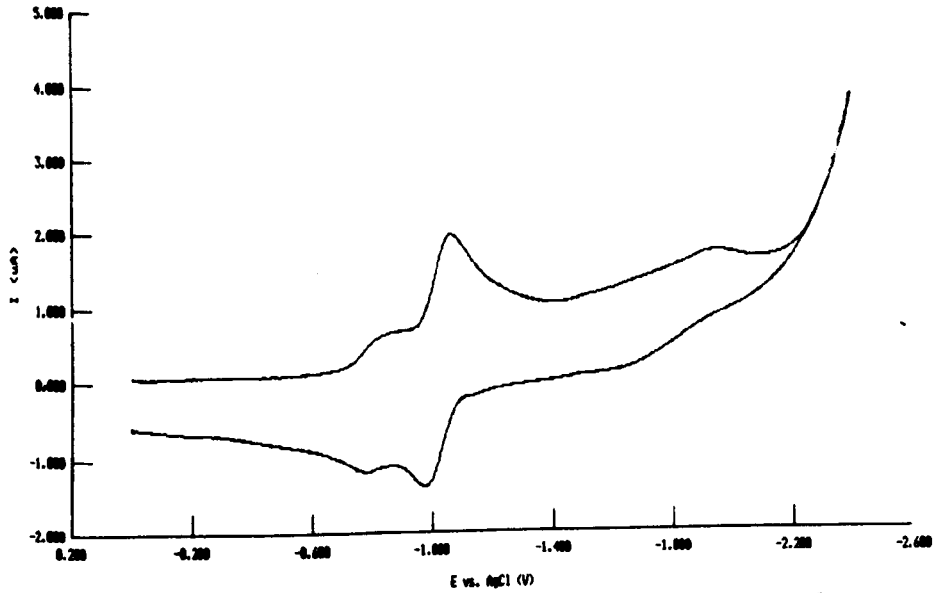

Figure4.15: CV of compound (127), sweep rate 200mVs^{-1}

Table 4.12: Peak potentials for (120)

$E_p^{R_1}$	$E_p^{O_1}$	$E_p^{R_2}$	$E_p^{O_2}$
-1.065	-0.9745	-1.951	*ca.* -1.6

Superscript R and O refer to reduction and oxidation peaks; all values are in volts relative to Ag/AgCl

As with both (120) and (127) there is a small pre-peak which is associated with sodium impurities. Again the addition of lithium ions has a large effect on the electrochemical behaviour, shifting both the first and the second reduction waves to less cathodic values. When half an equivalent of lithium is present two peaks for reduction of the complex and two for the free ligand can be seen. As with both the prevous compounds complexation appears to be incomplete as indicated by the difference in current of the first set of peaks i.e. the current for the complex is lower than that for the free ligand. There is also a small peak at *ca.* -0.9V which is associated with the sodium complex. Increasing the amount of lithium to one equivalent reduces the CV to that for the complex only. There is still a small peak visible however, for the sodium complex. When two equivalents of lithium perchlorate are present only adsorption is observed. Cyclic voltammograms of (128) with 0.5 and 1 equivalents of lithium perchlorate present are shown in Figures 4.16(a) and (b). Peak potentials are reported in Table 4.13.

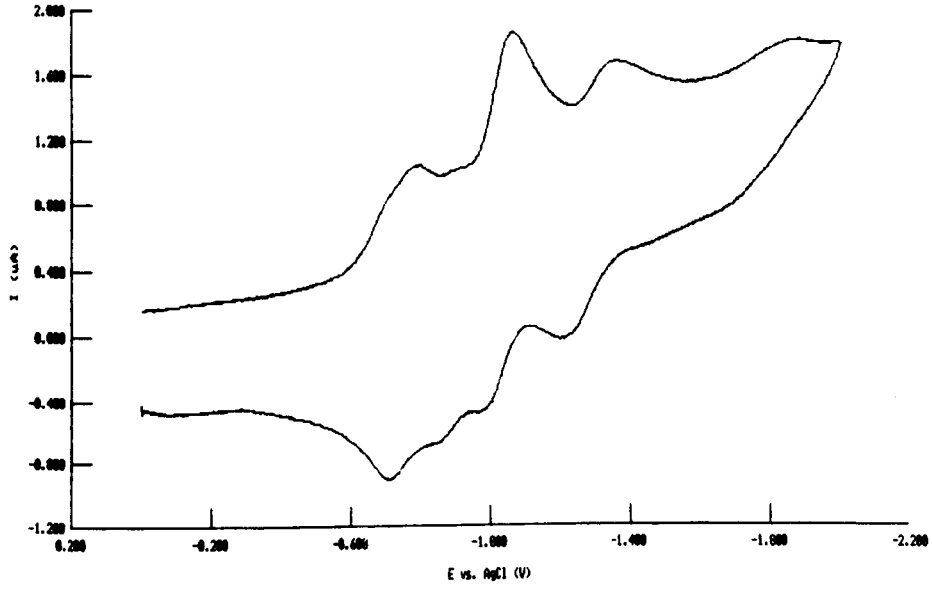

Figure 4.16(a): CV of (128) with 0.5 ≡ $LiClO_4$, sweep rate 200mVs^{-1}.

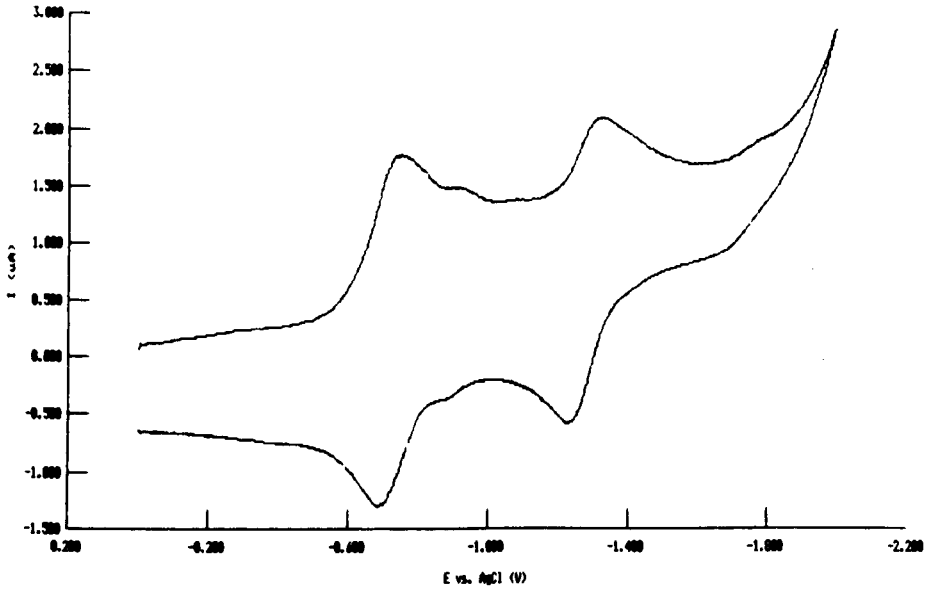

Figure 4.16(b): CV of (128) with 1 ≡ $LiClO_4$, sweep rate 200mVs^{-1}.

Table 4.13:Peak potentials for (128) in the presence of lithium perchlorate.

≡$LiClO_4$	$E_p^{R_1}$	$E_p^{O_1}$	$E_p^{R_2}$	$E_p^{O_2}$	$E_p^{R_{1'}}$	$E_p^{O_{1'}}$	$E_p^{R_{2'}}$	$E_p^{O_{2'}}$
0.5	-1.063	-0.97	-1.9	a	-0.796	-0.711	-1.363	-1.212
1	-	-	-	-	-0.754	-0.688	-1.474	-1.232
2	adsorption only							

Superscript R and O refer to reduction and oxidation peaks, R' and O' are the shifted potentials; (a) no peak could be discerned.

The addition of sodium ions also shifts the potentials to lower values. At half of an equivalent three peaks can be seen, which are be assigned to the reduction of the complex, the free ligand and the complex respectively. Increasing the amount of sodium to one equivalent leads to the observation of peaks for the complex only. Cyclic Voltammograms are shown in Figures 4.17(a), (b) and (c) with peak potentials given in Table 4.14.

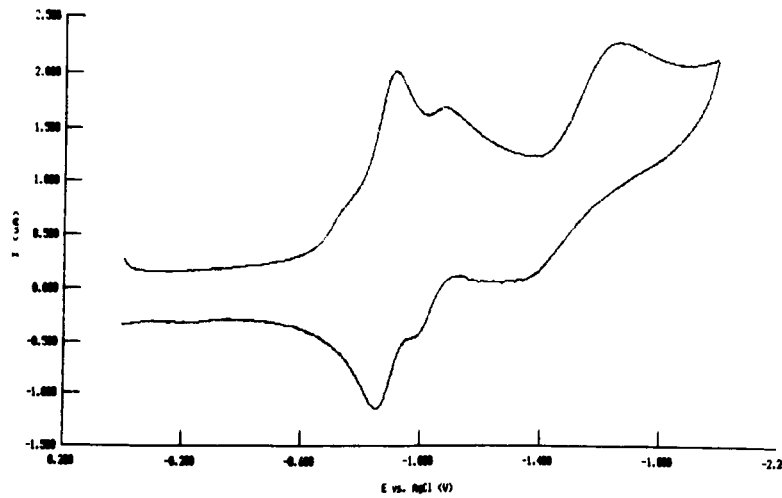

Figure 4.17(a): CV of (128) with 0.5 ≡ $NaClO_4$, sweep rate 200mVs^{-1}

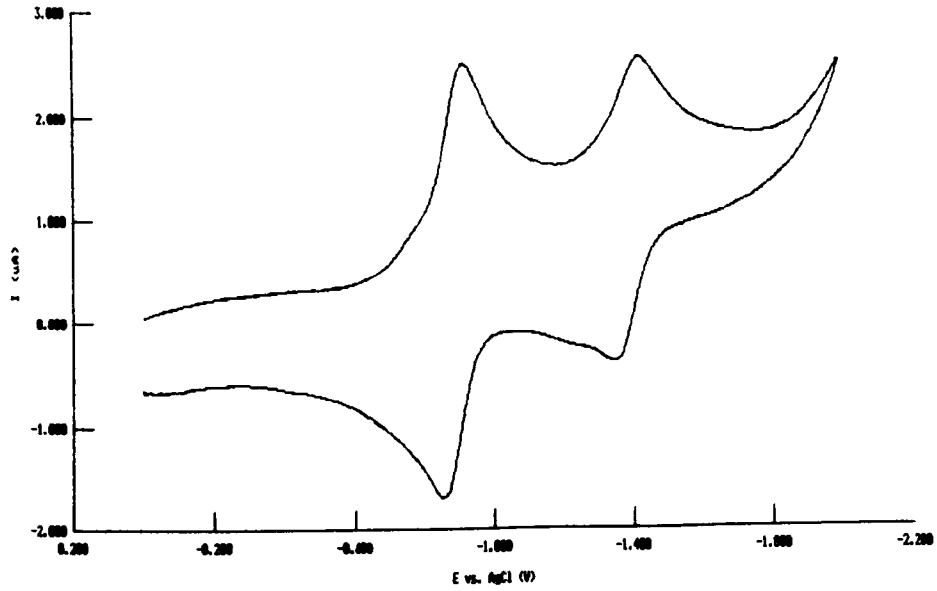

Figure 4.17(b): CV of (128) with 1 ≡ $NaClO_4$, sweep rate 200 mVs^{-1}.

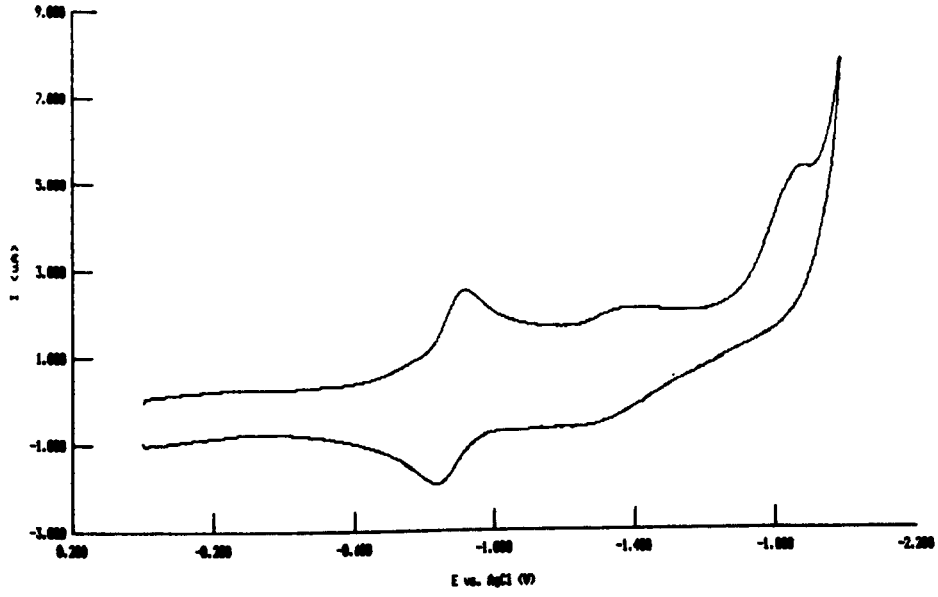

Figure 4.17(c): CV of (128) with 2 ≡ $NaClO_4$, sweep rate 200mVs^{-1}.

Table 4.14:Peak potentials for (128) in the presence of sodium perchlorate.

≡$NaClO_4$	$E_P^{R_1}$	$E_P^{O_1}$	$E_P^{R_2}$	$E_P^{O_2}$	$E_P^{R_{1'}}$	$E_P^{O_{1'}}$	$E_P^{R_{2'}}$	$E_P^{O_{2'}}$
0.5	-1.074	-0.97	a	a	-0.918	-0.856	-1.667[b]	-1.428
1	-	-	-	-	-0.918	-0.855	-1.425	-1.349
2	-	-	-	-	-0.920	-0.838	-1.398	a

Superscript R and O refer to reduction and oxidation peaks, R' and O' are the shifted potentials; (a) no peak could be discerned; (b) this peak is broad and may be two overlapping peaks.

Examination of Table 4.14 shows that when two equivalents of sodium are present adsorption is not seen, as was the case for both (120) and (127) with almost all the metals studied (the exception is compound (120) with potassium ions). There is, however an irreversible reaction which takes place at high potential. The reversible behaviour of (128) with sodium ions could be maintained for over 20 consecutive cycles, with eventual adsorption, provided the sweeps were reversed at -1.2V vs. Ag/AgCl. Conditioning of the working electrode at a relatively low potential (-3V) restored the previous behaviour.

Addition of potassium ions had relatively little effect on the electrochemical behaviour of (128). There is a small shift in the first reduction wave and a somewhat larger one for the second wave. At half an equivalent of potassium the first peak is quite broad; it is uncertain therefore whether this is a shifted peak for the free ligand or two very close overlapping peaks. It has been assigned to the complex as the oxidation peak associated with it is closer in magnitude to that for the complex. Cyclic voltammograms are shown in Figures 4.18(a), (b) and (c) with peak potentials given in Table 4.15.

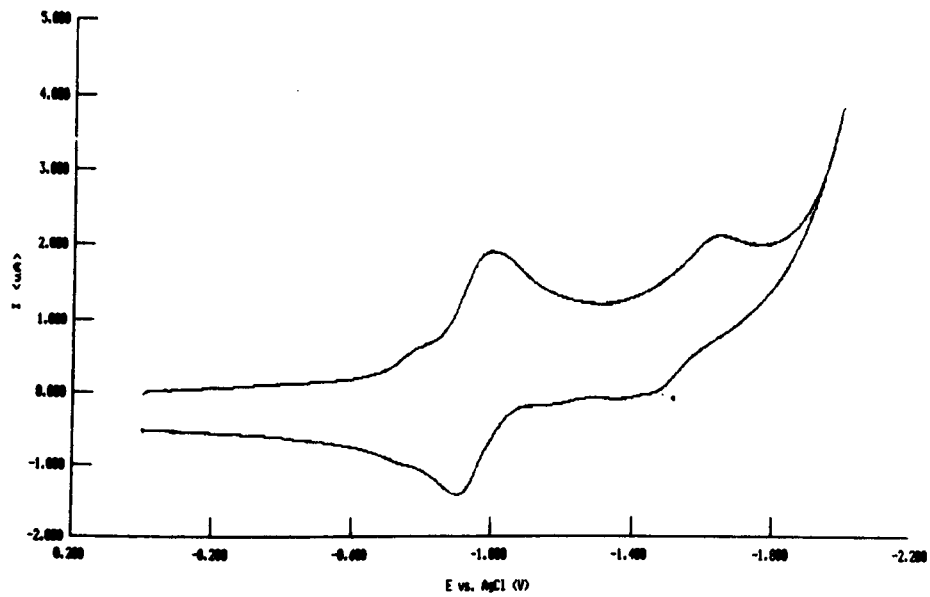

Figure 4.18(a): CV of (128) with 0.5 ≡ $KClO_4$, sweep rate 200mVs^{-1}.

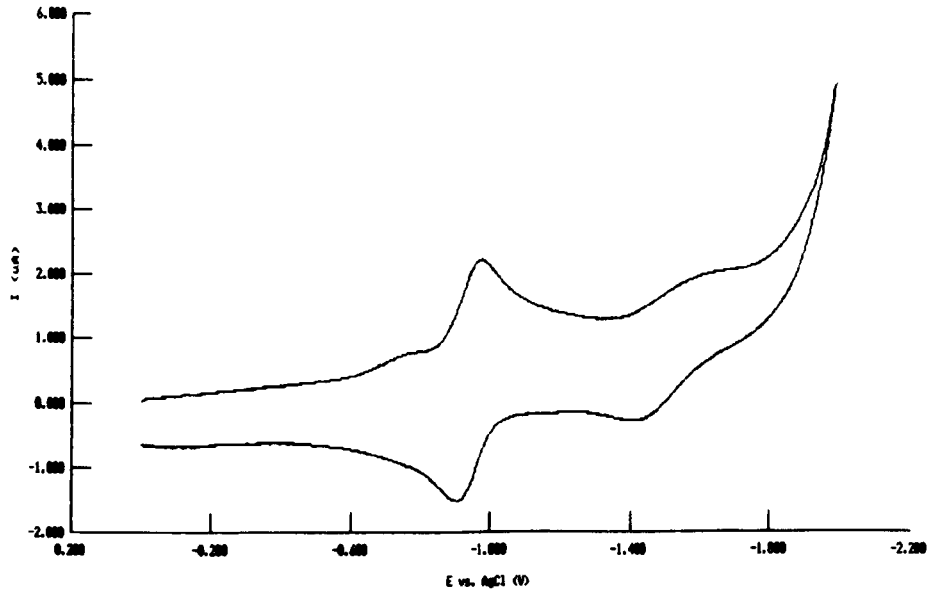

Figure 4.18(b): CV of (128) with 1 ≡ $KClO_4$, sweep rate 200mVs^{-1}.

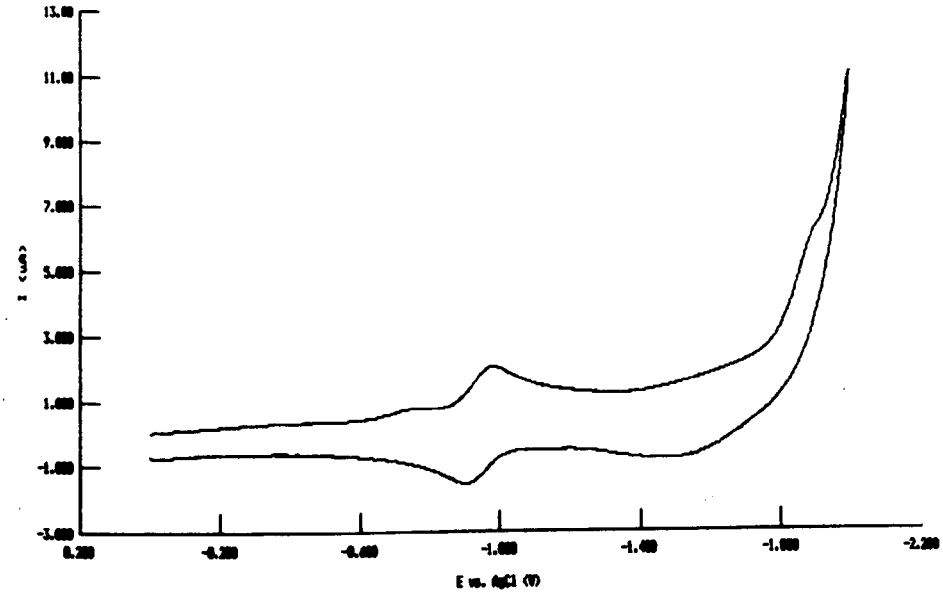

Figure 4.18(c): CV of (128) with 2 ≡ $KClO_4$, sweep rate 200mVs^{-1}.

Table 4.15:Peak potentials for (128) in the presence of potassium perchlorate.

≡$KClO_4$	$E_P^{R_1}$	$E_P^{O_1}$	$E_P^{R_2}$	$E_P^{O_2}$	$E_P^{R_{1'}}$	$E_P^{O_{1'}}$	$E_P^{R_{2'}}$	$E_P^{O_{2'}}$
0.5	-	-	-	-	-1.000	-0.9064	-1.648	-1.365
1	-	-	-	-	-0.979	-0.903	-1.672	-1.412
2	-	-	-	-	-0.980	-0.907	a	a

Superscript R and O refer to reduction and oxidation peaks, R' and O' are the shifted potentials; (a) no peak could be discerned.

Both rubidium and caesium ions had no effect, other than ion pairing, on the electrochemical behaviour. The potential shifts in the first reduction wave and the binding enhancement factors are given in Table 4.16.

Table 4.16: Summary of the shifts in the peak potentials for (128)

M^+	ΔE	BEF
Li^+	0.269	3.526×10^4
Na^+	0.147	3.05×10^2
K^+	0.086	28
Rb^+	-	-
Cs^+	-	-

Although the binding enhancement for sodium is rather low, that for lithium is significantly lower than those observed previously[34,36,39,40,48]. This combined with the very low binding for potassium and the apparent selectivity for sodium ions makes this an excellent sodium ionophore. This is a consequence of the well defined cavity in the molecule. The diethyl amide functions in the side arms may also play a role in this selectivity as they restrict the size of the entrance to the cavity thus excluding potassium ions.

Chapter 5

Molecular Modelling

Modelling of compound (106)

The failure of compound (106) to show any enhancement of binding upon electrochemical reduction has two possible explanations. The first is that the amide proton can "quench" the charge on the quinone oxygen by either hydrogen bonding or via a direct proton transfer. This seems unlikely as the model compound (129) and its N-methyl counterpart (130) behaved in a similar manner. If hydrogen bonding or proton transfer were involved one would expect the electrochemical behaviour of these compounds to be different. The second explanation is that steric constraints prevent the anthraquinone from interacting with the ionophoric cavity of the calixarene. If a ball and stick model is made of compound (106) one intuitively places the anthraquinone outside the cavity. Assessment of any barrier to rotation of the anthraquinone into the metal binding cavity however requires more sophisticated modelling. This was carried out using the Tripos program Sybyl on a Silicon Graphics Indigo Workstation at ICI, Blackley.

The structure of compound (106) was initially minimised to find a local energy minimum. The contributions by the various components, i.e. bond strain, van der Waals interactions, to the total energy of this conformation are given in Table 5.1. The structure is shown in stick format in Figure 5.1 and in CPK format in Figure 5.2.

Table 5.1: Energies for compound (106) in one of the conformations in which the anthraquinone unit is outside the cavity

Bond stretching energy:	4·34
Angle bending energy:	13·101
Torsional energy:	24·922
Out of plane bending energy:	0·194
1-4 van der Waals energy:	8·346
van der Waals energy:	-34·873
1-4 Electrostatic energy:	17·606
Electrostatic energy:	-3·484
Total energy:	30·151 kcals/mol

*Figure 5.1: Compound (**106**) in stick format, the hydrogens have been removed for clarity.*

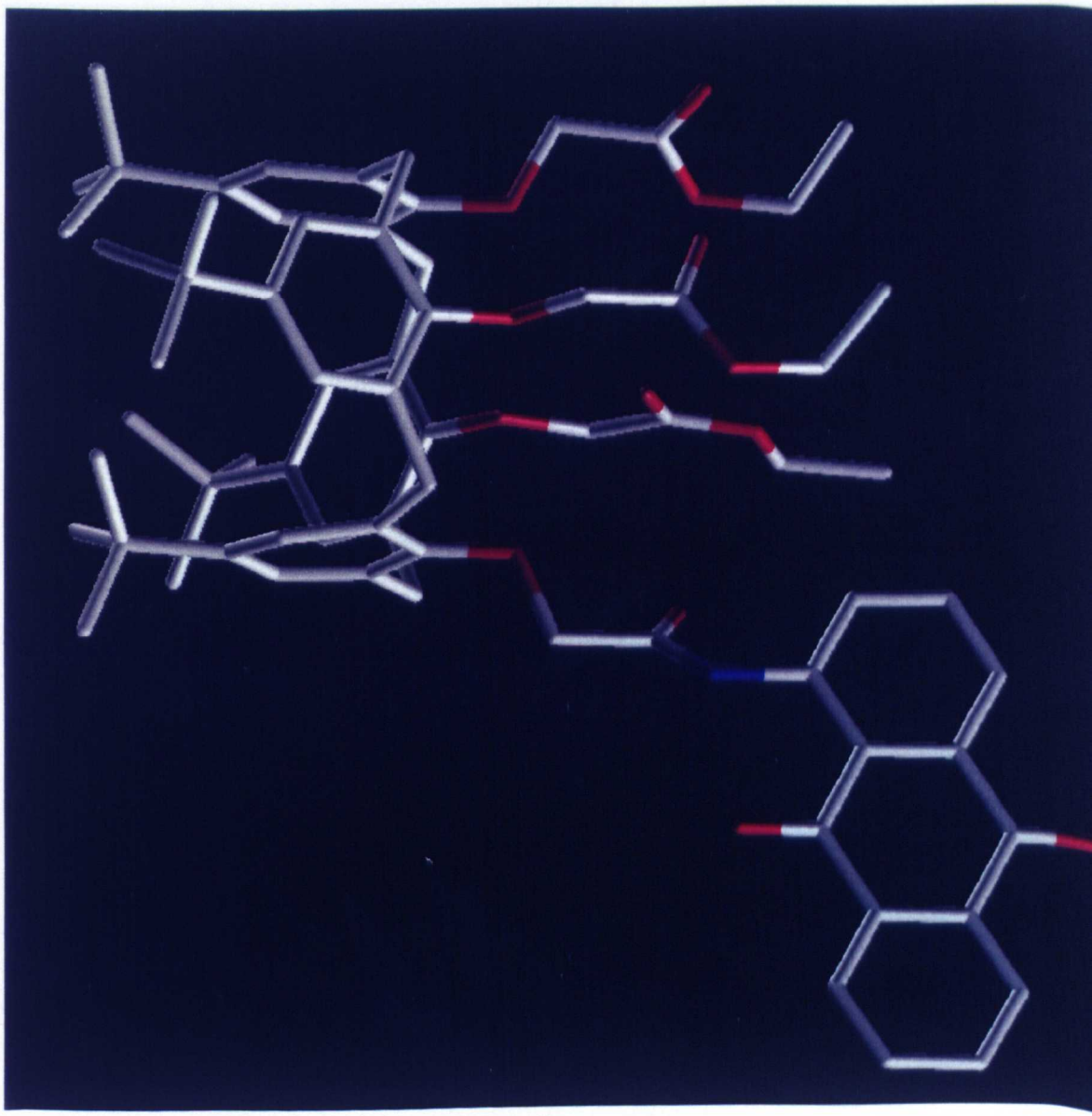

Carbon; white

Oxygen; red

Nitrogen; dark blue

*Figure 5.2: Compound (**106**) in CPK format*

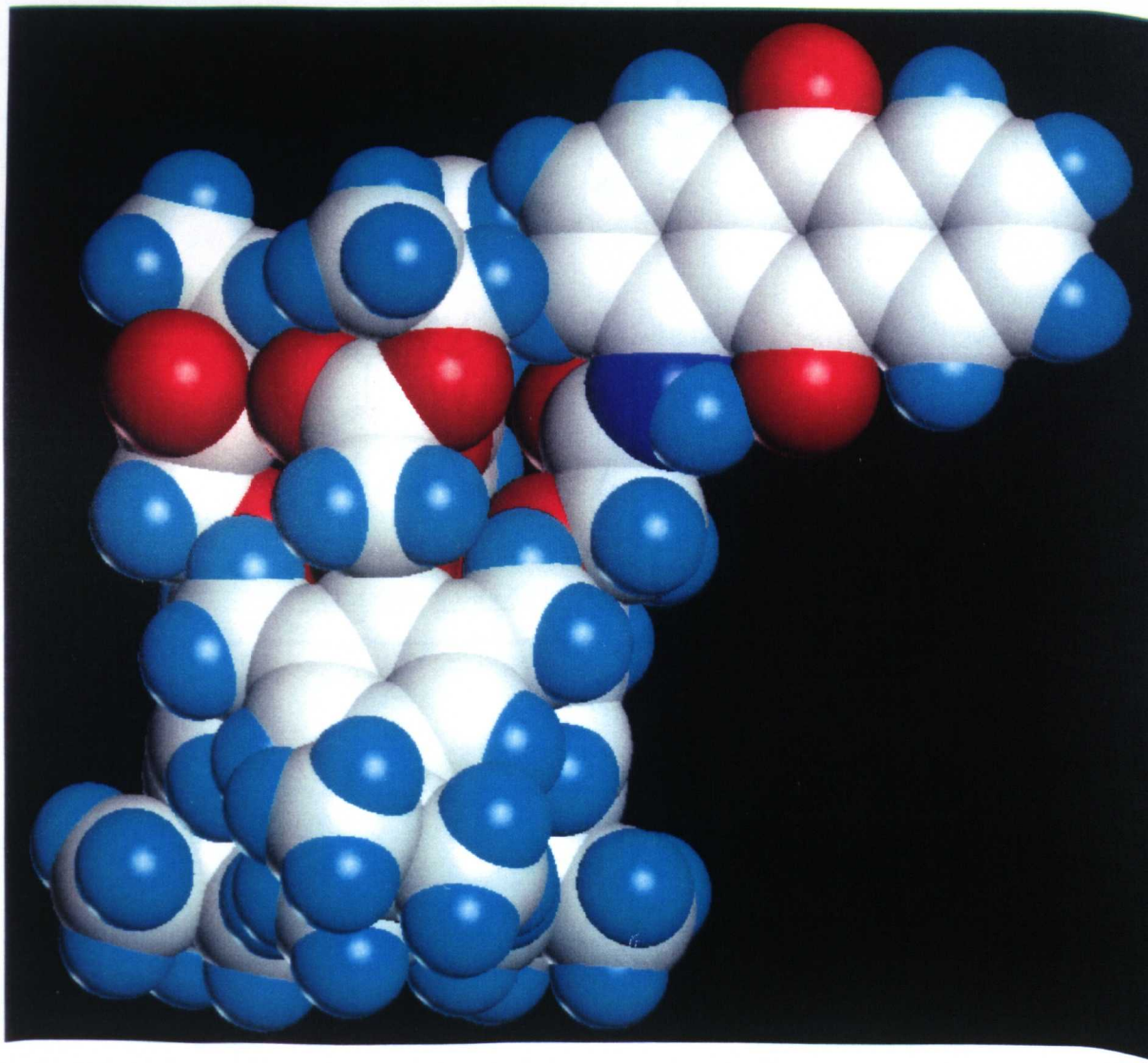

Carbon; white

Oxygen; red

Nitrogen; dark blue

Hydrogen; pale blue

A gridsearch was carried out on this compound in which the OCH_2—CONHAq bond was rotated about 360° in 15° steps as indicated in Fig 5.3. The energies for the conformations generated are given in Table 5.2

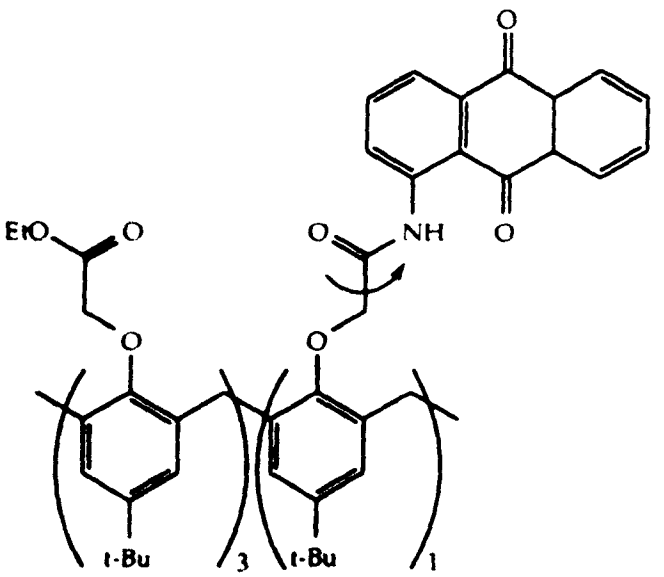

Fig 5.3

Table 5.2: Energies for the rotation of the OCH_2—CONHAq bond in compound (106)

Torsion/Deg	Energy/Kcal/mol
0	32·751
15	33·221
30	32·951
45	31·951
60	29·961
75	28·791
90	31·131
105	834·242
120	1482·873
135	2885·63
150	4714·673
165	31·721
180	44·641
195	2551·63
210	28·771
225	30·021
240	28·061
255	30·81
270	30·651
285	29·851
300	30·451
315	30·211
330	31·161
345	32·451
360	32·751

These energies are plotted versus the torsion angle of the OCH$_2$—CONHAq bond in Figure 5.4.

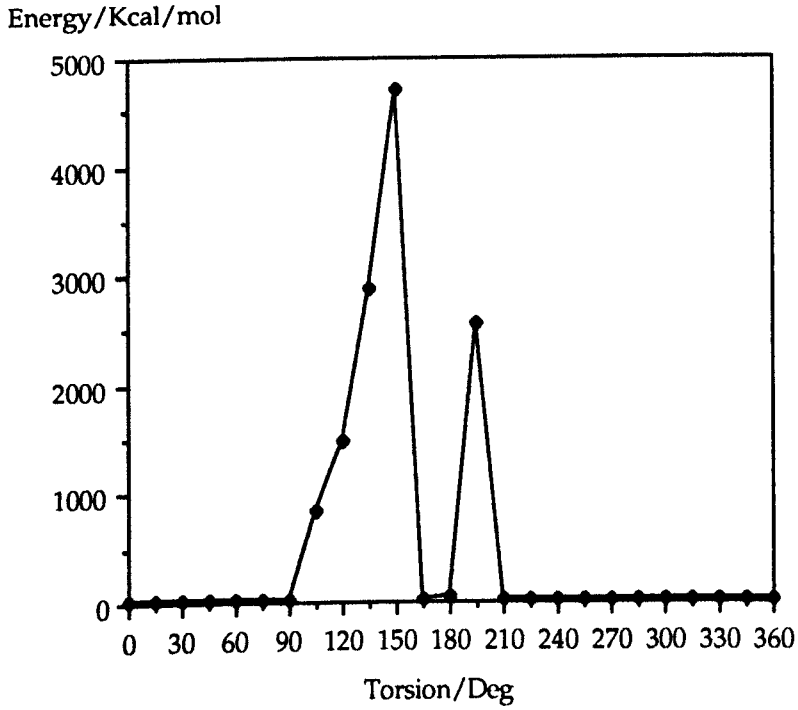

Figure 5.4: Energy Vs. Torsion angle between the OCH$_2$—CONHAq bond

This plot clearly shows that there is an energy barrier to rotation of the OCH$_2$—CONHAq torsion. The magnitude of this barrier is both high and unsymmetrical. The reason for this lies in the way in which the modelling program performs the rotation. The atoms are placed in their starting positions and the torsion angle then fixed at the relevant value. This occasionally results in a structure in which there is a serious conflict, e.g. an ethyl group poking through a ring of the anthraquinone. The program then attempts to minimise this structure. As it is unable to "drag" the ethyl group through the ring, rotate it out or disconnect, reposition and reconnect the group, the program simply performs the best minimisation that it can. This results in the unsymmetrical shape of the barrier and its unrealistically high value, 4687 kcal/mol above the lowest energy conformation. Figure 5.5 shows the structure for the torsion angle 105°, in which the energy is 834·242 kcal/mol (stick format, colour code as for Figure 5.1, hydrogens removed for clarity).

*Figure 5.5: Compound (**106**) at $\underline{O}\underline{C}H_2—\underline{C}\underline{O}NHAq$ torsion angle 105°, in stick format.*

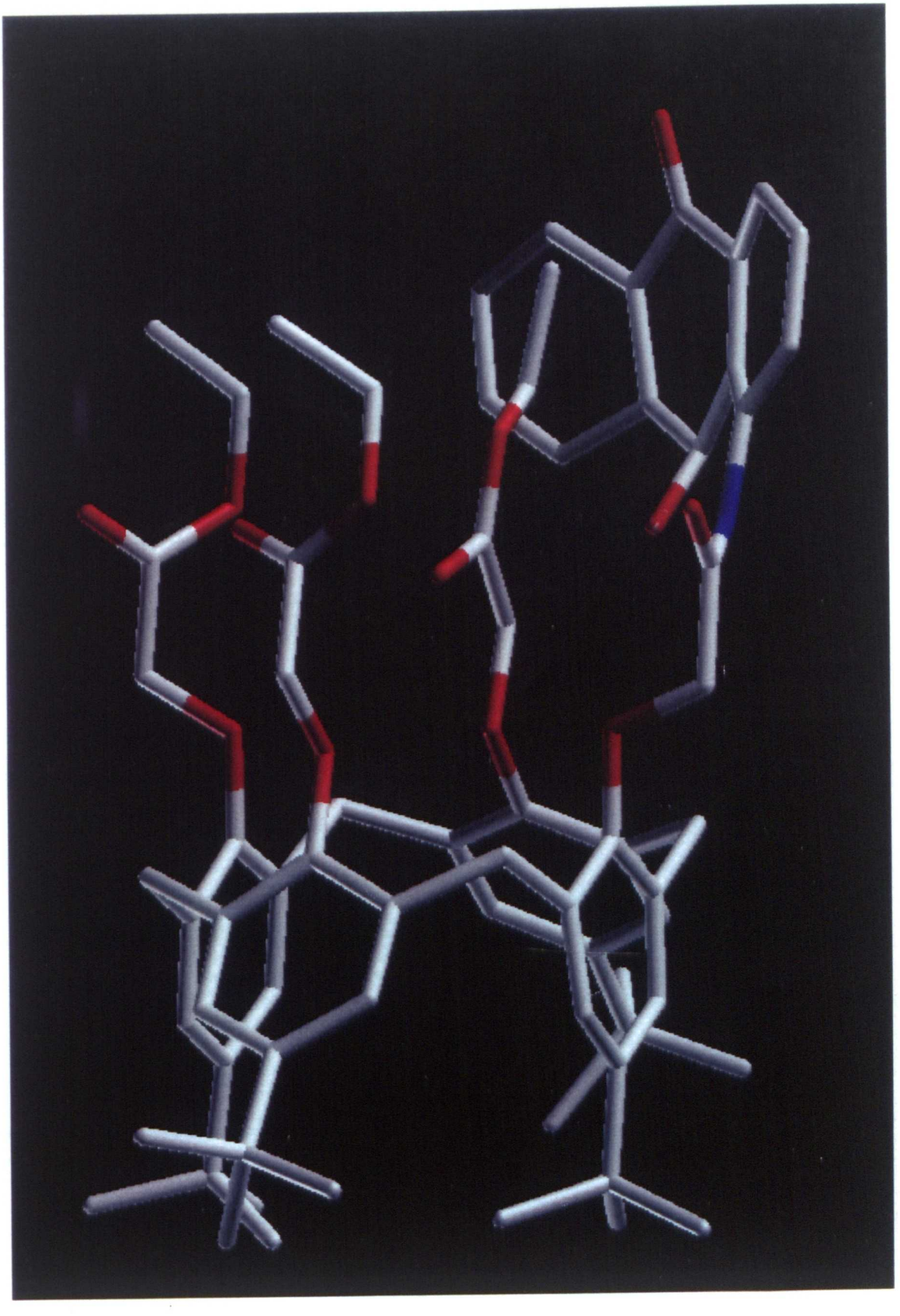

It can be seen that the anthraquinone is greatly distorted from its ideal planar geometry. Figure 5.6 shows the same structure in CPK format from a different angle, in this form it can be seen that there is a large steric interaction between the anthraquinone and the ester ethyl group. An analysis of the various contributions to the total energy clearly shows that the major contribution is from van der Waals interactions, i.e. steric interactions (Table 5.3).

Table 5.3: Energies for compound (106) in the conformations in which the anthraquinone unit is begining to interact with the ester groups.

Bond stretching energy:	72·845
Angle bending energy:	94·664
Torsional energy:	39·826
Out of plane bending energy:	94·081
1-4 van der Waals energy:	23·539
van der Waals energy:	494·891
1-4 Electrostatic energy:	17·727
Electrostatic energy:	-3·379
Total energy:	834·195 kcals/mol

A second feature of the plot is that there is an energy minimum of 31·721 kcal/mol at torsion angle 165° with a rise to 44·641 kcal/mol at 180°. It is not until the torsion angle reaches 195° that the energy rises dramatically again. The conformation in which the torsion angle is 165° is shown in stick format in Figure 5.7 and in CPK format in Figure 5.8. The energy values are given in Table 5.4

Table 5.4: Energies for compound (106) in the conformation in which the anthraquinone unit is inside the cavity defined by the ester groups.

Bond stretching energy:	4·605
Angle bending energy:	14·560
Torsional energy:	32·167
Out of plane bending energy:	0·236
1-4 van der Waals energy:	8·594
van der Waals energy:	-39·480
1-4 Electrostatic energy:	17·981
Electrostatic energy:	-6·940
Total energy:	31·723 kcals/mol

*Figure 5.6: Compound (**106**) at OCH$_2$—CONHAq torsion angle 105°, in CPK format.*

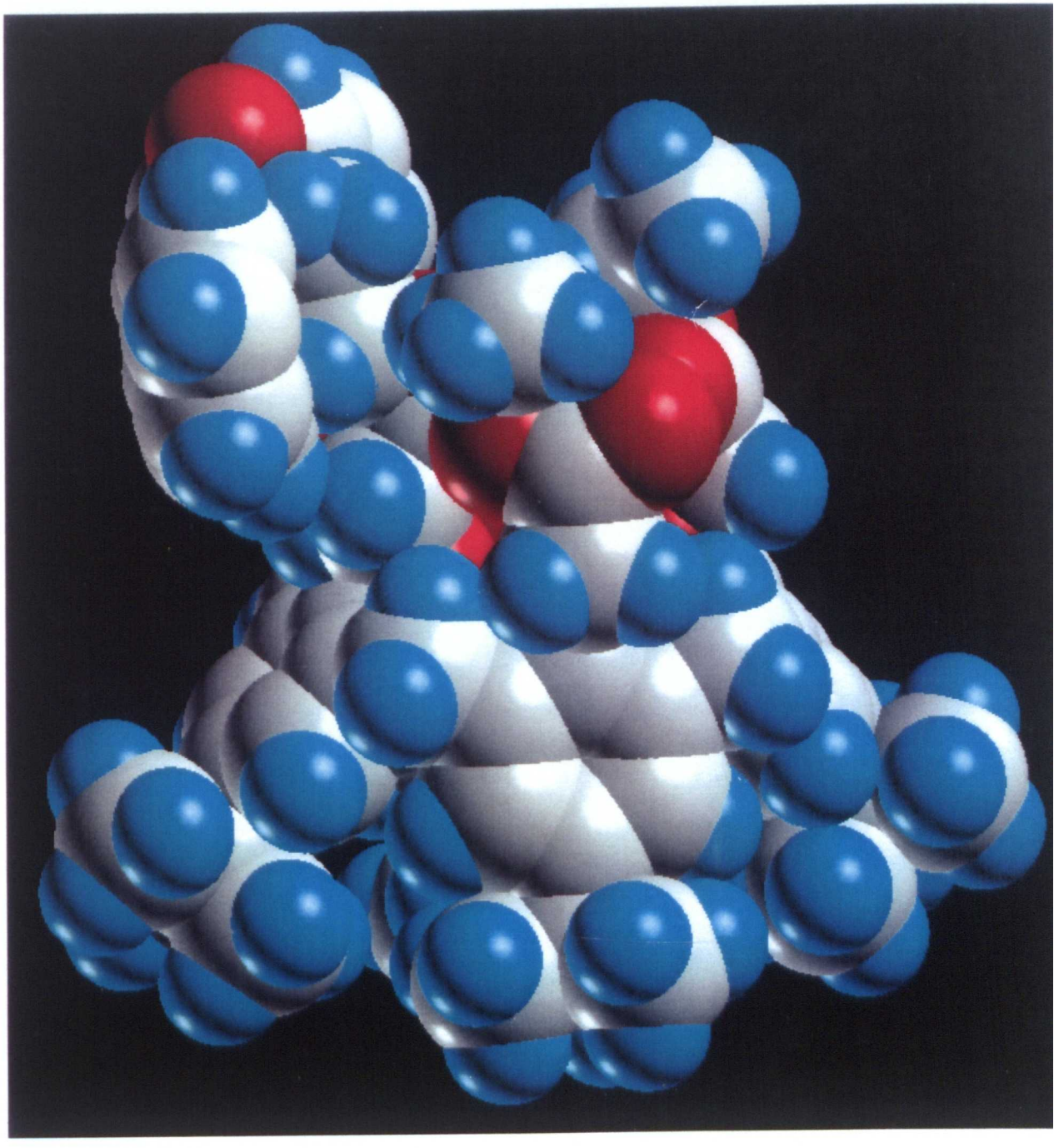

*Figure 5.7: Compound (**106**) at OCH$_2$—CONHAq torsion angle 165°, with the anthraqinone inside the cavity, in stick format*

*Figure 5.8: Compound (**106**) at* $\underline{OC}H_2$—$\underline{CO}NHAq$ *torsion angle 165°, with the anthraqinone inside the cavity, in CPK format*

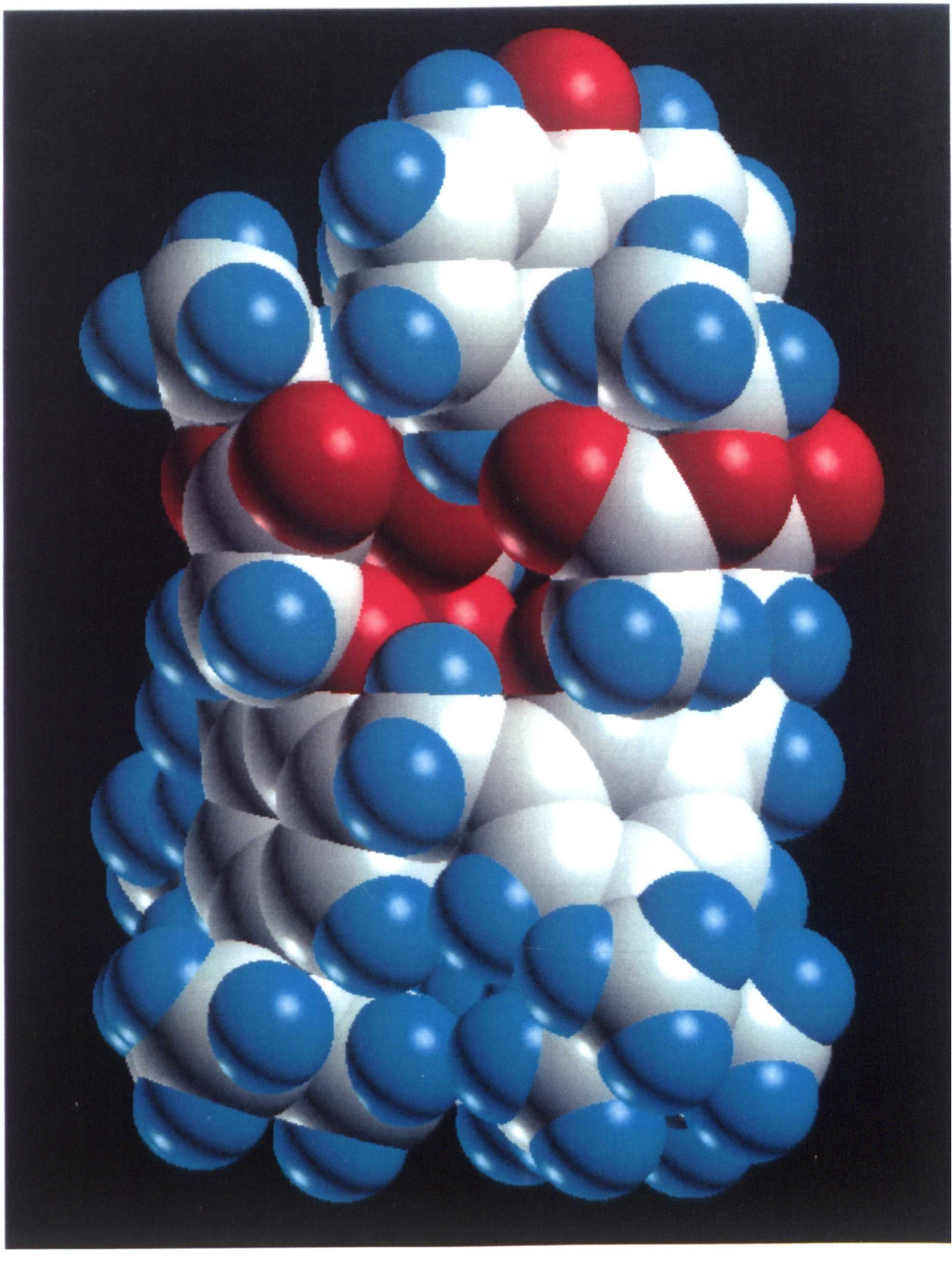

It is in this last conformation (torsion angle 165°) that the co-operative binding of the reduced anthraquinone and the ionophoric cavity was expected.

A similar search was performed on the rotation of the CONH—Aq bond in compound (**106**). This is not as important a rotation, for metal binding, as the OCH_2—CONHAq rotation since it does not bring the anthraquinone carbonyl function inside the cavity as effectively. This rotation, however also has a barrier to rotation (Table 5.5; Figure 5.9)

Table 5.5 : Energies for the rotation of the CONH—Aq bond in compound (**106**)

Torsion/Deg	Energy/Kcal/mol
0	33·77
15	33·89
30	30·58
45	30·42
60	31·63
75	33·72
90	34·98
105	33·96
120	32·43
135	32·03
150	32·58
165	36·52
180	42·67
195	2273·00
210	57·84
225	46·92
240	33·40
255	1009·36
270	36·06
285	31·09
300	30·15
315	30·23
330	31·27
345	33·55
360	33·77

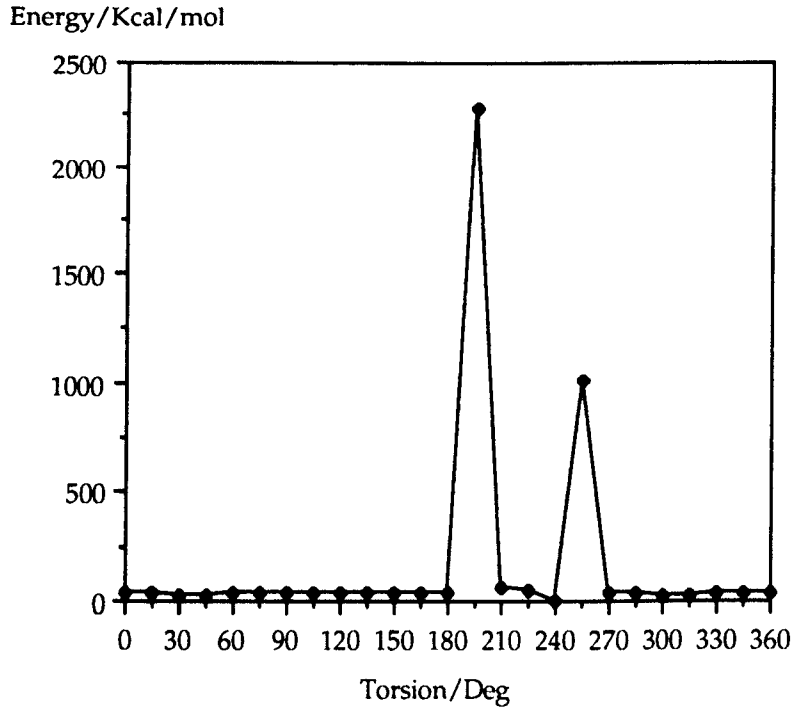

Figure 5.9: Ploy o f torsion angle Vs. Energy for the rotation of the CONH—Aq bond in compound (106)

A final search was performed on a modified version of compound (**106**) in which the ethyl groups of the ester functions were replaced by methyl groups to give compound (**131**). This reduces the size of the groups blocking the entry of the anthraquinone into the cavity and may lower the energy barrier sufficiently to facilitate rotation of the OCH_2—CONHAq bond. Thus the $\underline{OC}H_2$—$\underline{CO}$NHAq torsion was driven through 360° in 15° steps and a set of energies generated. These are given in Table 5.6 and plotted in Figure 5.10.

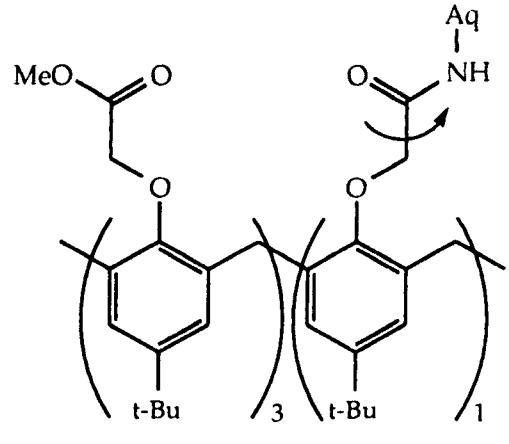

(**131**)

Table 5.6: Energies for the rotation of the CH_2—CO_2Me bond in compound (131)

Torsion/Deg	Energy/Kcal/mol
0	34·62
15	34·50
30	34·53
45	34·70
60	34·00
75	32·74
90	30·97
105	30·00
120	29·76
135	30·39
150	32·29
165	38·90
180	929·09
195	1782·23
210	1212·23
225	34·07
240	1959·75
255	91·04
270	36·23
285	32·00
300	32·15
315	32·64
330	33·44
345	34·03
360	34·62

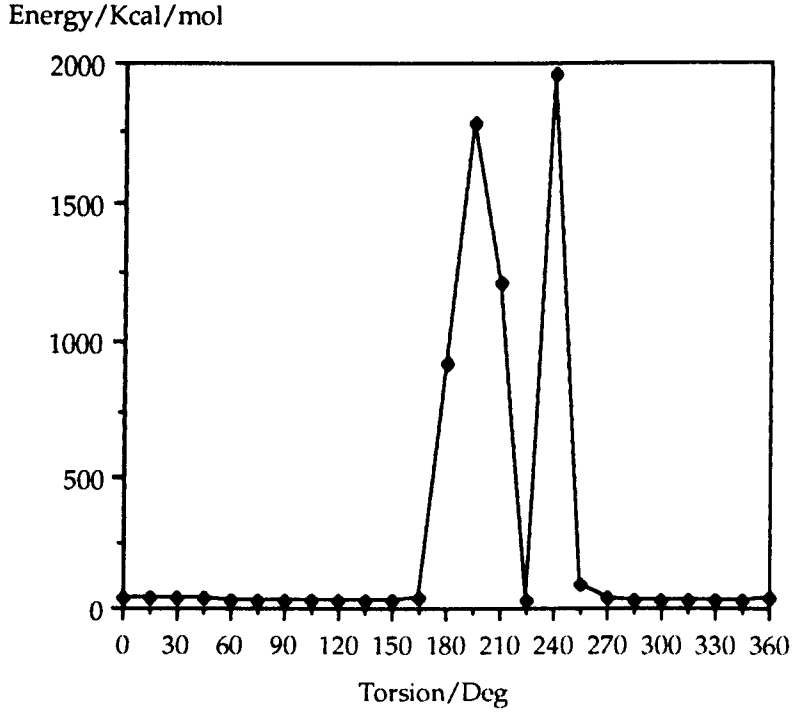

Figure 5.10: Plot of torsion angle vs. Energy for the rotation of the $\underline{O}CH_2$—$\underline{C}ONHAq$ bond in compound (131)

Again it can be seen that there is still a substantial barrier to the rotation of the OCH_2—CONHAq bond and that there is local minimum in which the anthraquinone is inside the cavity. On this evidence synthesis of compound (**131**) was not undertaken.

In the binding conformation of the compound (**59**), on which (**106**) was based, all the carbonyl functions are directed towards the centre of the cavity.[84,85] This is similar to the structure of the initial conformation of (**106**) [Fig. 5.1]. The energy barriers found in the modelling experiments demonstrate that in order for co-operative binding to take place many concerted molecular motions are required. One can conclude therefore that the rotation of the OCH_2—CONHAq is so severely restricted as to prevent the anthraquinone from moving to the inside of the cavity. Compound (**106**) therefore shows insufficient "pre-organisation" to act as an electrochemically enhanced ionophore. The molecular modelling experiments performed led us to abandon any further synthetic work towards compounds of this type.

Modelling of compound (120)

In compound (120) the anthraquinone is in a fixed position relative to the calixarene. Modelling of this compound was therefore restricted to finding the minimum energy conformation of the free ligand and the energies of the group I and calcium ion complexes. These energies are given in Tables 5.7-5.13. The free ligand is shown in stick format in Figure 5.11 and in CPK format in Figure 5.12.

Table 5.7: Energies for compound (120) as the free ligand.

Bond stretching energy:	3·895
Angle bending energy:	7·660
Torsional energy:	26·242
Out of plane bending energy:	0·078
1-4 van der Waals energy:	7·213
van der Waals energy:	-24·382
1-4 Electrostatic energy:	1·564
Electrostatic energy:	6·434
Total energy:	28·708 kcals/mol

Table 5.8: Energies for compound (120) as the Li^+ complex.

Bond stretching energy:	3·999
Angle bending energy:	8·388
Torsional energy:	25·126
Out of plane bending energy:	0·235
1-4 van der Waals energy:	8·454
van der Waals energy:	-25·256
1-4 Electrostatic energy:	1·972
Electrostatic energy:	-61·546
Total energy:	-38·546 kcals/mol

Table 5.9: Energies for compound (120) as the Na^+ complex.

Bond stretching energy:	3·833
Angle bending energy:	8·487
Torsional energy:	28·108
Out of plane bending energy:	0·381
1-4 van der Waals energy:	8·899
van der Waals energy:	-26·461
1-4 Electrostatic energy:	2·195
Electrostatic energy:	-62·597
Total energy:	-37·155 kcals/mol

*Figure 5.11: Compound (**120**) as the free ligand in stick fromat.*

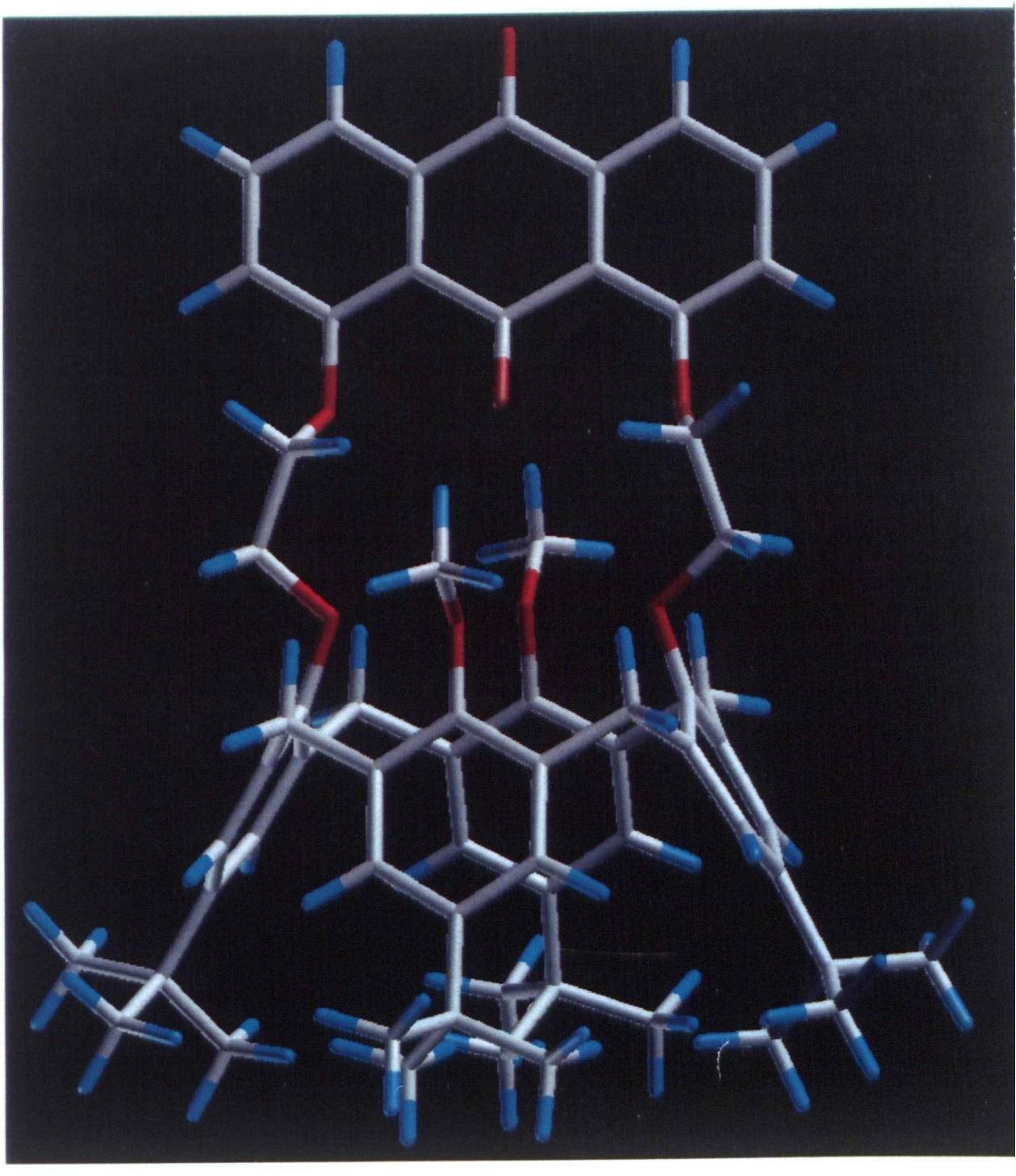

Figure 5.12: Compound (**120**) *as the free ligand in CPK fromat.*

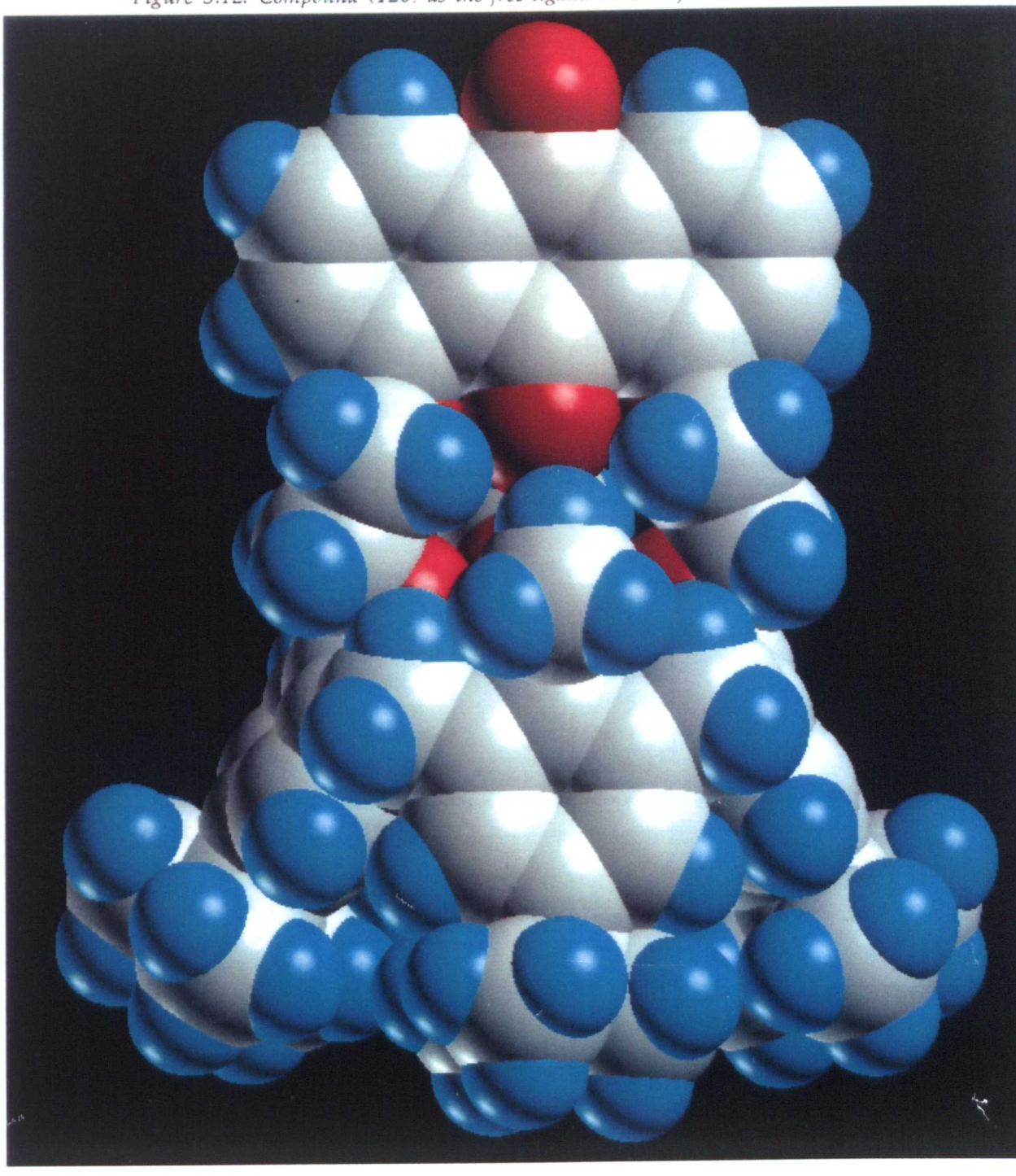

Table 5.10: Energies for compound (120) as the K^+ complex.

Bond stretching energy:	3·912
Angle bending energy:	8·364
Torsional energy:	24·784
Out of plane bending energy:	0·252
1-4 van der Waals energy:	8·902
van der Waals energy:	-25·052
1-4 Electrostatic energy:	1·990
Electrostatic energy:	-61·681
Total energy:	-38·531 kcals/mol

Table 5.11: Energies for compound (120) as the Rb^+ complex.

Bond stretching energy:	3·966
Angle bending energy:	7·518
Torsional energy:	26·574
Out of plane bending energy:	0·117
1-4 van der Waals energy:	6·790
van der Waals energy:	-17·184
1-4 Electrostatic energy:	2·429
Electrostatic energy:	-48·574
Total energy:	-18·363 kcals/mol

Table 5.12: Energies for compound (120) as the Cs^+ complex.

Bond stretching energy:	4·627
Angle bending energy:	8·541
Torsional energy:	28·758
Out of plane bending energy:	0·108
1-4 van der Waals energy:	5·696
van der Waals energy:	-13·719
1-4 Electrostatic energy:	2·612
Electrostatic energy:	-42·999
Total energy:	-6·376 kcals/mol

Table 5.8: Energies for compound (120) as the Ca^{2+} complex.

Bond stretching energy:	4·864
Angle bending energy:	12·557
Torsional energy:	24·606
Out of plane bending energy:	0·606
1-4 van der Waals energy:	10·933
van der Waals energy:	-18·254
1-4 Electrostatic energy:	2·625
Electrostatic energy:	-153·576
Total energy:	-115·576 kcals/mol

In the alkali metal series the energies of the Li^+, Na^+ and K^+ complexes are quite similar. If the energies followed the charge density of these ions the order of energies would be $Li^+ > Na^+ > K^+$. This suggests that compound (120) displays some selectivity towards potassium ions. The energies of the Rb+ and Cs+ complexes are both much smaller in magnitude than those for the Li^+, Na^+ and K^+ complexes; this indicates that these ions are too large to be accommodated in the cavity. The Ca^{2+} complexes energy however is large in magnitude, the largest contribution to this energy is the electrostatic energy. This is a charge density effect, the calcium ion is small and carries a charge of two. The other terms in the energy calculation are similar to those of the Rb^+ complex for which the "fit" is not good. There is also more strain in the Ca^{2+} complex. Calcium binding therefore is not likely to be very strong. In real situations the binding equilibrium will depend on the solvation state of the free M^+ ion and therefore the above energies must be viewed with some caution.

If we return to the series Li^+, Na^+ and K^+, selectivity between these ions is likely to be based on the complementarity of the cavity size and the ionic radius. Figures 5.11 and 5.12 however do not give much insight into the size of this cavity. Figure 5.11 does not show atomic radii and Figure 5.12 is crowded so that the donating oxygens cannot be seen. Figure 5.13 gives a better picture, here the donating oxygens are in CPK format and the rest of the molecule is in stick form. This shows the cavity size quite well. Figure 5.14 shows the sodium and potassium complexes of (120) in the same format. The "fit" of the potassium ion is much better than that of the sodium ion as it shows contact with the four phenolic ether oxygens and the anthraquinone carbonyl oxygen.

*Figure 5.13: Compound (**120**) as the free ligand with the donating oxygens in CPK format.*

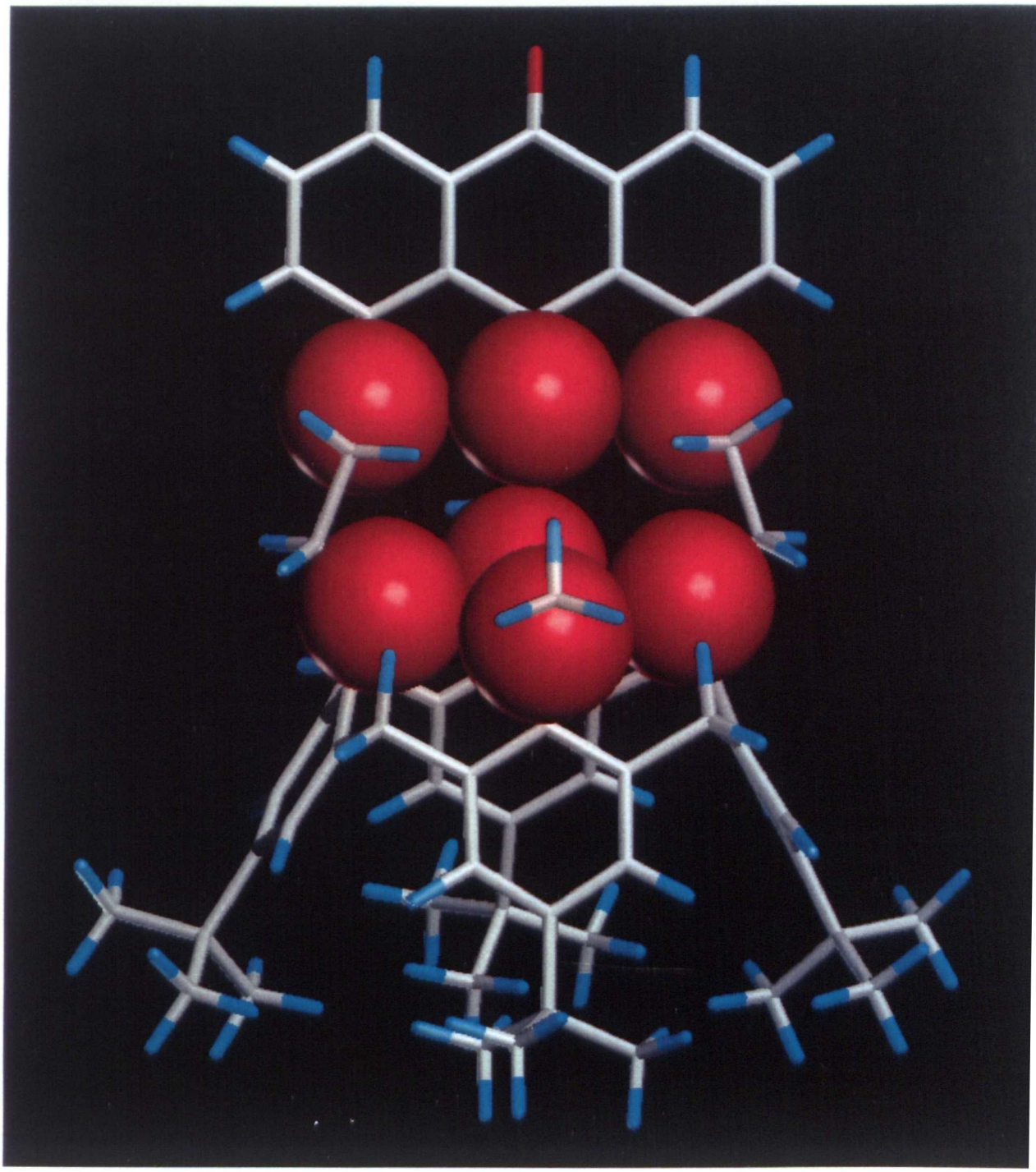

*Figure 5.14: The sodium (top) and potassium (bottom) complexes of Compound (**120**) with the donating oxygens and the metal ion in CPK format.*

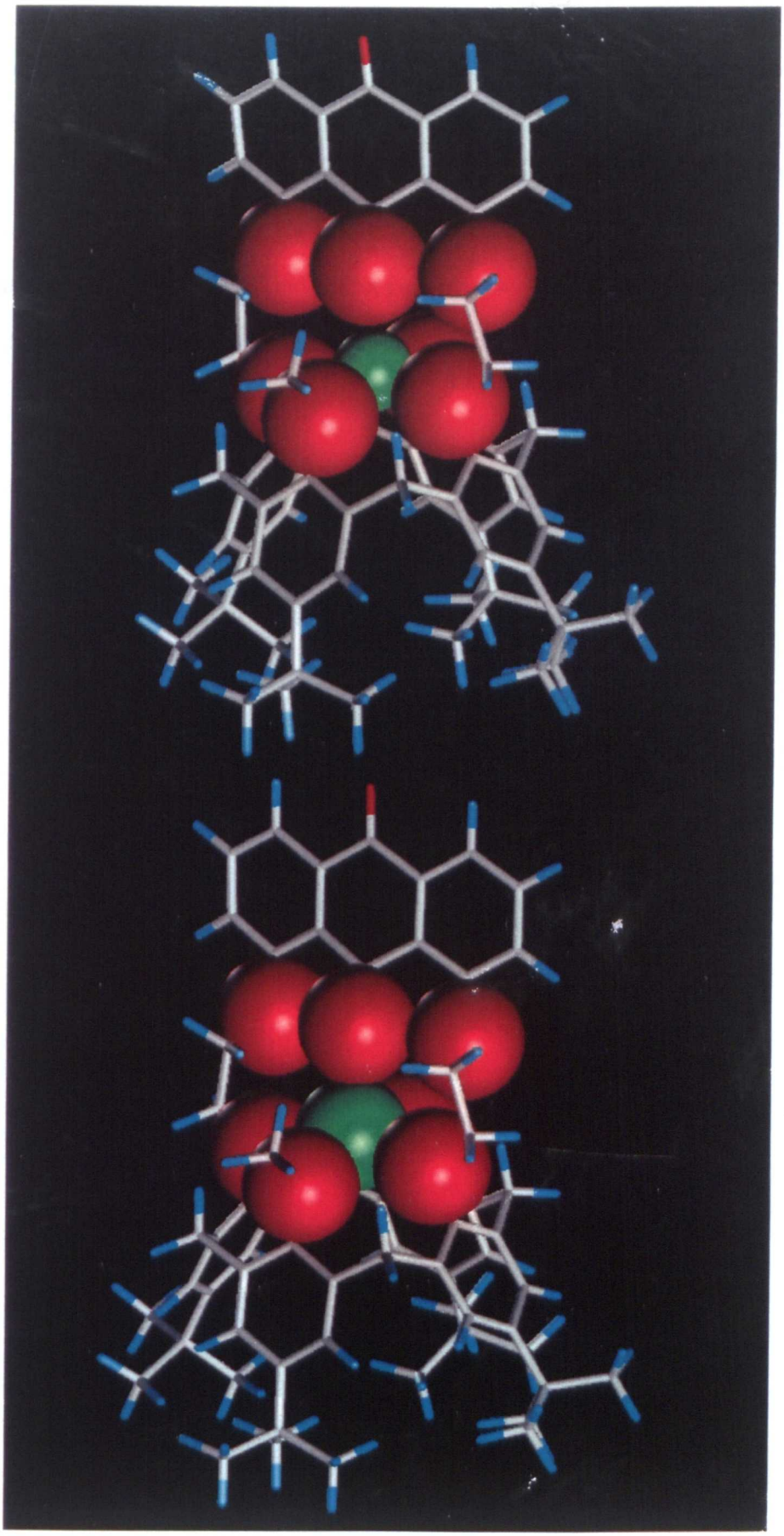

For the present study molecular modelling has proven to be a powerful tool in aiding molecular design. The Sybyl package correctly predicted that compound (**106**) would be unsuitable as switchable ionophore. It also predicted that compound (**120**) would be potassium selective, as proved to be the case. The results generated, however must always be treated with caution. As demonstrated by the unrealistically high energy barriers to rotation for compound (**106**). The results therefore must be confirmed experimentally. Thus the early use of an advanced modelling package may help to direct synthetic efforts along more productive pathways.

Experimental

Instrumentation and Experimental Techniques.

(a) Infrared (IR) spectra were recorded in the range 4000-600 cm^{-1} on a Perkin-Elmer 1320 or Perkin-Elmer 1720 fourier transform infrared spectrometers. Spectra of solid samples were recorded as nujol mulls or KBr discs.

(b) Nuclear magnetic resonance (NMR) spectra were recorded on a Bruker WM 200 (200MHz) spectrometer. Deuteriochloroform, with tetramethylsilane as internal standard, was used as solvent, unless otherwise stated. Spectra were recorded on the δ scale and signals are quoted in the form : chemical shift (multiplicity, number of protons, assignment), measured in ppm.

(c) Mass spectra were recorded on a VG7070E or a Fisons Instruments Trio 1000 spectrometer.

(d) Melting points were recorded on a Kofler hot stage apparatus.

(e) Thin layer chromatography (tlc) was carried out on Merck 5554 pre-coated silica plates

(f) Column chromatography was performed using Merck silica gel 60

(g) Ultraviolet (UV) solution spectra were recorded on a Hewlett Packard 8452A Diode Array Spectrophotometer.

(h) Cyclic Voltammograms were recorded on an EG&G model 173 potentiostat fitted with a 276 interface. The potential sweep was generated by an Apple II microcomputer which also served to collect data. Plots were recorded on an XY plotter.

Purification of reagents

Tetrahydrofuran was freshly distilled from sodium benzophenone ketyl, under a positive pressure of nitrogen , immediately prior to use.

Dry acetone was prepared by distilling from calcium sulphate, under a positive pressure of nitrogen , immediately prior to use.

Dry toluene was prepared by distilling from lithium aluminium hydride, under a positive pressure of nitrogen , immediately prior to use.

Pyridine was distilled and stored over sodium hydroxide pellets.

Acetonitrile for electrochemical experiments was taken from a freshly opened bottle and dried by passing it through a column of ICN Biochemicals alumina N super I.

Ozone was prepared using a Wallace and Tieman ozone generator.

All other reagents were used as received.

Experimental procedures.

5,11,17,23-tetra-*tert*-butyl-25,26,27,28-tetrahydroxycalix[4]arene (58)

Into a 3 litre, 3 neck flask, equipped with a mechanical stirrer, were placed, 4-*tert*-butylphenol (100g, 0.666 mol.), sodium hydroxide (1.2g, 0.03 mol.), formaldehyde solution (62.5ml, 37%, 0.666 mol.) and water (50ml). The mixture was heated on an oil bath to 120°C for 2 hr's, with stirring, where upon the mixture had turned a pale yellow colour, at this point nitrogen was blown across the surface of the mixture to facilitate the removal of water. The solution was converted into a thick toffee-like material. This was allowed to cool and broken into pieces, warm diphenyl ether (1l) was then added and the mixture stirred for 1 hour, to dissolve the solids. The flask was transferred to an isomantle, fitted with an air condenser and heated to reflux, (258°C), for 1-2hr's, blowing nitrogen across the surface for the first 30 minutes to remove water vapour. The mixture was allowed to cool, ethyl acetate (1.5 l) added and stirred for 15-30 minutes. The solution was then allowed to stand for 30 minutes. The precipitate was filtered off to yield an off-white solid, this was washed with ethyl acetate (2 x 100ml) and recrystallised from toluene to give white crystals. 46.38g, (43%). mp. 339°C (lit. 344-346°C)[66], IR (Nujol) 3177cm^{-1} (OH str.), NMR δ 10.35 (s, 1H, ArOH), 7.05 (s, 2H, ArH), 4.22 (br d, 1H, $ArCH_2Ar$), 3.52 (br d, 1H, $ArCH_2Ar$), 1.21 (s, 9H, $C(CH_3)_3$). Mass spec. (FAB, 3-NOBA), 648.4 ($C_{44}H_{56}O_4$ requires 648.418). Analysis calc for $C_{44}H_{56}O_4$, C 81.44; H 8.70. Found C 81.84; H 8.87.

5,11,17,23-tetra-*tert*-butyl-25,26,27,28-tetrakis(ethoxycarboxymethoxy)calix[4]arene (59)

p-tert-Butylcalix[4]arene (**58**) (10g, 15.41 mmol) was suspended in dry acetone(150ml) containing anhydrous potassium carbonate(6.39g, 46.23mmol) under nitrogen. The mixture was heated to reflux for 30 minutes and ethyl bromoacetate(20.59g, 0.123mol) added. The mixture was then refluxed for 5 days. The cooled mixture was partitioned between dichloromethane(100ml) and water(100ml). The organic layer was removed and the aqueous layer extracted further with dichloromethane(100ml). The

combined organic extracts were washed with water, dried over magnesium sulphate and the solvent removed *in vacuo* to yield a viscous oil. Excess ethyl bromoacetate was distilled from this at reduced pressure and the residue taken up in the minimum volume of hot ethanol. Upon cooling crystals were deposited, these were further purified by recrystalisation from ethanol/dichloromethane to yield ester (**59**) as white crystals. 10.72g, (70%); . mp 154-155°C (lit. 154-155°C)[84]; IR (Nujol) 1760cm^{-1} (C=O); NMR ^{1}H δ 1.07 (s, 36H, C(CH$_3$)$_3$), 1.29 (t, 12H, OCH$_2$CH$_3$), 3.19 (d, 4H, ArCH$_2$Ar), 4.20 (q, 8H, OCH$_2$CH$_3$), 4.81 (s, 8H, OCH$_2$C=O), 4.85 (d, 4H, ArCH$_2$Ar), 6.77(s, 8H, ArH), Mass spec. (FAB, 3-NOBA), [M+Na]$^+$ 1015.78, [M]$^+$ 992.76 (requires 992.565). Analysis calc for $C_{60}H_{80}O_{12}$, C 72.55; H 8.12, Found C 72.33; H 8.14.

5,11,17,23-tetra-*tert*-butyl-25,26,27-tris(ethoxycarboxymethoxy)-28-(hydroxycarboxymethoxy)calix[4]arene (**100**)

p-tert-Butyl-calix[4]arene tetraester (**59**) (5.00g, 5.034mmol) was dissolved in chloroform (100ml) containing 5% v/v ethanol and 1% v/v water. To this mixture was added trifluoroacetic acid (0.5ml). The mixture was stirred at room temperature for between 3 and 5 days. The reaction was monitored by disappearance of the ArH peak for (**59**) at 6.77ppm. The mixture was then washed with water (2x 100ml), dried over magnesium sulphate, filtered and the solvent removed *in vacuo* to yield an off-white solid(4.86g). Conversion was estimated at 96% by comparison of the intergrals for the ArH peaks in the NMR. The compound was used without further purification. mp 160°C (lit. 166-168°C)[113]; IR (Nujol) (C=O); NMR ^{1}H δ 0.82 (s, 18H, C(CH$_3$)$_3$), 1.29 (t, 3h, CH$_2$CH$_3$), 1.3 (t, 6H, CH$_2$CH$_3$) 1.31 (s, 9H, C(CH$_3$)$_3$), 1.32 (s, 9H, C(CH$_3$)$_3$), 3.19 (d, 2H, ArCH$_2$Ar), 3.25 (d, 2H, ArCH$_2$Ar), 4.21 (q, 4H, CH$_2$CH$_3$), 4.25 (q, 4H, CH$_2$CH$_3$), 4.35 (s, 2H, OCH$_2$CO$_2$Et), 4.57 (s, 2H, OCH$_2$CO$_2$Et), 4.59 (d, 2H, ArCH$_2$Ar), 4.86 (s, 2H, OCH$_2$CO$_2$Et), 4.94 (s, 2H, OCH$_2$CO$_2$Et), 4.96 (d, 2H, ArCH$_2$Ar), 6.53 (d, 2H, ArH), 6.62 (d, 2H, ArH), 7.13 (s, 2H, ArH), 7.14(s, 2H, ArH),. Mass spec. (FAB, 3-NOBA), [M+H]$^+$, 965.46, [M]$^+$, 964.45 (requires 964.534). Analysis calc for $C_{58}H_{76}O_{12}$, C, 72.17; H, 7.94, Found C, 72.41; H, 7.96.

5,11,17,23-tetra-*tert*-butyl-25,26,27,28-tetrakis(hydroxycarboxymethoxy)calix[4]arene (102)

p-tert-Butyl-calix[4]arene tetraester (59) (0.93g, 0.936mmol) was dissolved in ethanol (25ml) to which was added tetraethylammoniun hydroxide solution (40%aq. 1.73ml, 4.681mmol). This mixture was refluxed for 23hrs at which point the solution was pale yellow. The solution was allowed to cool and poured into HCl (2M, 10ml), this was extracted with ether (3x 20ml), washed with water (1x 10ml) and dried over magnesium sulphate, filtered and the solvent removed *in vacuo* to yield an off-white solid (0.68g; 82%). mp 270°C dec. (lit 270°C dec.)[110,111]; IR (KBr) 3624-2400cm^{-1}(broad OH), 1750cm^{-1} (C=O); NMR ^{1}H δ,1.2 (br., 36H, C(CH_3)$_3$), 3.3 (d, 4H, Ar$\underline{CH_2}$Ar) 4.6 (br., 12H, O$\underline{CH_2}$C=O & Ar$\underline{CH_2}$Ar), 6.9 (br., 8H, ArH). Mass spec. (FAB, 3-NOBA), [M+Na]$^+$, 903.40, [M+H]$^+$, 881.41, [M]$^+$ 880.40 (requires 880.44). Analysis calc for $C_{52}H_{64}O_{12}$, C, 70.89; H, 7.32, Found C, 70.46; H, 7.34.

5,11,17,23-tetra-*tert*-butyl-25,26,27,28-tetrakis(*tert*-butoxycarboxymethoxy)calix[4]arene (62)

p-tert-Butylcalix[4]arene (58) (5.05g, 7.78 mmol) was suspended in dry acetone(150ml) containing anhydrous potassium carbonate(3.23g, 23.37mmol) under nitrogen. The mixture was heated to reflux for 30 minutes and *tert*-butyl bromoacetate (12.14, 62.24mmol) added. The mixture was the refluxed for 7 days. The cooled mixture was partitioned between dichloromethane(100ml) and water(100ml). The organic layer was removed and the aqueous layer extracted further with dichloromethane (100ml). The combined organic extracts were washed with water, dried over magnesium sulphate and the solvent removed *in vacuo* to yield a viscous oil. Excess *tert*-butyl bromoacetate was distilled from this at reduced pressure. The residue was purified by recrystallisation from ethanol/dichloromethane to yield ester (62) as white crystals. 4.45, (52%); . mp 258-260°C (lit. 258-261°C)[83]; IR (Nujol) 1750cm^{-1} (C=O), 1720cm^{-1} (C=O); NMR ^{1}H δ 1.1 (s, 36H, C(CH_3)$_3$), 1.3 (s, 36H, C(CH_3)$_3$), 3.2 (d, 4H, Ar$\underline{CH_2}$Ar), 4.8 (q, 8H, O$\underline{CH_2}CH_3$), 4.9 (d, 4H,

Ar$\underline{CH_2}$Ar), 6.8(s, 8H, ArH), Mass spec. (FAB, 3-NOBA), $[M+K]^+$ 1143.55, $[M+Na]^+$ 1127.56, $[M]^+$ 1104.54 (requires 1104.690). Analysis calc for $C_{68}H_{96}O_{12}$, C 73.88; H 8.75, Found C 73.87; H 8.77.

5,11,17,23-tetra-*tert*-butyl-25,26,27-tris(ethoxycarboxymethoxy)-28-(1'-anthraquinonylamidocarboxymethoxy)calix[4]arene (106)

Tri-ester, mono-acid (**100**) (0.5g, 0.518mmol) was dissolved in thionyl chloride (25ml) and the mixture refluxed for 24hrs, under nitrogen. The excess thionyl chloride was distilled off under reduced pressure yielding a yellow oil. This was taken up in dry toluene (25ml) and added to a solution of 1-aminoanthraquinone (0.127g, 0.570mmol) in dry toluene (25ml). This mixture was refluxed for 16 hrs, whereupon it had changed colour from red to yellow. The solvent was removed *in vacuo* and the residue taken up in dichloromethane (40ml). This solution was washed with water (3 x 25ml), dried over magnesium sulphate and the solvent removed *in vacuo* to yield a yellow solid. This was purified by chromatography on silica (eluent DCM/Et_2O 0-50%) to yield (**106**) as a yellow solid. This was further purified by recrystallisation from methanol at -18°C to give yellow needles (0.250g, 41%). mp 130°C; IR (nujol) 1750cm^{-1} (EtOC=O), 1740cm^{-1} (RNHC=O); NMR ^1H δ 0.94 (s, 9H, $C(CH_3)_3$), 0.96 (t, 6H, $OCH_2\underline{CH_3}$), 1.04 (s, 9H, $C(CH_3)_3$), 1.18 (s, 18H, $C(CH_3)_3$), 3.22 (d, 2H, $ArCH_2Ar$), 3.27 (d, 2H, $ArCH_2Ar$), 3.84 (m, 4H, $O\underline{CH_2}CH_3$), 4.21 (q, 2H, $O\underline{CH_2}CH_3$), 4.72 (s, 2H, $ArO\underline{CH_2}$), 4.84 (s, 2H, $ArO\underline{CH_2}$), 4.85 (d, 2H, $ArCH_2Ar$), 5.04 (s, 2H, $ArO\underline{CH_2}$), 5.06 (d, 2H, $ArCH_2Ar$), 5.13(s, 2H, $ArO\underline{CH_2}$), 6.6 (s, 2H, ArH), 6.73 (s, 2H, ArH), 6.93 (s, 4H, ArH), 7.83 (m, 2H, AqH), 8.13 (m, 2H, AqH), 8.31 (m, 1H, AqH), 8.45 (m, 1H, AqH), 9.22 (m, 1H, AqH), 12.4 (s, 1H, NH). Mass spec. (FAB, 3-NOBA), $[M+Na]^+$ 1192.52, $[M+H]^+$ 1170.56.(requires 1169.586). Analysis calc for $C_{72}H_{83}NO_{13}$, C, 73.88; H, 7.15, N 1.28, Found C, 73.68; H, 7.10; N, 1.26.

5,11,17,23-tetra-*tert*-butyl-25,26,27-tris(ethoxycarboxymethoxy)-28-(2'-nitro-1'-anilinylamidocarboxymethoxy)calix[4]arene (107)

Tri-ester, mono-acid (**100**) (0.71g, 0.734 mmol) was dissolved in thionyl chloride (25ml) and the mixture refluxed for 2 hrs, under nitrogen. The excess thionyl chloride was

distilled off under reduced pressure yielding a yellow oil. This was taken up in dry toluene (25ml) and added to a solution of 2-nitroaniline (0.1067g, 0.772mmol) in dry toluene (25ml). This mixture was refluxed for 16 hrs, whereupon it had changed colour from orange to dark yellow. The solvent was removed *in vacuo* and the residue taken up in dichloromethane (40ml). This solution was washed with water (3 x 25ml), dried over magnesium sulphate and the solvent removed *in vacuo* to yield a yellow solid. This was purified by chromatography on silica (eluent DCM/Et_2O 0-50%) to yield (**106**) as a dirty yellow solid. This was further purified by dissolving in methanol and storing at -18°C for 1 week, wherupon a resinous precipitate had formed. The mother liquours were decanted from this and water added to give a pale yellow precipitate (0.480g, 60%). mp 96-98°C; IR (nujol) 1770cm^{-1} (EtOC=O), 1760cm^{-1} (RNHC=O); NMR ^1H δ 0.85 (s, 9H, $C(CH_3)_3$), 1.05 (s, 27H, $C(CH_3)_3$), 3.22 (d, 2H, $ArCH_2Ar$), 3.27 (d, 2H, $ArCH_2Ar$), 3.98 (m, 4H, $O\underline{CH_2}CH_3$), 4.24 (q, 2H, $O\underline{CH_2}CH_3$), 4.73 (s, 2H, $ArO\underline{CH_2}$), 4.75 (s, 2H, $ArO\underline{CH_2}$), 4.76 (d, 2H, $ArCH_2Ar$), 4.90 (s, 4H, $ArO\underline{CH_2}$), 4.95 (d, 2H, $ArCH_2Ar$), 6.72 (s, 2H, ArH), 6.80 (s, 2H, ArH), 6.82 (s, 4H, ArH), 7.24 (t, 1H, ArH), 7.66 (t, 1H, ArH), 8.18 (d, 1H, ArH), 8.48 (d, 1H, ArH), 10.08 (s, 1H, NH). Mass spec. (FAB, 3-NOBA), $[M+Na]^+$ 1107.56, $[M+H]^+$ 1085.58, (requires 1084.566). Analysis calc for $C_{64}H_{80}N_2O_{13}$, C, 70.83; H, 7.43; N 2.58, Found C, 70.33; H, 7.47; N, 2.10.

5,11,17,23-tetra-*tert*-butyl-25,27-bis(ethoxycarboxymethoxy)-26,28-hydroxycalix[4]arene(**111**)

p-tert-Butylcalix[4]arene (**58**) (5.03g, 7.75mmol) was suspended in dry acetone(100ml) containing anhydrous potassium carbonate(2.14g, 15.5mmol) under nitrogen. The mixture was heated to reflux for 30 minutes and ethylbromoacetate(2.59g, 15.5mmol) added. The mixture was the refluxed for 16 hrs. The cooled mixture was partitioned between dichloromethane(100ml) and water(100ml). The organic layer was removed and the aqueous layer extracted further with dichloromethane(100ml). The combined organic extracts were washed with water, dried over magnesium sulphate and the solvent removed *in vacuo* to yield a viscous oil. Excess ethyl bromoacetate was distilled from this at reduced

pressure to yield a viscous oily residue. This was recrystallised from ethanol/ dichloromethane to yield ester (**111**) as white crystals (4.32g, 68%). mp 181-184°C (lit 182-184°C)[114]; IR (nujol) 1750cm^{-1} (C=O); NMR ^{1}H δ; 0.97 (s, 18H, C(CH$_3$)$_3$), 1.29 (s, 18H, C(CH$_3$)$_3$), 1.37 (t, 6H, OCH$_2$CH$_3$), 3.34 (d, 4H, ArCH$_2$Ar), 4.31 (q, 4H, OCH$_2$CH$_3$), 4.37 (d, 4H, ArCH$_2$Ar), 4.69 (s, 4H, OCH$_2$CO$_2$Et), 6.74 (s, 4H, ArH) 7.03 (s, 4H, ArH). Mass spec. (FAB, 3-NOBA), [M+Na]$^+$, 843.51, [M+H]$^+$, 821.53, [M]$^+$ 820.52 (requires 820.49). Analysis calc for $C_{52}H_{68}O_8$, C 76.06, H 8.35, Found C, 76.01; H, 8.37.

5,11,17,23-tetra-*tert*-butyl-25,27-bis(methoxy)26,28-hydroxycalix[4]arene(**114**)

p-tert-Butylcalix[4]arene (**58**) (1.06g, 1.633mmol) was suspended in dry acetone(100ml) containing anhydrous potassium carbonate(0.5g, 3.62mmol) under nitrogen. The mixture was heated to reflux for 30 minutes and methyl iodide(1.00g, 7.05mmol) added. The mixture was then refluxed for 16 hrs. The cooled mixture was partitioned between dichloromethane(100ml) and water(100ml). The organic layer was removed and the aqueous layer extracted further with dichloromethane(100ml). The combined organic extracts were washed with water, dried over magnesium sulphate and the solvent removed *in vacuo* to yield an off-white solid. This was recrystallised from chloroform/methanol to yield ether (**114**) as white crystals (0.8g, 72%). mp 160-162°C ; IR (nujol) 3450cm^{-1} (OH); NMR ^{1}H δ; 0.97 (s, 18H, C(CH$_3$)$_3$), 1.31 (s, 18H, C(CH$_3$)$_3$), 3.34 (d, 4H, ArCH$_2$Ar), 3.94 (s, 6H, OMe), 4.29 (d, 4H, ArCH$_2$Ar), 6.83 (s, 4H, ArH), 7.09 (s, 4H, ArH), 7.34 (s, 2H, ArOH). Mass spec. (FAB, 3-NOBA), [M]$^+$ 676.39 (requires 676.449). Analysis calc for $C_{46}H_{60}O_4$, C 81.61, H 8.93; Found C, 81.56; H, 8.90.

5,11,17,23-tetra-*tert*-butyl-25,27-bis(allyloxy)26,28-hydroxycalix[4]arene(**115**)

p-tert-Butylcalix[4]arene (**58**) (5.09g, 7.84mmol) was suspended in dry acetone(100ml) containing anhydrous potassium carbonate(2.17g, 15.7mmol) under nitrogen. The mixture was heated to reflux for 30 minutes and allylbromide(2.85g, 23.5mmol) added. The mixture was then refluxed for 16 hrs. The cooled mixture was partitioned between

dichloromethane(100ml) and water(100ml). The organic layer was removed and the aqueous layer extracted further with dichloromethane(100ml). The combined organic extracts were washed with water, dried over magnesium sulphate and the solvent removed *in vacuo* to yield an off-white solid. This was recrystallised from chloroform/methanol to yield ether (**115**) as white crystals (4.88g, 85%). mp 165-166°C ; IR (nujol) 3400cm^{-1} (OH); NMR ^{1}H δ; 1.05 (s, 18H, C(CH$_3$)$_3$), 1.29 (s, 18H, C(CH$_3$)$_3$), 3.34 (d, 4H, ArCH$_2$Ar), 4.29 (d, 4H, ArCH$_2$Ar),4.53 (m, 4H, OCH$_2$CHCH$_2$) 5.39 (m, 2H, OCH$_2$CHCH$_2$), 5.72 (m, 2H, OCH$_2$CHCH$_2$), 6.28 (m, 2H, OCH$_2$CHCH$_2$), 6.90 (s, 4H, ArH), 7.05 (s, 4H, ArH), 7.71 (s, 2H, ArOH). Mass spec. (FAB, 3-NOBA), [M+H]$^+$, 729.56, [M]$^+$ 728.55 (requires 728.4805). Analysis calc for $C_{50}H_{64}O_4$, C 82.37, H 8.85, Found C, 82.43; H, 8.86.

5,11,17,23-tetra-*tert*-butyl-25,27-bis(allyloxy)26,28-bis(methoxy)calix[4]arene (**116**)

Di-ether (**115**) (3.49g, 4.61 mmol) was added to a suspension of NaH (0.69g, 80% oil suspension, 23.05 mmol)in dry THF (100ml). This mixture was refluxed for 30 mins. and methyl iodide (3.27g, 23.05 mmol) added. The mixture was then refluxed for a further 16 hrs. The excess sodium hydride was quenched by careful addition of water (10ml) and the solvent removed *in vacuo* . The residue was partioned between dichloromethane (150ml) and water (150ml) and the organic layer separated. The aqueous layer was further extracted with dichloromethane (150ml). The combined organic extracts were washed with water (1 x 100ml) dried over magnesium sulphate, filtered and the solvent removed *in vacuo* to give a white solid. This was recrystallised from chloroform/methanol to give colourless needles (3.17g, 87%). mp. 183-184°C; NMR appears to be a mixture of conformers; ^{1}H δ; 0.82, 1.06, 1.35 (br s, 36H, C(CH$_3$)$_3$), 3.18 (br d, 4H, ArCH$_2$Ar), 3.21 (br s, OCH$_3$), 3.59-4.26 (br m, OCH$_3$ + ArCH$_2$Ar), 4.35 (br m, 4H, OCH$_2$CHCH$_2$) 5.15-5.41 (br m, 4H, OCH$_2$CHCH$_2$), 6.18 (br m, 2H, OCH$_2$CHCH$_2$), 6.41-6.68, 6.85-7.32 (br m, 8H, ArH); Mass spec. (FAB, 3-NOBA), [M]$^+$ 756.50 (requires 756.5118). Analysis calc for $C_{52}H_{68}O_4$, C 82.49, H 9.05; Found C, 82.60, H, 9.10.

5,11,17,23-tetra-*tert*-butyl-25,27-bis(hydroxycarboxymethoxy)26,28-bis(methoxy)calix[4]arene(113)

Tetra ether (**116**) (0.21g, 0.277 mmol) was dissolved in dichloromethane (50ml) and cooled to -78°C in a solid CO_2/*iso* -propanol bath. Ozone was passed through the solution until it had taken upon a grey/blue colour. The reaction mixture was then flushed with nitrogen, to remove excess ozone, and hydrogen peroxide (10ml) in methanol (30ml)added. The mixture was removed from the cooling bath and allowed to reach room temperature, with vigourous stirring. The organic layer was separated and washed water (2 x 50ml). The organic layer was dried over magnesium sulphate, filtered and the solvent removed *in vacuo* to yield an oily solid (0.398g, 95%). IR (nujol) 3750-3100cm^{-1} (OH), 1732cm^{-1} (C=O); NMR, only broad poorly resolved peaks; mass spec. (FAB, 3-NOBA), no $[M]^+$ or $[M+Na]^+$, CI (NH_3) no $[M]^+$ or $[M+NH_4]^+$ (requires 792.4601). Analysis calc for $C_{50}H_{64}O_8$, C 75.73, H 8.13; Found C, 73.19, H, 8.17.

5,11,17,23-tetra-*tert*-butyl-25,27-bis(2'-hydroxyethoxy)26,28-bis(methoxy)calix[4]arene (118)

Tetra ether (**116**) (0.21g 0.528 mmol) was dissolved in chloroform (40ml) and cooled to -78°C in a solid CO_2/*iso* -propanol bath. Ozone was passed through the solution until it had taken upon a grey/blue colour. The reaction mixture was then flushed with nitrogen to remove excess ozone and sodium borohydride (0.1g, 2.64 mmol) in ethanol (30ml) added. The mixture was removed from the cooling bath and allowed to reach room temperature, with vigourous stirring. The organic layer was separated and washed with $HCl_{(aq)}$ (1 x 20ml, 2N) and then with water (2 x 50ml). The organic layer was dried over magnesium sulphate, filtered and the solvent removed *in vacuo* to yield an oily solid (0.132g, 62%). IR (nujol) 3600-3100cm^{-1} (OH); NMR, δ 0.5-1.7 (br m, 36H, $C(CH_3)_3$), 2.7-4.8 (br m, 18H, $ArCH_2Ar$ + $ArOCH_2CH_2OH$), 6.5-7.5 (br m, 8H, ArH); mass spec. (FAB, 3-NOBA), $[M+Na]^+$ 787.40 $[M+H]^+$ 765.40, (requires 764.5016). Analysis calc for $C_{50}H_{68}O_6$, C 78.49, H 8.96; Found C, 69.5, H, 8.64.

1,8-dichloro-4,5-dinitroanthraquinone (47)

1,8-Dichloroanthraquinone (27.7g, 0.1mol) was suspended in 98% sulphuric acid (60ml) and heated to 80°C and stirred mechically. The heat source was removed and a mixture of nitric acid (25ml, sp. gr. 1.5) and 98% sulphuric acid (10ml) added dropwise so as to maintain a temperature of 100-110°C. Nitric acid (70ml, sp. gr. 1.42) was then added in a single portion and the mixture heated to 80°C for 2Hrs. The heat source was removed and the mixture stirred overnight. The mixture was then poured into water (500ml) stirred for 20 mins and filtered. The filtred solids were washed with water until no longer acidic and then with dichloromethane until the washings show no colouration. The resulting solids were dried under vacumn to give (47) as a yellow powder (25g, 70%). mp 344-345°C (dec.); IR 1680cm^{-1} (C=O), 1535cm^{-1} (NO_2), 1380cm^{-1} (NO_2); NMR ^{1}H (DMF) δ; 8.24 (s, ArH); (DMSO) δ; 8.28 (s, ArH); ^{13}C (DMF) δ; 127.83, 128.82, 133.26, 136.48, 139.20, 147.59 (C-NO_2), 178.31 (C=O), 212.50 (C=O). Mass spec. (EI), $[M]^+$, 369.80 (11.87, $^{37}Cl_2$), 367.81 (66.14 $^{37}Cl^{35}Cl$), 365.79 (100, $^{35}Cl_2$), (requires 365.945). Analysis calc for $C_{14}H_4Cl_2N_2O_6$, C 45.81, H 1.10, N 7.63 Found C, 45.99; H, 1.09, N 7.64.

2,4,6-Tribromo-3,5-dimethylphenol(131)

3,5-Dimethylphenol (3.2g, 26.19mmol) was dissolved in acetic acid (50ml) and an acetic acid solution of bromine (4ml Br_2 in 25ml) added with swirling. The mixture was alowed to stand overnight and then poured into a dilute solution of sodium metabisulphite. The mixture was extracted with ether (3 x 75ml) and the combined organic extracts washed with water and then dried over magnesium sulphate. The solvent was removed *in vacuo* to yield a white solid. This was recrystallised from petrol (40-60)/dichloromethane to give (131) as long white needles. (7.5g, 80%) mp 164°C(lit. 164°C)[127]; IR 3400cm^{-1} (OH); NMR ^{1}H δ; 6.00 (s, 1H, ArH) 2.59 (s, 6H, ArMe); . Mass spec. (EI), $[M]^+$, 361.77 (32.11, $^{81}Br_3$), 359.76 (97.75, $^{81}Br_2{}^{79}Br$), 357.74 (100, $^{81}Br^{79}Br_2$), 355.76 (34.03, $^{79}Br_3$), (requires 355.805). Analysis calc for $C_8H_7Br_3O$, C 26.78, H 1.97 Found C 26.84; H 1.95.

2,6-Dibromo-3,5-dimethyl-1,4-benzoquinone(132)

2,4,6-Tribromo-3,5-dimethylphenol (**131**) (3.56g, 9.92mmol) was sprinkled onto fuming nitric acid (50ml, sp.gr. 1.5). The mixture became orange/red. It was then heated until red fumes appeared, cooled and poured into water (500ml). The yellow precipitate was extracted with ether (2x 50ml) and the combined organic extracts washed with water until no longer acidic. The solution was dried over magnesium sulphate, filtered and the solvent removed *in vacuo* to yield a yellow solid. this was recrystallised from petrol (40-60)/dichloromethaneto give (**132**) as yellow plates. (2.05g, 70%) mp 168°C (lit. 168°C)[127]; IR 1650cm^{-1} (C=O); NMR ^{1}H δ; 2.23 (s, Me); . Mass spec. (EI), [M]$^{+}$, 295.86 (22.35, $^{81}Br_2$), 293.85 (43.64, $^{81}Br^{79}Br$), 291.85 (22.08, $^{79}Br_2$), (requires 291.8735). Analysis calc for $C_8H_6Br_2O_2$, C 32.69, H 2.06 Found C 32.60; H 2.04.

2,6-Dibromo-3,5-bis(bromomethyl)-1,4-benzoquinone (119)

2,6-Dibromo-3,5-dimethyl-1,4-benzoquinone (**132**) (1.00g, 3.40mmol) was treated with N-bromosuccinimide (1.33g, 7.48mmol) in carbon tetrachloride (100ml) in the presence of a catalytic amount of benzoyl peroxide under intense light at reflux for 16 hrs. The mixture was cooled and the solid succinimide filtered off. The solvent was removed from the filtrate *in vacuo* to yield a brown solid. This was recrystallised from ethanol to give (**119**) as a red brown solid. (0.44g, 29%). mp. 125-126°C; NMR ^{1}H δ; 4.89 (s, CH_2Br); . Mass spec. (EI), [M]$^{+}$, 455.56 (7.29, $^{81}Br_4$), 453.54 (29.26, $^{81}Br_3{}^{79}Br$), 451.54 (44.95, $^{81}Br_2{}^{79}Br_2$), 449.51 (30.68, $^{81}Br^{79}Br_3$), 447.53 (7.90, $^{79}Br_4$), (requires for $C_8H_4{}^{79}Br_4O_2$, 447.694). Analysis calc for $C_8H_4Br_4O_2$, C 21.27, H 0.89; Found C 21.46, H 0.93.

1,8-bis(2'bromoethoxy)-anthraquinone (122)

1,8-Dihydroxyanthraquinone (5g, 20.82 mmol) was dissolved in dry DMF (100ml), by heating to 40°C, to which was added caesium carbonate (15g, 46.04 mmol) portion-wise. The colour changed from orange to purple. To this mixture was added 1,2-dibromoethane

(20ml, 232 mmol) and the mixture was heated to 80°C for 3 hrs. The mixture was allowed to cool, filtered through a Celite pad and the solvent removed *in vacuo*. The residue was chromatographedon silica (0-4% methanol/dichloromethane) and the product collected as the second fraction. This was further purified by recrystallisation from ethyl acetate to give (**122**) as yellow/orange needles (3.84g, 40%). mp 153-154°C (lit. 153-154°C)[46]; NMR ^{1}H δ; 3.76 (t, 4H, CH_2Br), 4.44 (t, 4H, $ArOCH_2$), 7.31 (d, 2H, Ar H-2 and H-7), 7.62 (t, 2H, Ar H-3 H-6), 7.87 (d, 2H, Ar H-4 H-5); Mass spec. EI $[M]^+$ 452 (Br_2 pattern), $[M-Br]^+$ 373 (one Br), (requires 451.926, ^{79}Br); Analysis calc for $C_{18}H_{14}Br_2O_4$, C 47.61, H 3.11; Found C 47.53, H 3.11.

1,8-Oxybis(-25-ethyleneoxy(5,11,17,23-tetra-*tert*-butyl-26,28-hydroxycalixaryl)-27-ethyleneoxy)anthraquinone (123)

Compound (**122**) (3.04g, 6.694 mmol), *p-tert*-butylcalix[4]arene(**58**) (4.344g, 6.694 mmol), sodium carbonate (5.676g, 53.5 mmol) and sodium iodide (8.03g, 53.5 mmol) were suspended in butyronitrile (200ml) and heated to reflux for 18 hrs. The solvent was removed in vacuo and the residue partitioned between dichloromethane (100ml) and HCl (100ml, 2N) and filtered. The organic layer was separated and washed with water (2 x 100ml), dried over magnesium sulphate, filtered and the volume of solvent reduced to ≈ 50ml. This solution was filtered again to remove unreacted (**58**) (0.447g)and the volume of solvent removed *in vacuo* . The residue was recrystallised from dichloromethane/petrol (bp 40-60) yielding a crop of crystals (1.53g), these were filtered off and the solvent removed from the mother liquors *in vacuo*. The residue was recrystallised from chloroform/methanol and the mother liquors retained [these solids contained the polymeric materials (**124**) and (**125**) along with some (**123**)]. The solvent was removed from these liquors*in vacuo* and the residue recrystallised from dichloromethane/petrol (bp 40-60) yielding a second crop of crystals (0.4842g). These were combined with the first crop to give (**123**) (2.0142g, 36% based on recovered (**58**)). mp 303-304°C (dec); IR 1680cm^{-1} (AqC=O), 1590cm^{-1} (AqC=O); NMR ^{1}H δ; 1.09 (s, 18H, $C(CH_3)_3$), 1.19 (s, 18H, $C(CH_3)_3$), 3.24 (d, 4H, $ArCH_2Ar$), 4.23 (d, 4H, $ArCH_2Ar$), 4.48 (m, 4H, $ArOCH_2$) 4.68 (m, 4H, $AqOCH_2$), 6.93 (s, 4H, ArH), 6.96 (s, 4H,

ArH), 7.24 (d, 2H, Ar H-2 and H-7), 7.58 (t, 2H, Ar H-3 H-6), 7.81 (d, 2H, Ar H-4 H-5), 8.13 (s, 2H, ArOH); mass spec. (FAB, 3-NOBA), $[M+H]^+$ 941.41, $[M]^+$ 940.40 (requires 940.4914). Analysis calc for $C_{62}H_{68}O_8$, C, 79.12, H, 7.28; for $C_{62}H_{68}O_8NaCl$, C, 74.49 H, 6.86; Found C, 75.64, H, 6.97.

1,8-Oxybis(ethyleneoxy-25-(5,11,17,23-tetra-*tert*-butyl-26,28-(methoxy)calixaryl)-27-ethyleneoxy)anthraquinone (120)

Anthraquinone calixarene crown (**123**) (0.5g, 0.53 mmol), sodium hydride (0.1g, 80% oil suspension 3.18 mmol) and dimethyl sulphate (0.234g, 2.22 mmol) were dissolved in dry THF (50ml). The mixture was heated to reflux for 16 hrs. The reaction mixture was allowed to cool and hydrochloric acid (5ml, 2N) added to quench excess sodium hydride. The mixture was partitioned between dichloromethane (75ml) and water (75ml). The organic layer was separated and washed with water (2 x 30ml), dried over magnesium sulphate, filtered and the solvent removed *in vacuo*. The residue was recrystallised from dichloromethane/methanol to yeild (**120**) as a yellow powder (0.2565g, 50%). mp 180-183°C (dec); IR, 1700cm^{-1}(AQC=O), 1610cm^{-1}(AQC=O); MNR ^1H δ; 0.81 (s, 18H, $C(CH_3)_3$), 1.29 (s, 18H, $C(CH_3)_3$), 3.13 (d, 4H, $ArCH_2Ar$), 4.00 (s, 6H, ArOMe), 4.23 (d, 4H, $ArCH_2Ar$), 4.41 (m, 4H, $ArOCH_2$), 4.79 (m, 4H, $AqOCH_2$), 6.51 (s, 4H, ArH), 7.08 (s, 4H, ArH), 7.32 (d, 2H, Ar H-2 and H-7), 7.62 (t, 2H, Ar H-3 H-6), 7.78 (d, 2H, Ar H-4 H-5); mass spec. (FAB, 3-NOBA), $[M+H]^+$ 969.34, $[M]^+$ 968.33 (requires 968.5227). Analysis calc for $C_{64}H_{72}O_8$, C, 79.31, H, 7.49; Found C, 78.82, H, 7.69.

1,8-Oxybis(ethyleneoxy-25-(5,11,17,23-tetra-*tert*-butyl-26,28-(ethoxycarboxymethoxy)calixaryl)-27-ethyleneoxy)anthraquinone (127)

Anthraquinone calixarene crown (**123**) (0.5g, 0.53 mmol), sodium hydride (0.1g, 80% oil suspension 3.18 mmol) and ethyl bromoacetate (0.3448g, 2.22 mmol) were dissolved in dry THF (50ml). The mixture was heated to reflux for 16 hrs. The reaction mixture was allowed to cool and hydrochloric acid (5ml, 2N) added to quench excess sodium hydride.

The mixture was partitioned between dichloromethane (75ml) and water (75ml). The organic layer was separated and washed with water (2 x 30ml), dried over magnesium sulphate, filtered and the solvent removed *in vacuo*. The residue was recrystallised from dichloromethane/methanol to yeild (**127**) as yellow needles (0.4206g, 71%). mp 306-307°C (dec); IR, 1780cm^{-1} (C=OOEt), 1690cm^{-1}(AQC=O), 1610cm^{-1}(AQC=O); MNR ^{1}H δ; 0.83 (s, 18H, $C(CH_3)_3$), 1.06 (t, 6H, $OCH_2\underline{CH_3}$), 1.31 (s, 18H, $C(CH_3)_3$), 3.16 (d, 4H, $ArCH_2Ar$), 3.86 (q, 4H, $O\underline{CH_2}CH_3$), 4.33 (s, 4H, $ArO\underline{CH_2}CO_2Et$), 4.42 (d, 4H, $ArCH_2Ar$), 4.57 (m, 4H, $ArOCH_2$) 4.71 (m, 4H, $AqOCH_2$), 6.48 (s, 4H, ArH), 7.10 (s, 4H, ArH), 7.34 (d, 2H, Ar H-2 and H-7), 7.60 (t, 2H, Ar H-3 H-6), 8.00 (d, 2H, Ar H-4 H-5); mass spec. (FAB, 3-NOBA), $[M+H]^+$ 1113.45, $[M]^+$ 1112.44 (requires 1112.5650). Analysis calc for $C_{70}H_{80}O_{12}$, C, 75.51, H, 7.24; Found C, 75.30, H, 7.22.

1,8-Oxybis(ethyleneoxy-25-(5,11,17,23-tetra-*tert*-butyl-26,28-(NN-diethylamidocarboxymethoxy)calixaryl)-27-ethyleneoxy)anthraquinone (**128**)

Anthraquinone calixarene crown (**123**) (0.5g, 0.53 mmol), sodium hydride (0.1g, 80% oil suspension 3.18 mmol), sodium iodide (0.2389g, 1.59 mmol) and N,N-diethyl-2-chloroacetamide (0.3179, 2.22 mmol) were dissolved in dry THF (50ml). The mixture was heated to reflux for 16 hrs. The reaction mixture was allowed to cool and hydrochloric acid (5ml, 2N) added to quench excess sodium hydride. The mixture was partitioned between dichloromethane (75ml) and water (75ml). The organic layer was separated and washed with water (2 x 30ml), dried over magnesium sulphate, filtered and the solvent removed *in vacuo*. The residue was chromatographed on 10% w/w NaCl loaded silica (eluent 1/ dichloromethane, 2/ ethyl acetate, 3/ ethanol) The last fraction was recrystallised from ethanol, with activated charcoal treatment, to yeild (**128**) as a yellow powder (0.1536g, 25%). mp 170-172°C; IR, 1700cm^{-1} (C=ONEt$_2$), 1690cm^{-1}(AQC=O), 1610cm^{-1}(AQC=O); MNR ^{1}H δ; 0.81 (s, 18H, $C(CH_3)_3$), 1.08 (t, 12H, $NCH_2\underline{CH_3}$), 1.36 (s, 18H, $C(CH_3)_3$), 2.98 (q, 4H, $N\underline{CH_2}CH_3$), 3.17 (d, 4H, $ArCH_2Ar$), 3.42 (q, 4H, $N\underline{CH_2}CH_3$), 4.32 (s, 4H, $ArO\underline{CH_2}CONEt_2$), 4.35 (d, 4H, $ArCH_2Ar$), 4.54 (m, 4H, $ArOCH_2$) 4.84 (m, 4H, $AqOCH_2$), 6.44 (s, 4H, ArH), 7.16 (s, 4H, ArH), 7.32 (d, 2H, Ar H-2 and H-7), 7.56 (t, 2H, Ar H-3 H-6),

8.03 (d, 2H, Ar H-4 H-5); mass spec. (FAB, 3-NOBA), $[M+Na]^+$ 1189.61, $[M+H]^+$ 1167.59 (requires 1166.6595). Analysis calc for $C_{74}H_{90}N_2O_{10}$, C, 76.13, H, 7.77, N, 2.40; Found C, 74.50, H, 7.71, N, 2.27.

N-acetyl-1-aminoanthraquinone (**129**)

1-Aminoanthraquinone (1.52g, 6.81 mmol) was dissolved in acetic anhydride (30ml) and heated to reflux for 10 mins. The mixture was allowed to cool slightly and then poured into water (500ml) and boiled to decompose the excess anhydride. The mixture was filtered and the solid washed well with water until the washings were no longer acidic. The solids were then dried at room temperature under vacumn and recrystallised from ethanol to give (**129**) as a bright yellow powder (1.5g, 83%). mp 216-217°C (lit 216-217°C)[128], IR 1710 cm^{-1} (NHC=O), 1580cm^{-1} (AQC=O); NMR ^1H δ; 2.35 (s, 3H, Me) 7.6-8.4 (m, 6H, ArH), 9.2 (d, 1H, Ar H-2), 12.33 (s, 1H, NH). Mass spec. EI $[M]^+$ 265.07 (requires 265.0739); Analysis calc for $C_{16}H_{11}NO_3$, C, 72.45, H, 4.18, N, 5.28; Found C, 72.68, H, 4.16, N, 5.14.

N-Methyl-N-acetyl-1-aminoanthraquinone (**130**)

1-Methylaminoanthraquinone (3.14g, 13.23 mmol) was dissolved in acetic anhydride (60ml) and heated to 100°C and a drop of H_2SO_4(conc.) added, the mixture changed from red to yellow almost immediatelyand heating was ceased. The mixture was allowed to cool slightly and then poured into water (500ml) and boiled to decompose the excess anhydride. The mixture was extracted with dichloromethane (3 x 100ml), and the combined organic extracts washed with water until the washings were no longer acidic. The organic extracts were dried over magnesium sulphate, filtered and the solvent removed *in vacuo*. The residue was dry flash chromatographed on silica (eluent 1/ dichloromethane, 2/ diethyl ether). the second fraction was recrystallised from ethanol to give (**130**) as golden yellow plates (2.21g, 60%). mp 210-212°C (lit 210-212°C)[129], IR 1650cm^{-1} (NHC=O), 1580cm^{-1} (AQC=O); NMR ^1H δ; 1.8 (s, 3H, C=OMe), 3.2 (s, 3H, NMe), 7.6-8.6 (m, 6H, ArH). Mass spec. EI $[M]^+$ 279.03 (requires 279.0895); Analysis calc for $C_{17}H_{13}NO_3$, C, 73.11, H, 4.69, N, 5.04; Found C, 73.31, H, 4.67, N, 5.01.

1. C.J. Pedersen, *J.Am.Chem.Soc.*, **1967**,*89*, 2495,

2. C.J. Pedersen, *J.Am.Chem.Soc.*, **1967**,*89*, 7017,

3. J. Dale and P.O. Kristiansen, *J.C.S.Chem. Comm.* , **1971**, 2105; *Acta. Chem. Scand.* , **1972**, *26* , 1471,

4. R.N. Greene, *Tet. Lett.* , **1972**, 1793,

5. G.W. Gokel, D.J. Cram, C.L. Liotta, H.P. Harris and F.L. Cook, *J.O.C.*, **1974**, *39* , 2445

6.G. Johns, C.J.Ransom and C.B. Reese, *Synthesis* , **1976**, 515

7. See S. Patai, Ed., "*Crown Ethers and Analogs.*" Part of the series "*The chemistry of functional groups.*", John Wiley & Sons Chichester, 1989

8. H.K. Frensdorff, *J.Am.Chem.Soc.*, **1971**,*93* , 600,

9. B. Dietrich, J.-M. Lehn and J.-P. Sauvage, *Tetrahedron Letters*, **1969**, 2885, 2889

10. B. Dietrich, J.-M. Lehn, J.-P. Sauvage and J. Blanzat, *Tetrahedron*, **1973**, *29*, 1629

11. B. Dietrich, J.-M. Lehn and J.-P. Sauvage, *Tetrahedron*, **1973**, 29, 1647

12. B.G. Cox, H. Schneider and J. Stroka, *J.Am.Chem.Soc.*, **1978**, *100* , 4746

13. D.J. Cram, T. Kaneda, R.C. Helgeson and G.M. Lein, *J.Am.Chem.Soc.*, **1979**, *101*, 6752

14. G.M. Lein and D.J. Cram, *J.C.S.Chem.Comm.*, **1982**, 301

15.S. Shinkai, T. Minami, Y. Kusano and O. Manabe, *Tetrahedron Letters* , **1982**, 23 , 2581

16. S. Shinkai, K. Shigematsu, Y. Kusano and O. Manabe, *J. C. S. Perkin I* , **1981**, 3279

17. S. Shinkai, T. Ogawa, Y. Kusano, O. Manabe, K. Kikukawa, T. Goto and T. Matsuda, and O. Manabe, *J.Am.Chem.Soc.*, **1982**, 1960

18. S. Shinkai, T. Minami, T. Kouno, Y. Kusano and O. Manabe, *Chem. Lett.* , **1982**, 499

19. S. Shinkai, T. Minami, Y. Kusano and O. Manabe, *J.Am.Chem.Soc.*, **1982**, *104*, 1967

20. S. Shinkai, K. Inuzka, O. Miyazaki and O. Manabe, *J.Am.Chem.Soc.*, **1985**, *107*, 3950

21. H. Nakamura, H. Nishida, M. Takagi and K. Ueno, *Anal. Chim. Acta.* , **1982** *139* , 219,

22. R.M. Izatt, J.D. Lamb, R. T. Hawkins, P. R. Brown, S. R. Izatt and J. J. Christensen, *J.Am.Chem.Soc.*, **1983**, *105* , 1782

23. M. Tazaki, K. Nita, M. Takagi and K. Ueno, *Chem. Lett.* , **1982**, 571

24. S. Shinkai, H. Kinda, Y. Araragi, and O. Manabe, *Bull. Chem. Soc. Jpn.* , **1983**, *56* , 559

25. a) H. Stetter and W. Frank, *Angew. Chem. Int. Ed. Eng.* , **1976**, *15* , 686; b) H. Stetter, W. Frank and R. Mertens, *Tetrahedron* , **1981**, *37* , 767

26. M. Takahshi and S. Takamoto, *Bull. Chem. Soc. Jpn.* , **1977**, *50* , 3413

27. H. Tsukube, *J.Chem.Soc. Perkin Trans. I*, **1983**, 29

28. A. Kaifer, L. Echegoyen, D.A. Gutowski, D.M. Goli and G.W. Gokel, *J.Am.Chem.Soc.*, **1983**, *105*, 7168

29. H. Togo, K. Hashimoto, K. Morihashi and O. Kikuchi, *Bull. Chem. Soc. Jpn.* , **1988**, *61* , 3026

30. C.R. Morgan, D.A. Gutowski,T.P. Cleary, L. Echegoyen and G.W. Gokel, *J. O.C.*, **1984**, *49* , 5008

31. D.A. Gutowski, L. Echegoyen, D.M. Goli, A. Kaifer, R.A. Schultz and G.W. Gokel, *J.Am.Chem.Soc.*, **1984**, *106* , 1633

32. A. Kaifer, D.A. Gutowski, L. Echegoyen, V.J. Gatto, R.A. Schultz, T.P. Cleary, C.R. Morgan, D.M. Goli, A. M Rios and G.W. Gokel, *J.Am.Chem.Soc.*,**1985**, *107* , 1958

33. M. Delgado, L. Echegoyen, V.J. Gatto, D.A. Gutowski and G.W. Gokel, *J.Am.Chem.Soc.*,**1986**, *108* , 4135

34. J.M. Caridade Costa, B. Jeyashri and D. Bethell, *J. Electroanal. Chem.* **1993***351*, 259

35. L. Echegoyen, D.A. Gutowski, V.J. Gatto and G.W. Gokel, *J. C. S. Chem Comm.*, **1986**, 220

36. D.A. Gutowski, M. Delgado, V.J. Gatto, L. Echegoyen and G.W. Gokel, *Tetrahedron Letters*, **1986**, *27*, 3487

37. L. Echeverria, M. Delgado, V.J. Gatto, G.W. Gokel and L. Echygoyen, *J.Am.Chem.Soc.*, **1986**, *108* , 6825

38. L.E. Echegoyen, H. Kim Yoo, V.J. Gatto, G.W. Gokel and L. Echygoyen, *J.Am.Chem.Soc.*, **1989**, *111* , 2440

39. D.A. Gutowski, M. Delgado, V.J. Gatto, L. Echegoyen and G.W. Gokel, *J.Am.Chem.Soc.*, **1986**, *108* , 7553

40. M. Delgado, D.A. Gutowski, H. Kim Yoo, V.J. Gatto, G.W. Gokel and L. Echegoyen, *J.Am.Chem.Soc.*, **1988**, *110* , 119

41. J.P. Dix and F. Vögtle, *Chem. Ber.*, **1981**, *114*, 638

42. S. Nakatsuji,Y. Ohmori, M. Iyoda, K. Nakashima and S. Akiyama, *Bull. Chem. Soc. Jpn.* , **1983**, *56*, 3185

43. T. Lu, H. Kim Yoo, H. Zhang, S. Bott, J.L. Atwood, L. Echegoyen and G.W. Gokel, *J.O.C.*, **1990**, *55*, 2269

44. H. Kim Yoo, D.M. Davis, Z. Chen, L. Echegoyen and G.W. Gokel, *Tetrahedron Letters*, **1990**, *31*, 55

45. J. Fang, T. Lu, H. Kim, I. Delgado, P. Geoffroy, J.L. Atwoodand G.W. Gokel, *J.O.C.*, **1991**, *56*, 7059

46. H. Kim, O.F. Schall, J. Fang, J. E. Trafton, T. Lu, J.L. Atwood and G.W. Gokel, *J. Phys. Org. Chem.*, **1992**, *5*, 482

47. J. Hancox, M.Sc. Thesis, Liverpool University, 1993

48. Z. Chen, O.F. Schall, M.A. Icalá, Y. Li, G.W. Gokel and L. Echegoyen, *J.Am.Chem.Soc.*, **1992**, *114* , 444

49. K. Sugihara, H. Kamiya, M. Yamaguchi, T. Kaneda and S. Misumi, *Tetrahedron Letters*, **1981**, *22*, 1619

50. H. Bock, B. Hierholzer, F. Vögtle and G. Hollmann, *Angew. Chem. I. E. E.* ,**1984**, *23* ,57

51. (a) R.E. Wolf and S.R. Cooper, *J.Am.Chem.Soc.*, **1984**, *106* , 4646; (b) M. Delgado, R.E. Wolf, J.A.R. Hartmann, G. McCafferty, R. Yagbasan, S.C. Rawle, D.J. Watkin and S.R. Cooper, *J.Am.Chem.Soc.*, **1992**, *114* , 8983

52. K. Maruyama, H. Sohmiya and H. Tsukube, *Tetrahedron Lett.* , **1985**, *26*, 3583

53. C.D. Gutsche, *Acc. Chem. Res.*,**1983**, *16*, 161

54. C.D. Gutsche, *Topics in Curr. Chem.*, **1984**, *123*, 1

55. Chemical Abstracts, Registry number [74568-07-3], American Chemical Society, Columbus, Ohio

56. A. Zinke and E. Ziegler, *Ber.*, **1941**, *B74*, 1729

57. A. Zinke and E. Ziegler, *Ber.*, **1944**, *77*, 264

58. B.T. Hayes and R.F. Hunter, *Chem. Ind.*, **1956**, 193

59. B.T. Hayes and R.F. Hunter, *J. Appl. Chem.*, **1958**, *8*, 743

60. J.W. Conforth, P. D'Arcy Hart, G.A. Nicholls, R.J.W. Rees and J.A. Stock, *Br. J. Pharmacol.*, **1955**, *10*, 73

61. J.W. Conforth,E.D. Morgan, K.T. Potts and R.J.W. Rees, *Tetrahedron*, **1973**, *29*, 1659

62. R.S. Buriks, A.R. Fauke and F.E.Mange, U.S. Patent, 4,032,514, **1977**

63. R.S. Buriks, A.R. Fauke and F.E.Mange, U.S. Patent, 4,098,717, **1978**

64. R.S. Buriks, A.R. Fauke and J.H. Munch, U.S. Patent, 4,259,464, **1981**

65. C.D. Gutsche, A.E. Gutsche and A.I. Karautov, *J. Inclusion Phenom.*, **1985**, 3, 447

66. C.D. Gutsche, *Organic syntheses*, **1989**, *68*, 234

67. C.D. Gutsche *"Monographs in Supramolecular Chemistry, No. 1, Calixarenes`"*, Royal Society of Chemistry, Cambridge, (1989)

68. *"Calixarenes: A Versatile Class of Macrocyclic Compounds"*, eds. J. Vicens and V. Böhmer, Kluwer Academic Publishers, Dordrecht, (1991)

69. G. Happel, B. Mathiasch and H. Kämmerer, *Makromol. Chem.*, **1975**, *176*, 3317

70. J.H. Munch, *Makromol. Chem.*, **1977**, *178*, 69

71. C.D. Gutsche and L.J. Bauer, *J.Am.Chem.Soc.*, **1985**, *107*, 6052

72. P.D.J. Grootenhois, P.A.Kollman, L.C. Groenen, D.N. Reinhoudt, G.J. van Hummel, F. Ugozzoli and G.D. Andreeti, *J.Am.Chem.Soc.*, **1990**, *112*, 4165

73. C.D. Gutsche and L.J. Bauer, *Tetrahedron Lett.*, **1981**, *22*, 4763

74. K. Iwamoto, K. Araki and S. Shinkai, *J. Org. Chem.*, **1991**, *56*, 4955

75. V. Böhmer, H. Goldmann, W. Vogt, E.F. Paulus, F.L. Tobiason and M.J. Thielman, *J.C.S.Perkin Trans. 2*, **1990**, 1769

76. C.D. Gutsche B. Dhawan, J.A. Levine K.H. No and L.J. Bauer, *Tetrahedron*, **1983**, *39*, 409

77. K. Iwamoto, K. Fujimoto, T. Matsuda and S. Shinkai, *Tetrahedron Lett.*, **1990**, *31*, 7169

78. A. Casnati, A. Pochini, R. Ungaro, R. Caccicpaglia and L. Mandolini, *J.C.S.Perkin Trans. 1*, **1991**, 2052

79. W. Verboom, S. Datta, Z. Asfari, S. Harkema and D.N. Reinhoudt, *J.O.C.*, **1992**, *57*, 5394

80. K. Iwamoto, K. Araki and S. Shinkai, *Tetrahedron*, **1991**, *47*, 4325

81. S.K. Chang, S.K. Kwon and I. Cho, *Chem. Lett.*, **1987**, 947

82. M.A. McKervey, E.M. Seward, G. Ferguson, B.L. Ruhl and S.J. Harris, *J. Chem. Soc. Chem. Commun.*, **1985**, 388

83. A. Arduini, A. Pochini, S. Reverberi and R. Ungaro, *Tetrahedron*, **1986**, *42*, 2089

84. F. Arnaud-Neu, E.M. Collins, M. Deasy, G. Ferguson, S.J. Harris, B. Kaitner, A.J. Lough, M.A. McKervey, E.M. Marques, B.L. Ruhl, M.J. Schwing-Weill and E.M. Seward, *J. Am.Chem. Soc.*, **1989**, *111*, 8681

85. A. Arduini, E. Ghidini, A. Pochini, R. Ungaro, G.D. Andreetti, G. Calestani and F. Ugozzoli, *J. Inclusion Phenom.*, **1988**, *6*, 119

86. F. Arnaud-Neu, G. Barrett, S. Cremin, M. Deasy, G. Ferguson, S.J. Harris, A.J. Lough, L. Guerra, M.J. Schwing-Weill and P. Schwinte, *J. Chem. Soc. Perkin Trans. 2*, **1992**, 1119

87. See (a) M.J. Schwing-Weill and M.A. McKervey and (b) A. Pochini and R. Ungaro in ref 68, pp. 149-171 and 127-145

88. T. Nagasaki and S. Shinkai, *Bull. Chem. Soc. Jpn.*, **1992**, *65*, 471

89. C. Alfieri, E. Dradi, A. Pochini, R. Ungaro and G.D. Andreetti, *J. Chem. Soc. Chem. Commun.*, **1983**, 1075

90. D.N. Reinhoudt, P.J. Dijksitra, P.J.A. in't Veld, K.E. Bugge, S. Harkema, R. Ungaro and E. Ghidini, *J.Am.Chem.Soc.*, **1987**, *109*, 4761

91. D. Kraft, R. Arnecke, V. Böhmer and W. Vogt, *Tetrahedron*, **1993**, *49*, 6019

92. G. Deng, T. Sakaki, K. Nakashima, S. Shinkai, *Tetrahedron Lett.*, **1992**, *33*, 2163

93. G. Deng, T. Sakaki, K. Nakashima, S. Shinkai, *Chem. Lett.*, **1992**, 1287

94. S. Shinkai, H. Koreishi, K. Ueda, O. Manabe, *J. Chem. Soc. Chem. Commun.*, **1986**, 233

95. S. Shinkai, H. Koreishi, K. Ueda, T. Akimura, O. Manabe, *J.Am.Chem.Soc.*, **1987**, *109*, 6371

96. A.M. King, C.P. Moore, K.R.A.S. Sandanayake and I.O. Sutherland, *J. Chem. Soc. Chem. Commun.*, **1992**, 582

97. M. McCarrick, B. Wu, S.J. Harris, D. Diamond, G. Barretand M.A. McKervey, *J. Chem. Soc. Chem. Commun.*, **1992**, 1287

98. Y. Kubo, S. Hamaguchi, K. Kotani and K. Yoshida, *Tetrahedron Lett.*, **1991**, *32*, 7419

99. H. Shimizu, K. Iwamoto, K. Fujimoto and S. Shinkai, *Chem. Lett.*, **1991**, 2147

100. K. Iwamoto, K. Araki, H. Fujimoto, and S. Shinkai, *J. Chem. Soc. Perkin Trans. 1*, **1992**, 1885

101. T. Jin, k. Ichikawa and T. Koyama, *J. Chem. Soc. Chem. Commun.*, **1992**, 499

102. C. Pérez-Jiménez, S.J. Harris and D. Diamond, *J. Chem. Soc. Chem. Commun.*, **1993**, 480

103. I. Aoki, T. Sakaki and S. Shinkai, *J. Chem. Soc. Chem. Commun.*, **1992**, 731

104. I. Yoshida, N. Yamamoto, F. Sugara, K. Ueno, D. Ishii and S. Shinkai, *Chem. Lett.*, **1991**, 2105

105. S. Shinkai, S. Mori, T. Tsubaki, T. Sone and O. Manabe, *Tetrahedron Lett.*, **1984**, *25*, 5315

106. S. Shinkai, S. Mori, H. Korishi, T. Tsubaki, T. Sone and O. Manabe, *J.Am.Chem.Soc.*, **1986**, *108*, 2409

107. F. Hamada, T. Fukugaki, K. Murai, G.W. Orr and J.L. Atwood, *J. Inclusion Phenom.*, **1991**, *10*, 57

108. C.P. Andrieux, A. Merz, J.-M. Saveant and R. Tomahogh*J. Am. Chem. Soc.*, **1984**, *106*,

109. For example 1-methoxyanthraquinone Ep^1 -0.9 V (in reference 35)

110. G. Barrett, V. Böhmer, G. Ferguson, J.F. Gallagher, S.J. Harris, R.G. Leonard, M.A. McKervey, M. Owens, M. Tabatabai, A. Vierengel and W. Vogt, *J. Chem. Soc. Perkin Trans. 2*, **1992**, 1595

111. A. Arduini, A. Pochini, S. Reverberi and R. Ungaro, *J. Chem. Soc. Chem. Commun.*, **1984**, 981

112. S.K. Chang and I. Cho, *J. Chem. Soc. Perkin Trans. 1*, **1986**, 211

113. V. Bohmer, W. Vogt, S.J. Harris, R.G Leonard, E.M. Collins, M. Deasy, M.A. McKervey and M. Owens, *J. Chem. Soc. Perkin Trans. 1*, **1990**, 431

114 . E.M. Collins, M.A. McKervey and S.J. Harris, *J. Chem. Soc. Perkin Trans. 1*, **1989**, 372

115.R. Ungaro, A. Pochini and G.D. Andreetti, *J. Inclusion Phenom.*, **1984**, *2*, 199

116. J.D. Van Loon, A. Arduini, L. Coppi, W. Verboom, A. Pochini, R. Ungaro, S. Harkema and D.N. Reinhoudt, *J. Org. Chem.*, **1990**, *55*, 5639

117. S. Shinkai, *Tetrahedron*, **1993**, *49*, 8933

118.S. Shinkai, K. Araki, H. Koreishi, T. Tsubaki and O. Manbe, *Chem. Lett.*, **1986**, 1351

119.K. Araki, K. Iwamoto, S. Shinkai and T. Matsuda, *Bull. Chem. Soc. Jpn.*, **1990**, *63*, 3480

120.A. Arduini, A. Casnati, L. Dodi, A. Pochini and R. Ungaro, *J. Chem. Soc. Chem. Commun.*, **1990**, 1597

121.L.C. Groenen, B.H.M. Ruël, A. Casnati, P. Timmerman, W. Verboom, S. Harkema, A. Pochini, R. Ungaro and D.N. Reinhoudt, *Tetrahedron Lett.*, **1991**, *32*, 2675

122. P.A. Chritensen and A. Hamnett *"Techniques and Mechanisms in Electrochemistry"*, Blackie Academic & Professional, London, (1994)

123. C.M.A. Brett and A.M.O. Brett, *"Electrochemistry Principles, Methods and Applications"*, Oxford science Publications, Oxford, (1993)

124. V.D. Parker and M. Tilset, *J. Am. Chem. Soc.*, **1987**, *109*, 2521

125. S. Millar, D. Gutowski, Z. Chen, G. Gokel, L. Echegoyen and A. Kaifer, *Anal. Chem.*, **1988**, *60*, 2021

126. aq + li ref find

127. Tribromo-sym-xylenol was prepared according to the method of Raiford and Scott, who also reported 2,6-dibromoxyloquinone. The latter, however, was prepared by the superior method of Raiford and Kaiser, for the analogous 2,6-dichloroxyloquinone.
(a)L.C. Raiford and J.H. Scott, *J. Org. Chem.*, (1937), **2**, 213; (b) L.C. Raiford and D.W. Kaiser, *J. Org. Chem.*, (1939), **4**, 555

128. pp 442, "Elselviers Encyclopedia of Organic Chemistry" Series III, Volume 13, Elselvier Publishing Co. Inc., New York, (1946)

129. *Chemisches Zentralblatt*, **1908** I, 571